

AD-A100 436

MASSACHUSETTS INST OF TECH LEXINGTON LINCOLN LAB
WORLD-WIDE LINK AVAILABILITY FOR GEOSTATIONARY AND CRITICALLY I--ETC(U)

F1962R-80-C-0002

NL

JAN 81 L M SCHWAB

UNCLASSIFIED

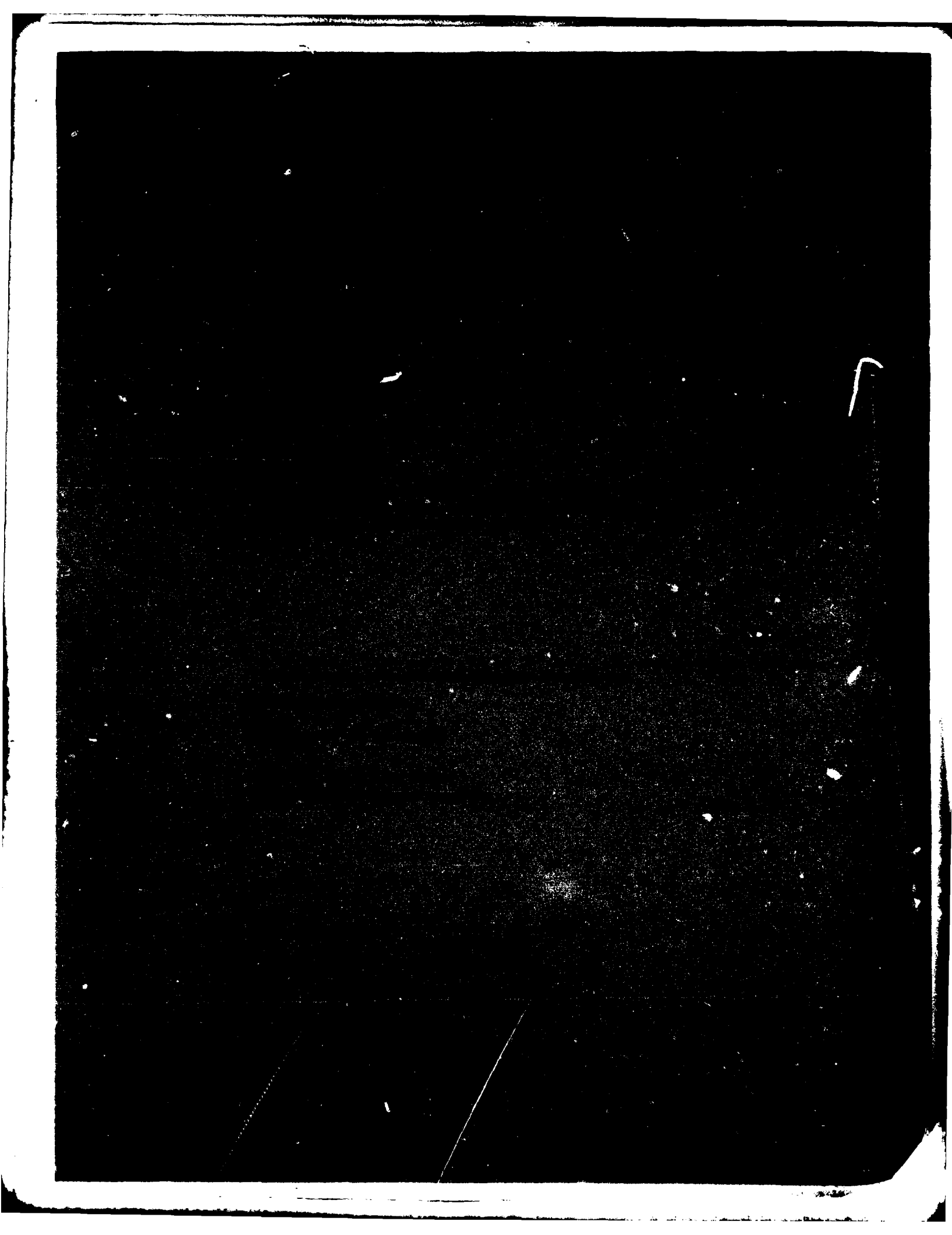
DCA-9

ESD-TR-81-5

1 of 1
A7-20436

END
DATE
7-8-81
DTIC

AD 1976



**MASSACHUSETTS INSTITUTE OF TECHNOLOGY
LINCOLN LABORATORY**

**WORLD-WIDE LINK AVAILABILITY
FOR GEOSTATIONARY AND CRITICALLY
INCLINED ORBITS INCLUDING RAIN ATTENUATION EFFECTS**

L.M. SCHWAB

Group 61

PROJECT REPORT DCA-9

27 JANUARY 1981

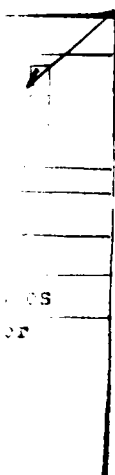
Approved for public release; distribution unlimited.

LEXINGTON

MASSACHUSETTS

Abstract

Link availability for constellations of satellites in geostationary and critically inclined orbits is computed using a predictor model based on the Crane 8 region worldwide rain attenuation model. The results are contrasted to percent Earth visibility computations which do not include rain attenuation. For geostationary satellite constellations, the quantitative relationship of Earth coverage vs link margin vs availability vs number of satellites is described by a set of parametric curves.



CONTENTS

Abstract	iii
List of Illustrations	vi
I. INTRODUCTION	1
II. PERCENT EARTH COVERAGE COMPUTATIONS	3
A. Geostationary Orbit: Geometric Visibility Only	3
B. Geostationary Orbit: Weather Factor Included	6
C. Critically Inclined Orbit: Geometric Visibility Only	11
D. Critically Inclined Orbit: Weather Factor Included	29
E. Relationship of Earth Coverage to Link Margin for Geostationary Orbits	37
III. LINK AVAILABILITY COVERAGE PROFILE MAPS	41
IV. SATELLITE ANTENNA SUBSYSTEM DIRECTIVITY ALLOCATION CONSIDERATIONS	61
V. CONCLUSIONS	70
Acknowledgments	71
References	72

ILLUSTRATIONS

- | | |
|--|----|
| 1. Crossover latitude vs number of equi-spaced geostationary satellites | 4 |
| 2. Percent Earth area coverage vs number of equi-spaced geostationary satellites for 10° minimum elevation angle visibility to 1, 2, 3, and 4 or more satellites | 5 |
| 3. Percent Earth coverage as a function of link availability for a constellation of three equi-spaced geostationary satellites starting at 30° East longitude. Frequency is fixed at 44 GHz link margin is varied over the range from 6 to 18 dB | 8 |
| 4. Percent Earth coverage as a function of link availability for a constellation of four equi-spaced geostationary satellites starting at 30° East longitude. Frequency is fixed at 44 GHz and link margin is varied over the range from 6 dB to 18 dB | 9 |
| 5. Percent Earth coverage as a function of link availability for a constellation of five equi-spaced geostationary satellites starting at 30° East longitude. Frequency is fixed at 44 GHz and link margin is varied over the range from 6 dB to 18 dB | 10 |
| 6(a). Percent Earth coverage as a function of orbit time relative to perigee. Two satellites in critically inclined orbits; 12 hour periods; each satellite is phased by 6 hours with satellites in the same orbital plane. Top curve illustrates terminal visibility to one or more satellites; bottom curve is visibility to 2 or more satellites | 16 |
| 6(b). Percent Earth coverage as a function of orbit time relative to perigee. Two satellites in critically inclined orbits; 12 hour periods; each satellite is phased by 6 hours with satellites in orthogonal orbital planes. Top curve illustrates terminal visibility to one or more satellites; bottom curve is visibility to 2 or more satellites. This case represents a configuration yielding identical ground tracks for the 2 satellites | 17 |
| 6(c). Percent Earth coverage as a function of orbit time relative to perigee. Three satellites in critically inclined orbits; 12 hour periods; each satellite is phased by 4 hours with satellites in the same orbital plane. Top curve illustrates terminal visibility to one or more satellites; bottom curve is visibility to 3 or more satellites | 18 |

ILLUSTRATIONS (Cont'd)

6(d). Percent Earth coverage as a function of orbit time relative to perigee. Four satellites in critically inclined orbits; 12 hour periods; each satellite is phased by 3 hours with satellites in the same orbital plane. Top curve illustrates terminal visibility to one or more satellites; bottom curve is visibility to 4 or more satellites

19

6(e). Percent Earth coverage as a function of orbit time relative to perigee. Four satellites in critically inclined orbits; 12 hour periods; each satellite is phased by 6 hours with satellites in orthogonal orbital planes. This case represents a configuration of 2 identical ground tracks separated by 90° longitude. Top curve illustrates terminal visibility to one or more satellites; bottom curve is visibility to 4 or more satellites

20

6(f). Percent Earth coverage as a function of orbit time relative to perigee. Three satellites in critically inclined orbits; 12 hour periods; each satellite is phased by 4 hours with orbital planes separated by 60° . This case represents a configuration yielding identical ground tracks for the 3 satellites

21

7(a). Percent Earth coverage as a function of orbit time relative to perigee. Two satellites in critically inclined orbits; 24 hour periods; each satellite is phased by 12 hours with satellites in the same orbital plane. Top curve illustrates terminal visibility to one or more satellites; bottom curve is visibility to 2 or more satellites

22

7(b). Percent Earth coverage as a function of orbit time relative to perigee. Two satellites in critically inclined orbits; 24 hour periods; each satellite is phased by 12 hours with satellites in orbital planes 180° apart. This case represents a configuration yielding identical ground tracks for the satellites. Top curve illustrates terminal visibility to one or more satellites; bottom curve is visibility to 2 or more satellites

23

7(c). Percent Earth coverage as a function of orbit time relative to perigee. Three satellites in critically inclined orbits; 24 hour periods; each satellite is phased by 8 hours with satellites in the same orbital plane. Top curve illustrates terminal visibility to one or more satellites; bottom curve is visibility to 3 or more satellites

24

7(d). Percent Earth coverage as a function of orbit time relative to perigee. Four satellites in critically inclined orbits; 24 hour periods; each satellite is phased by 6 hours with satellites in

ILLUSTRATIONS (Cont'd)

- the same orbital plane. Top curve illustrates terminal visibility to one or more satellites; bottom curve is visibility to 4 or more satellites 25
- 7(e). Percent Earth coverage as a function of orbit time relative to perigee. Four satellites in critically inclined orbits; 24 hour periods; each satellite is phased by 12 hours with satellites in orthogonal orbital planes. Top curve illustrates terminal visibility to one or more satellites; bottom curve is visibility to 4 or more satellites 26
- 7(f). Percent Earth coverage as a function of orbit time relative to perigee. Three satellites in critically inclined orbits; 24 hour periods; each satellite is phased by 8 hours with orbital planes separated by 120° . This case represents a configuration yielding identical ground tracks for the 3 satellites 27
8. Northern Hemisphere coverage for 0.99 link availability: 14 dB link margin at 44 GHz. Critically inclined orbit with 12 hour period. 4 hours before apogee: 45.7N, 76.0E; $3.72*Re$ Altitude 31
9. Northern Hemisphere coverage for 0.99 link availability. 14 dB link margin at 44 GHz. Critically inclined orbit with 12 hour period. Apogee: 63.4N, 75.0E; $6.16*Re$ Altitude 32
10. Northern Hemisphere coverage for 0.99 link availability. 14 dB link margin at 44 GHz. Critically inclined orbit with 12 hour period. 2 hours after apogee: 59.9N, 75.5E; $5.6*Re$ Altitude 33
11. Northern Hemisphere coverage for 0.99 link availability. 14 dB link margin at 44 GHz. Critically inclined orbit with 24 hour period. 4 hours before apogee: 61.5N, 112.2E; $10.13*Re$ Altitude 34
12. Northern Hemisphere coverage for 0.99 link availability. 14 dB link margin at 44 GHz. Critically inclined orbit with 24 hour period. Apogee: 63.4N, 75.0E; $11.05*Re$ Altitude 35
13. Northern Hemisphere coverage for 0.99 link availability. 14 dB link margin at 44 GHz. Critically inclined orbit with 24 hour period. 8 hours after apogee: 53.2N, 2.8E; $7.06*Re$ altitude 36
14. Earth coverage as a function of link margin for parametric values of link availability. A constellation of 3 equi-spaced geostationary satellites and an operating frequency of 44 GHz are assumed 38

ILLUSTRATIONS (Cont'd)

- 15. Earth coverage as a function of link margin for parametric values of link availability. A constellation of 4 equi-spaced geostationary satellites and an operating frequency of 44 GHz are assumed 39
- 16. Earth coverage as a function of link margin for parametric values of link availability. A constellation of 5 equi-spaced geostationary satellites at an operating frequency of 44 GHz are assumed 40
- 17. Coverage area (unshaded) for 0.99 link availability for a constellation of 3 equi-spaced geostationary satellites. Operating frequency is 44 GHz and link margin equals 14 dB 42
- 18. Coverage area (unshaded) for 0.99 link availability for a constellation of 3 equi-spaced geostationary satellites. Operating frequency is 44 GHz and link margin equals 10 dB 43
- 19. Coverage area (unshaded) for 0.99 link availability for a constellation of 3 equi-spaced geostationary satellites. Operating frequency is 44 GHz and link margin equals 6 dB 44
- 20. Coverage area (unshaded) for 0.98 link availability for a constellation of 3 equi-spaced geostationary satellites. Operating frequency is 44 GHz and link margin equals 14 dB 45
- 21. Coverage area (unshaded) for 0.98 link availability for a constellation of 3 equi-spaced geostationary satellites. Operating frequency is 44 GHz and link margin equals 10 dB 46
- 22. Coverage area (unshaded) for 0.98 link availability for a constellation of 3 equi-spaced geostationary satellites. Operating frequency is 44 GHz and link margin equals 6 dB 47
- 23. Coverage area (unshaded) for 0.99 link availability for a constellation of 4 equi-spaced geostationary satellites. Operating frequency is 44 GHz and link margin equals 14 dB 48
- 24. Coverage area (unshaded) for 0.99 link availability for a constellation of 4 equi-spaced geostationary satellites. Operating frequency is 44 GHz and link margin equals 10 dB 49
- 25. Coverage area (unshaded) for 0.99 link availability for a constellation of 4 equi-spaced geostationary satellites. Operating frequency is 44 GHz and link margin equals 6 dB 50

ILLUSTRATIONS (Cont'd)

- | | |
|--|----|
| 26. Coverage area (unshaded) for 0.98 link availability for a constellation of 4 equi-spaced geostationary satellites.
Operating frequency is 44 GHz and link margin equals 14 dB | 51 |
| 27. Coverage area (unshaded) for 0.98 link availability for a constellation of 4 equi-spaced geostationary satellites.
Operating frequency is 44 GHz and link margin equals 10 dB | 52 |
| 28. Coverage area (unshaded) for 0.98 link availability for a constellation of 4 equi-spaced geostationary satellites.
Operating frequency is 44 GHz and link margin equals 6 dB | 53 |
| 29. Coverage area (unshaded) for 0.99 link availability for a constellation of 5 equi-spaced geostationary satellites.
Operating frequency is 44 GHz and link margin equals 14 dB | 54 |
| 30. Coverage area (unshaded) for 0.99 link availability for a constellation of 5 equi-spaced geostationary satellites.
Operating frequency is 44 GHz and link margin equals 10 dB | 55 |
| 31. Coverage area (unshaded) for 0.99 link availability for a constellation of 5 equi-spaced geostationary satellites.
Operating frequency is 44 GHz and link margin equals 6 dB | 56 |
| 32. Coverage area (unshaded) for 0.98 link availability for a constellation of 5 equi-spaced geostationary satellites.
Operating frequency is 44 GHz and link margin equals 14 dB | 57 |
| 33. Coverage area (unshaded) for 0.98 link availability for a constellation of 5 equi-spaced geostationary satellites.
Operating frequency is 44 GHz and link margin equals 10 dB | 58 |
| 34. Coverage area (unshaded) for 0.98 link availability for a constellation of 5 equi-spaced geostationary satellites.
Operating frequency is 44 GHz and link margin equals 6 dB | 59 |
| 35. (a). Idealized Earth coverage uplink receive pattern before reallocation (solid line) and after reallocation (dashed line);
(b). Isometric sketch of reallocated gain pattern showing fringe area increase in relative directive gain | 63 |
| 36. Enhanced directive gain G_r (dB) as a function of angular width ($\Delta\theta$) for two 90° sector pattern fringes and parametric values of difference in directive gains from 0 to 18 dB with increments of 3 dB. | 65 |

ILLUSTRATIONS (Cont'd)

37. Projection of an enhanced fringe area satellite antenna pattern on Earth's surface. Fringe sectors are 90° wide (azimuth sense) and 1° deep (polar sense) as measured from a line between the Earth center and the satellite (Mercator Projection). 66
38. Average rain cell size (km) as a function of rain rate.
(From ITU/CCIR Rep. 563) 69

I. INTRODUCTION

The effects of weather, especially rain, upon the operational quality of millimeter wave military satellite communications (MILSATCOM) systems cannot be ignored.¹ MILSATCOM link outage time can be bounded in the worst case by assuming that a link's signal-to-noise ratio (SNR) is so far degraded during any rain that the link is not usable, i.e., not available. For most parts of the world, there is measurable rain between 5 and 10% of a typical year. The resulting 90 to 95% link availability bound is far too poor to be of interest to all but the most unconcerned or low priority users.

The millimeter wave MILSATCOM problem is a classic one in the sense of the need to provide maximum possible Earth coverage for the maximum possible daily access time using a minimum number of satellites. The bulk of past and current experiments have concentrated on determining propagation loss statistics for specific locations in lieu of a more general world-wide weather related predictor model. The results reported here describe the Earth coverage area for millimeter wave MILSATCOM links computed by using a link availability predictor tool recently derived.² The coverage areas computed on the basis of geometry only are provided as a basis for comparison with the coverage areas computed with weather effects included. The geometric visibility results incorporated in this report are presented in a different format than prior publications³ which have emphasized probability of visibility as a function of latitude.

Section II of this report provides the numerical data on the percent Earth coverage for single and multiple satellites in geostationary and critically inclined orbits computed without rain effects (i.e., geometric visibility only) and with rain effects (i.e., using the link availability predictor model). Plots of percent Earth coverage as a function of link availability for the cases of 3, 4, and 5 equally spaced geostationary satellites are provided. In part (E) of Section II, the Earth coverage data is presented in the alternative form of percent Earth coverage vs link margin for parametric values of availability. Separate plots are provided for constellations of 3,

4, and 5 geostationary satellites each. These curves provide the MILSATCOM system designer with a potent tool for addressing the classic trade-off of coverage vs margin vs availability vs number of satellites.

Section III presents coverage profiles for the cases of 3, 4, and 5 equally spaced geostationary satellites with an operating frequency of 44 GHz and link margins of 14 dB, 10 dB, and 6 dB. These coverage profiles consist of joined segmented Mercator maps which provide the geographic distribution of global areas below a constant value of link availability - taken here as 0.98 and 0.99.

Section IV discusses reallocation of the satellite antenna directive gain to overcome localized weather effects. Antenna patterns are modeled for which typical directive gain differentials are computed and related to requirements for aperture size and number of beams.

II. PERCENT EARTH COVERAGE COMPUTATIONS

A. Geostationary Orbit: Geometric Visibility Only

All of the Earth coverage area calculations described in this report are performed for $\theta > 10^\circ$ where θ is the elevation angle of the satellite measured at the terminal. The visibility limit contour for any single geostationary satellite with no orbit inclination is given by Eqn. (1). For the assumption of at least 3 equally spaced geostationary satellites, Eqn. (1) can be directly solved for the crossover latitude. This crossover latitude

$$\lambda = [\pm \cos^{-1} \left(\frac{\cos 71.43^\circ}{\cos \phi} \right) + \lambda_s] \quad (1)$$

where λ, λ_s = longitudes of the visibility limit contour and satellite subpoint, respectively
 ϕ = latitude of visibility contour corresponding to the longitude λ

represents the minimum value of latitude for which at least one geostationary satellite is visible. Fig. 1 shows the crossover latitude as a function of the number of equi-spaced geostationary satellites.

Any of several methods of numerical surface integration may be utilized to compute the percent Earth area coverage from which one or more geostationary satellites are visible with at least a 10° terminal elevation angle. Standard spherical integration was used to compute the data presented in the Fig. 2 histogram of percent Earth area coverage to at least M satellites ($M=1,2,3,4$) as a function of the number N of equi-spaced geostationary satellites ($N=1,2,3,4,5,6,7,8$). Fig. 2 clearly shows that for the case of three equi-spaced geostationary satellites, most of the Earth area (91%) is covered with access to at least one satellite vs a maximum possible coverage area of 96.1% which would be achieved with an infinite number of equi-spaced satellites. Requiring simultaneous access to at least 2 satellites (for reasons of redundancy, or otherwise) results in a minimum number of 7 equi-spaced

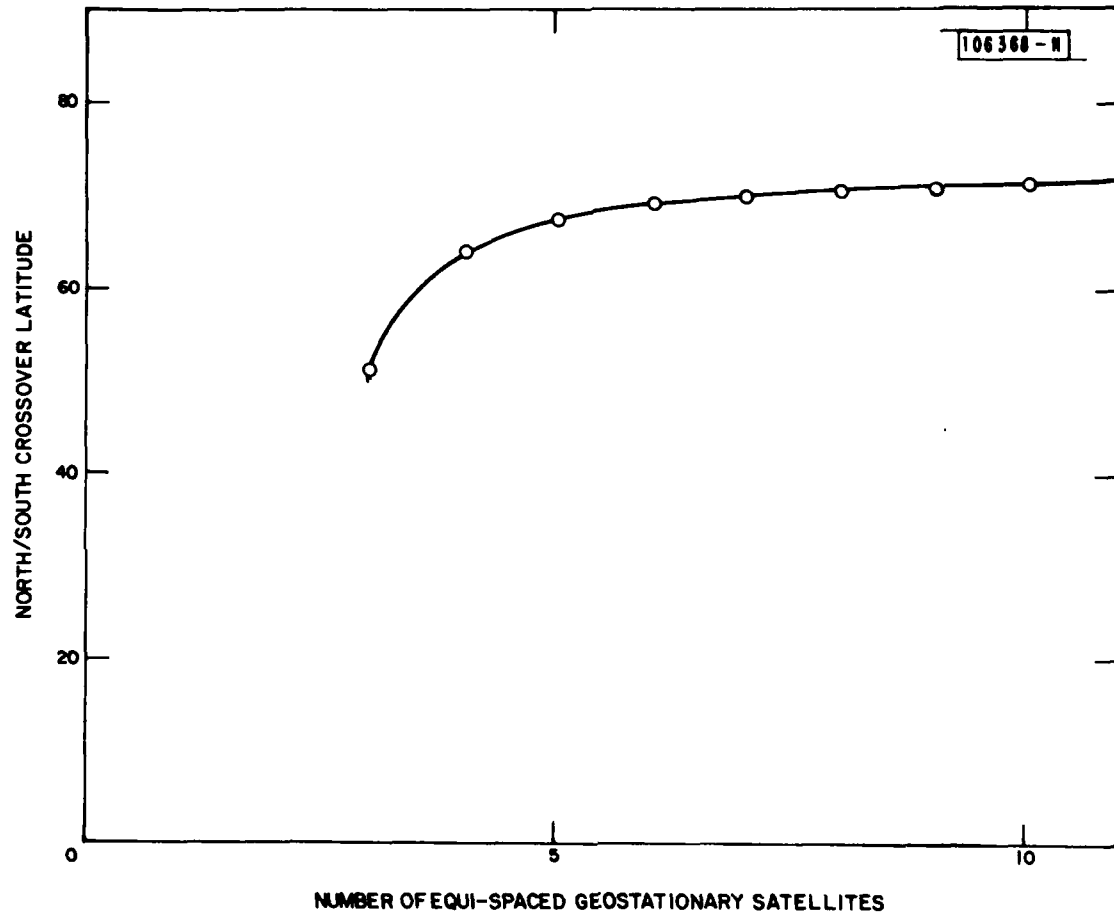


Fig. 1. Crossover latitude vs number of equi-spaced geostationary satellites.

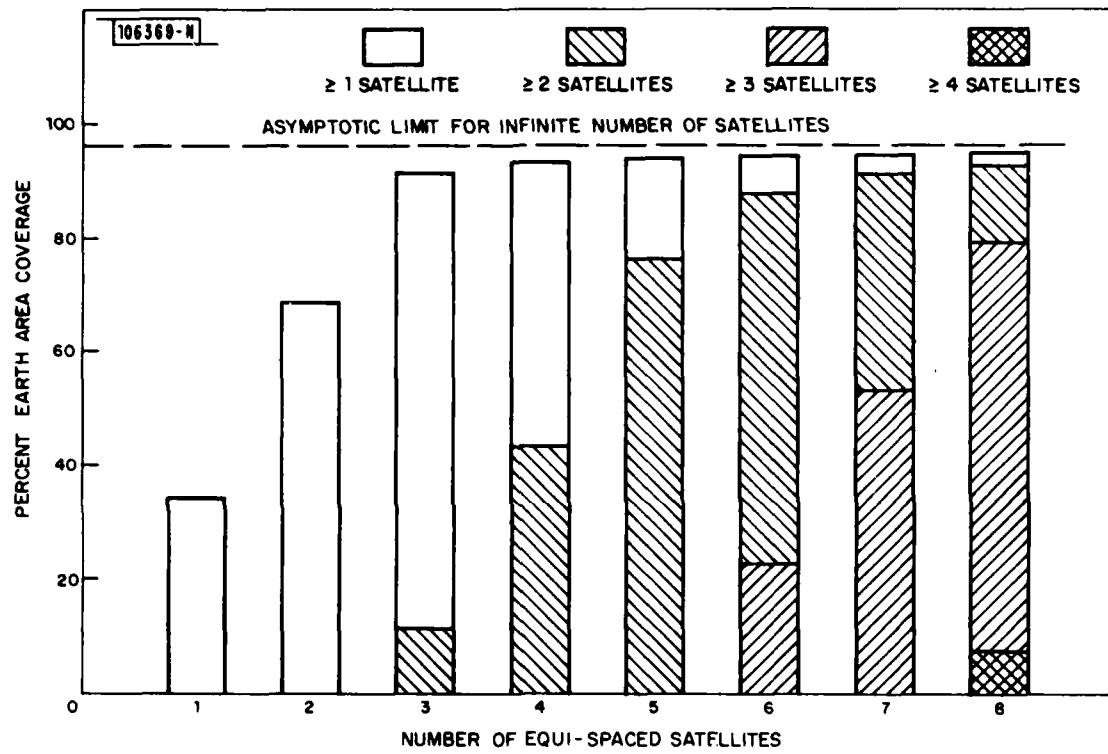


Fig. 2. Percent Earth area coverage vs number of equi-spaced geostationary satellites for 10° minimum elevation angle visibility to 1, 2, 3, and 4 or more satellites.

satellites to exceed the 91% coverage factor for single satellite access using only 3 satellites.

The three types of shaded areas in Fig. 2 represent the 2-fold, 3-fold, and 4-fold coverage overlap areas on the Earth's surface. In all cases, it is understood the bottom end of all the areas, shaded or clear, is the zero ordinate. For example, in the case of 6 equally spaced satellites, the percent Earth area visible to 2 and only 2 satellites can be directly found by subtracting the ordinate value for > 3 satellite visibility from the ordinate value for > 2 satellite visibility. Equivalently, one can measure the bar segment coded for > 2 satellite visibility with a pair of dividers.

B. Geostationary Orbit: Weather Factor Included

When the effects of rain are included in the computations of coverage area, the percent Earth area covered becomes a function of the those link parameters which are related to rain attenuation, i.e., link margin (dB), required availability and choice of satellite subpoint (in addition to the simple elevation angle dependence for geometric coverage). That is, for any given satellite subpoint and any terminal location (regardless of climate region), an arbitrarily high value of link availability is achievable at the expense of providing a large link margin via large antenna apertures, high transmit power, and/or a low value of receive system noise temperature.

The software package SAPM (System Availability Predictor Model) was used to compute the percent coverage area including effects of rain for geostationary satellites. Reference 2 contains a description of the numerical techniques used (and the coding thereof) in predicting SHF and EHF MILSATCOM system availability in the presence of rain. References 4 and 5 provide details on the rain rate data and climate region designations used in the Crane rain attenuation model which is modeled in the SAPM software. A subroutine employing conventional spherical integration ($\Delta\text{Area} = r^2 \sin\theta \Delta\theta \Delta\phi$) was appended to the SAPM program and coupled with a test on the values of link availability stored in the output array.

The cases which were treated using the expanded SAPM program were all equi-spaced geostationary satellite constellations consisting of 3, 4, and

5 satellites. In each case, the initial satellite subpoint was chosen as 30°E and subsequent subsatellite points in each constellation were placed at intervals of 360°/No. of satellites. These subsatellite points all satisfied the requirement of providing geometric Earth coverage to several specific areas of sponsor interest. The frequency was fixed at 44 GHz for all cases and the link margin was sequentially increased in 2 dB increments starting at 6 dB and ending at 18 dB. These bounding values of link margin were selected on the basis of (a) approaching unsatisfactory bit error rates for negligibly low margins and (b) the cost limitations associated with implementing systems with excessively high values of margin. Fig. 3 graphs the integrated percent Earth coverage as a function of one-way link availability at 4 successive levels of link margin for the constellation of 3 equi-spaced geostationary satellites. Similarly, Figs. 4 and 5 address the 4 and 5 equi-spaced geostationary satellite constellations.

The abscissa scale used in Figs. 3, 4, and 5 is a "reversed logarithmic" function which has the effect of compressing the scale in the region about zero value rather than the usual logarithmic compression in the region of unity value. Assuming the horizontal scale was 100 units in length, the reverse logarithmic function which compresses availability values in the range of

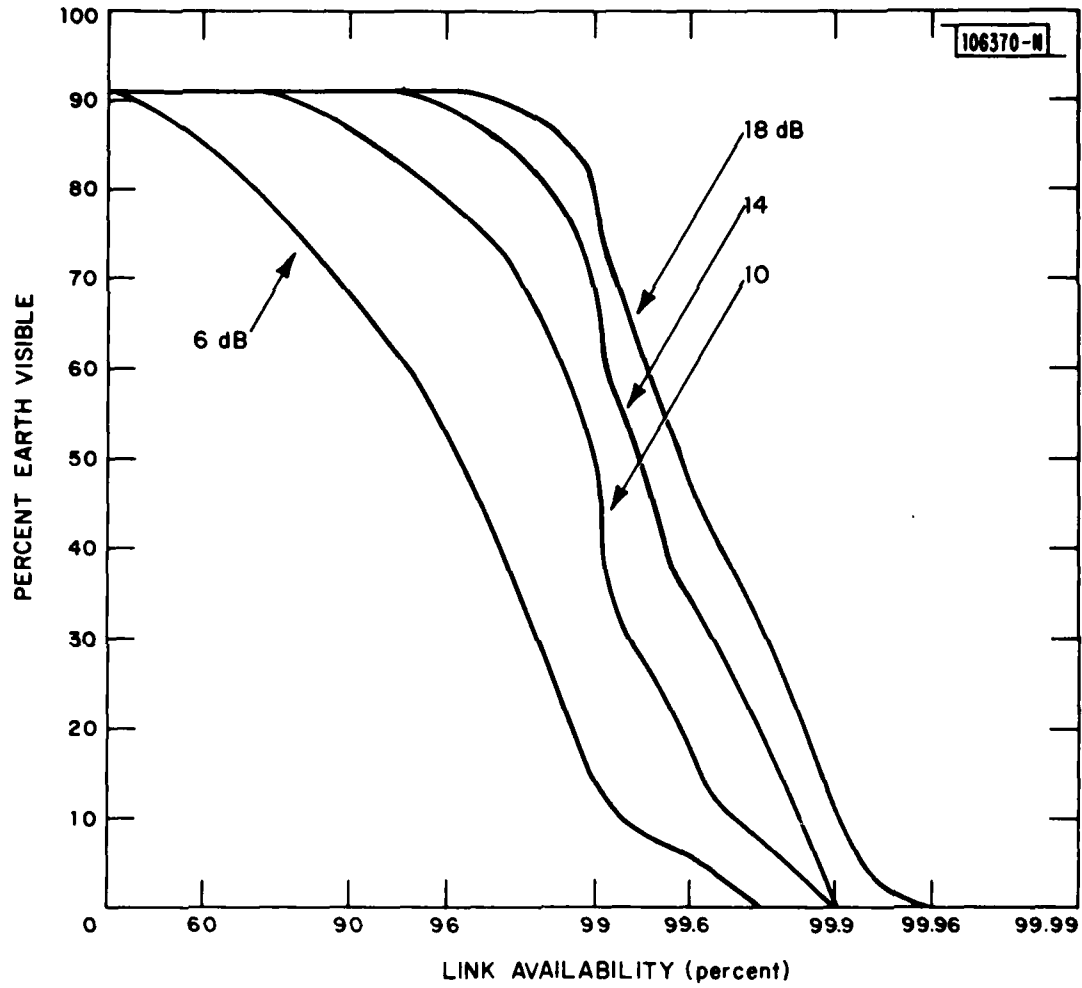
$$0\% < A < 99.99\%$$

into the horizontal scale is given by Eqn. (2)

$$A' = 100 - 25 \log_{10} (10000 - 100A) \quad (2)$$

where A' = the reversed logarithmic compressed value

This relationship can be modified to provide any number of reverse logarithmic cycles as required with the first cycle always starting at zero and cycle boundaries occurring at 90.0%, 99.0%, 99.9%, 99.99%, etc.



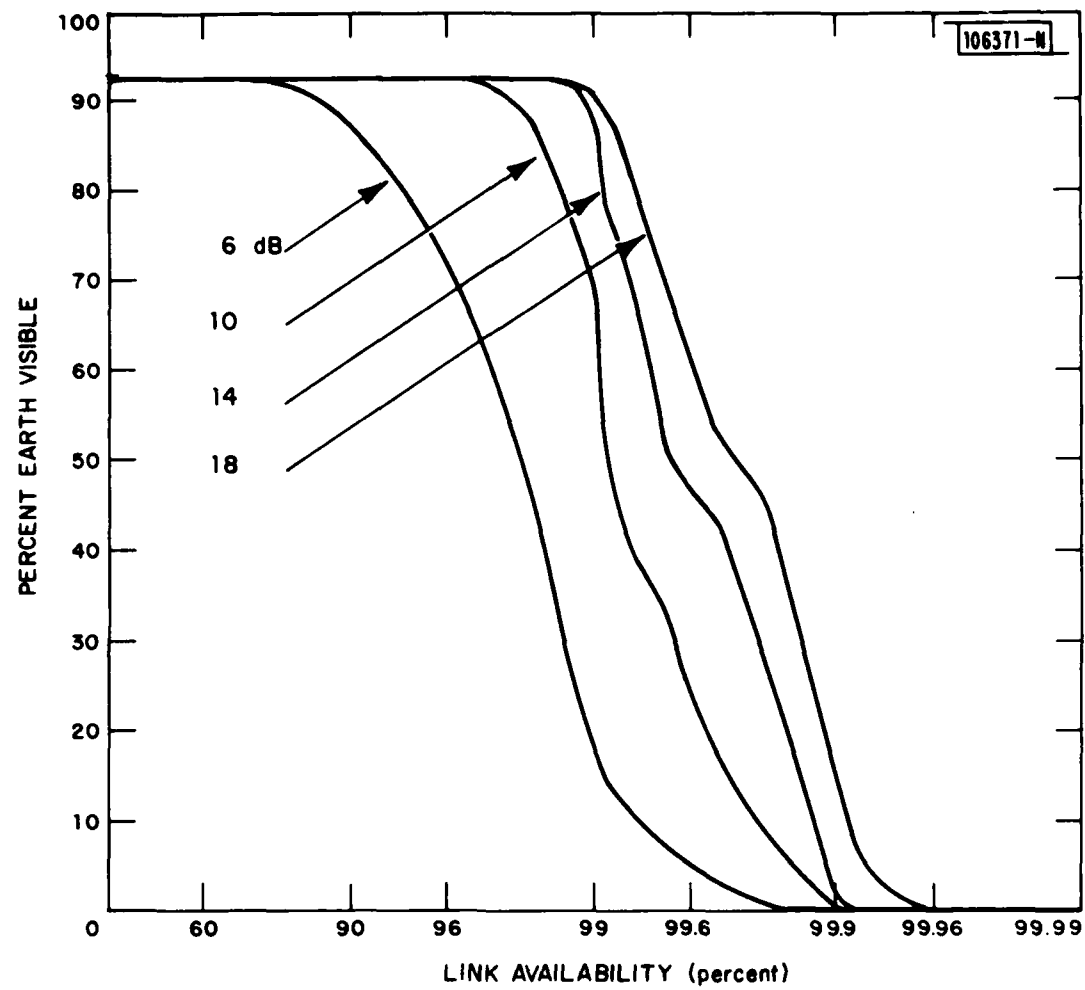


Fig. 4. Percent Earth coverage as a function of link availability for a constellation of four equi-spaced geostationary satellites starting at 30° East longitude. Frequency is fixed at 44 GHz and link margin is varied over the range from 6 dB to 18 dB.

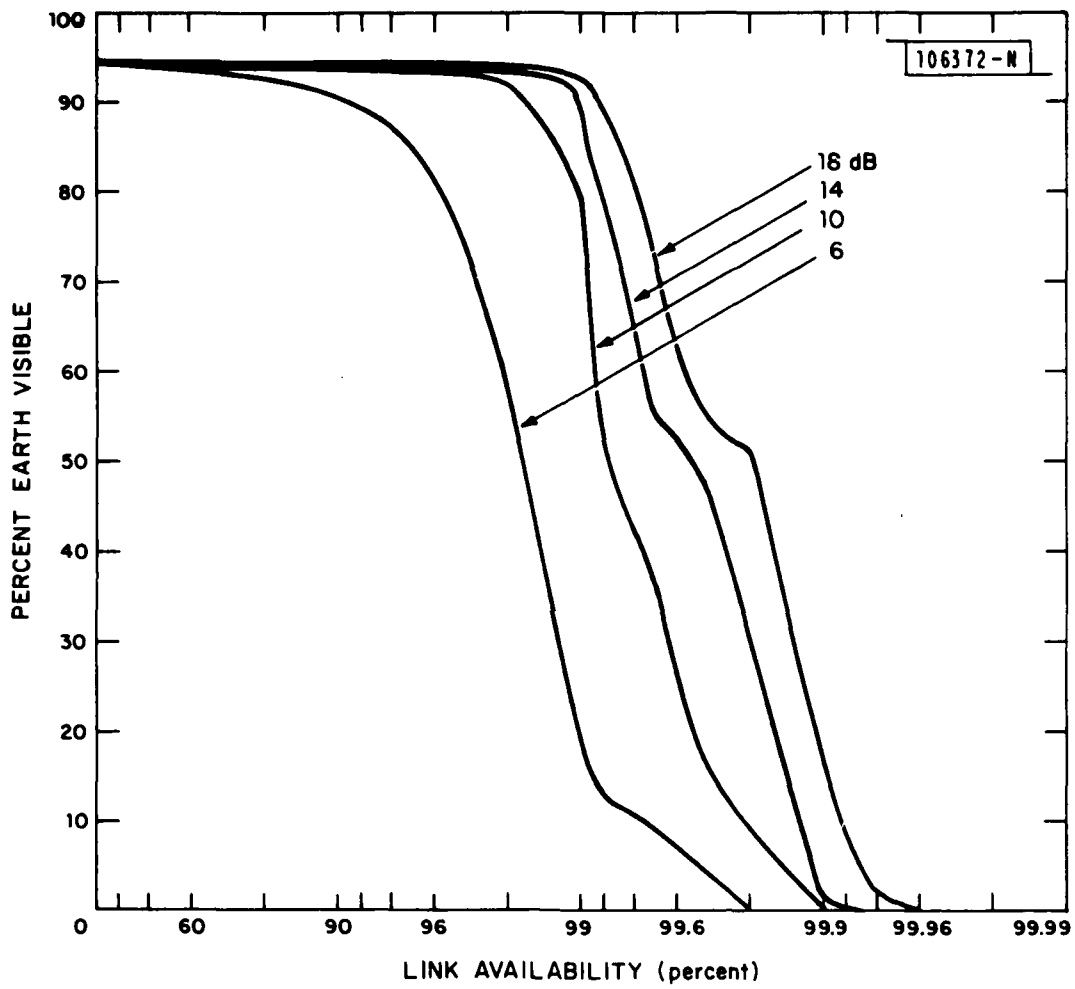


Fig. 5. Percent Earth coverage as a function of link availability for a constellation of five equi-spaced geostationary satellites starting at 30° East longitude. Frequency is fixed at 44 GHz and link margin is varied over the range from 6 dB to 18 dB.

All the curves given in Figs. 3, 4 and 5 possess the general S-character shape for which the extreme values of availability represent physical limitations which cannot be overcome. For low values of availability, the curves all approach the asymptotic value represented by the geometric coverage value as computed earlier and given in Fig. 2. For high values of availability, the minimum rain rate distribution values given by Crane's rain rate Region A definition (see References 2, 4, or 5 for details of distributions and climate region definitions) can be related to maximum possible availability values. Obviously, the only means of extending the zero percent visibility limit to higher levels of availability is by increasing the link margin. Indeed, that effect can be observed in any of the sequences given in Figs. 3, 4, or 5 for increasing link margin. Slight inflections found in several of the curves were caused by various aspects of the numerical solution process. The digitization of the Crane climate region map was carried out on a 2.5° latitude by 2.5° longitude basis² thereby yielding some conversion error. The climate region map boundaries were derived and drawn by Crane on the basis of multiple rain data sources who usually used differing measurement approaches and data reporting formats. Lastly, the Earth area integration process was limited to using the same 2.5° intervals applied to the map digitization simply by virtue of accuracy limitation, i.e., no additional accuracy can be achieved using finer resolution increments than those used in a preceding step. The integration process incurs second order errors at the Earth disk boundary as well as at the boundaries of constant longitude separating coverage areas of adjacent satellites.

The primary value of the sequence of curves given in Figs. 3-5 is in determining the region of the knee of each curve, below which the Earth area coverage rapidly drops. For example, the 14 dB and 18 dB margin cases with 4 and 5 satellite constellations show that the coverage falls rapidly for availability requirements above 0.990.

C. Critically Inclined Orbits: Geometric Visibility Only

The percent Earth coverage results given in Section II(A) for the case of geostationary satellites were straightforward to compute and present due to

constancy of the geometry with time. For the case of critically inclined elliptical orbits, the percent Earth coverage results must be presented as a function of time. The plots presented here use relative orbit time (in hours) with the starting point reference being a perigee for one of the satellites. Unambiguous designation of the reference satellite is not necessary for computation only of percent coverage because of the symmetry and repetitive nature of the curves.

The plots of percent Earth coverage vs time presented in this section, like those given in Section A for geostationary satellites, indicate only a coverage factor unrelated to specific geographical locations. For example, a value of 50% coverage at two different times does not mean that the same 50% of the Earth is visible. Rather, it means that some 50% is covered. This method of presentation contrasts with others^{6,7} where, for a specified area of interest on the Earth's surface (usually, the northern hemisphere) the percent of the specified area which has continuous 100% time coverage is computed. Also, in this study specific ground station locations are neither assumed nor given *a priori*. Hence, the general coverage approach used in this section appeared to be more appropriate to the problem at hand. It should also be noted that the specification of ground coverage with mutual visibility to a fixed ground station site represents a statement of conditional probability. Use of straightforward satellite visibility geometry for spacecraft at or near geostationary orbit altitudes shows that 100% Earth coverage would never be achievable without use of inter-satellite links when a mutual visibility requirement is specified. Given this physical limitation as well as the current level of interest in the MILSATCOM community with inter-satellite links, it was decided to compute and present Earth coverage data on an unconditional basis with respect to ground station locations, i.e., no requirement for mutual visibility.

The desirability of the critically inclined elliptical orbits can be briefly summarized as follows. These orbits provide coverage to Earth areas at extreme latitudes (for argument of perigee $\omega=270^\circ$, apogee is at northern latitudes; for $\omega=90^\circ$, apogee is at southern latitudes). For a specific choice of orbital plane inclination ($I=63.43^\circ$), the effects of a non-spherical Earth

in solving the two-body motion problem are compensated such that orbit degradation (primarily due to drag forces near perigee) is minimized.

Selection of an orbit period which is synchronous or semi-synchronous with the Earth rotation causes the satellite to reappear at the same time and same place in the sky every day. The desirability of using critically inclined orbits is not restricted just to extreme latitudes. In fact, appropriately chosen constellations of satellites in only critically inclined orbits can provide approximately complete coverage to the entire Earth (or, alternately, a smaller number of satellites in inclined orbit in conjunction with a set of equi-spaced geostationary satellites).

The parameters of the critically inclined orbits used in this portion of the study addressing percent Earth coverage are summarized in Table I. The choice of values for the longitude of the ascending node is important only in the relative sense when evaluating percent coverage for a constellation of several satellites with different orbits. The remaining parameter which must be specified is the relative time of perigee passage.

Twelve different cases of critically inclined orbit satellite constellations are treated in this section. They break down into 6 cases for 12 hour semisynchronous orbits and 6 cases for 24 hour synchronous orbits. Briefly, the cases are summarized as follows:

12 Hour Period Orbits

Fig. 6(a): 2 Satellites; Same Orbital Plane; Perigees Phased by 6 hours

Fig. 6(b): 2 Satellites; Orbital Planes Separated by 90° ; Perigees Phased by 6 hours (Identical Ground Track)

Fig. 6(c): 3 Satellites; Same Orbital Plane; Perigees Phased by 4 hours

Fig. 6(d): 4 Satellites; Same Orbital Plane; Perigees Phased by 3 hours

Fig. 6(e): 4 Satellites; Orbital Planes Separated by 90° ; Perigees Phased by 6 hours

Fig. 6(f): 3 Satellites; Orbital Planes Separated by 60° ; Perigees Phased by 4 hours (Identical Ground Track)

24 Hour Period Orbits

Fig. 7(a): 2 Satellites; Same Orbital Plane; Perigees Phased by 12 hours

Fig. 7(b): 2 Satellites; Orbital Planes Separated by 180° ; Perigees
Phased by 12 hours (Identical Ground Track)

Fig. 7(c): 3 Satellites; Same Orbital Plane; Perigees Phased by 8 hours

Fig. 7(d): 4 Satellites; Same Orbital Plane; Perigees Phased by 6 hours

Fig. 7(e): 4 Satellites; Orbital Planes Separated by 90° ; Perigees Phased
by 12 hours

Fig. 7(f): 3 Satellites; Orbital Planes Separated by 120° ; Perigees
Phased by 8 hours (Identical Ground Track)

All the orbits are given the value 270° for the argument of the perigee which has the effect of placing the apogees all in the northern hemisphere; if the constellations were each doubled by appending analogous satellites with 90° values for argument of perigee, the effect would be to approximately double the values of percent Earth visible. Small amounts of overlapped area at the northern and southern hemispheres as well as small unusable visibility areas near perigee will reduce the coverage to a lower effective value. The single hemisphere apogee constellations were used simply to conserve computing resources. The abscissa scale of orbit time relative to the reference satellite's time of perigee passage spans a 24 hour interval. This interval was selected on the basis of depicting a minimum of one complete cycle of the curves.

The data given in Figs. 6(a) through (f) and 7(a) through (f) should be interpreted as follows. For an N satellite case ($N=2,3,4$), the lowest curve represents the percent Earth area which is visible to all N satellites simultaneously as a function of time over the 24 hour interval. The next higher curve represents the percent Earth area visible to at least $(N-1)$ satellites simultaneously. The highest curve gives the Earth area visible to one or more satellites in the constellation. One of the advantages to presenting the data in this fashion is that it allows the user the option of easily determining the percent Earth area visible to specifically M satellites

TABLE I
CRITICALLY INCLINED ORBIT PARAMETERS

12 Hour Period Orbit (Apogee = 6.16 Earth radii altitude)

$I = 63.43^\circ$ (inclination)
 $\omega = 270^\circ$ (argument of perigee)
 $e = 0.722$ (eccentricity)
 $T = 43200$ sec (period)
 $\Omega = \text{arbitrary}$ (ascending node)

24 Hour Period Orbit (Apogee = 11.08 Earth radii altitude)

$I = 63.43^\circ$
 $\omega = 270^\circ$
 $e = 0.825$
 $T = 86400$ sec
 $\Omega = \text{arbitrary}$

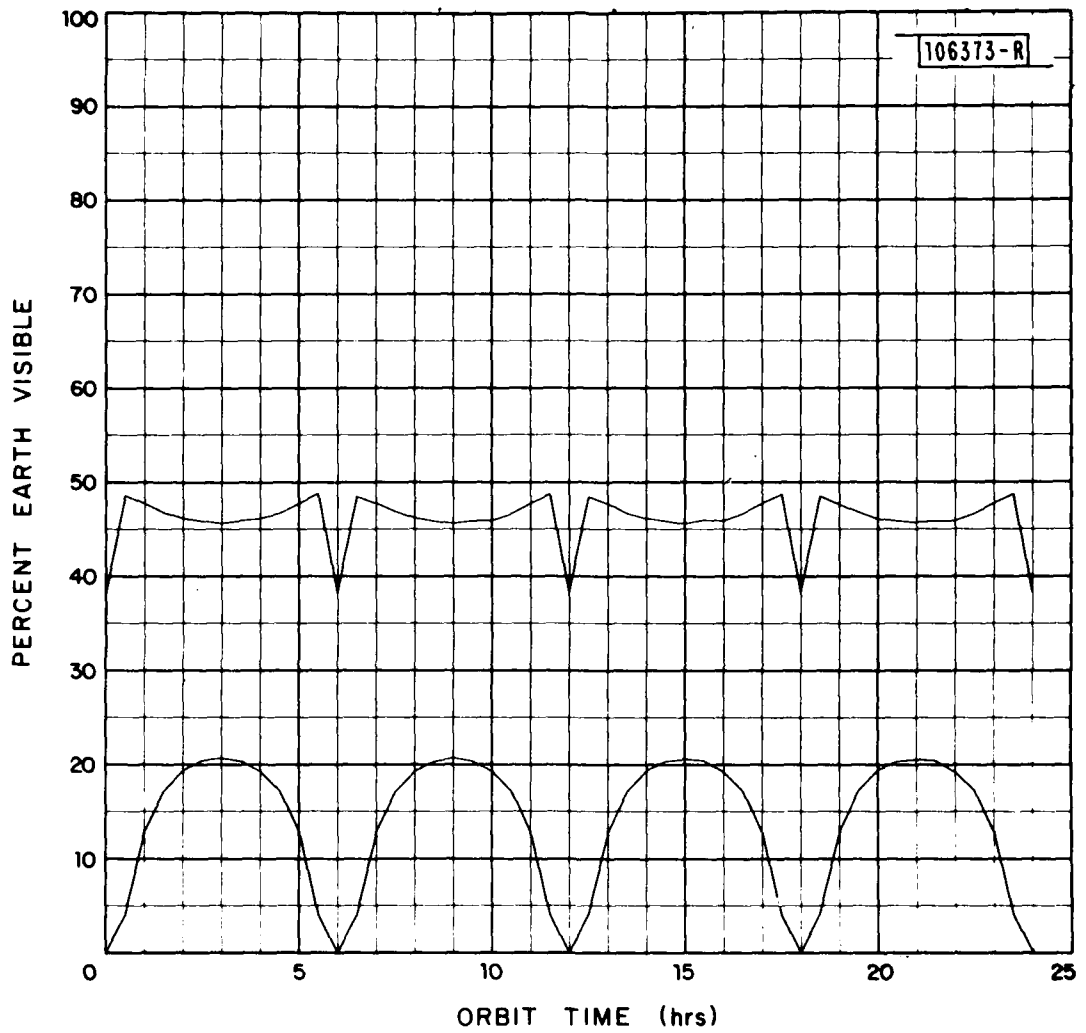


Fig. 6(a). Percent Earth coverage as a function of orbit time relative to perigee. Two satellites in critically inclined orbits; 12 hour periods; each satellite is phased by 6 hours with satellites in the same orbital plane. Top curve illustrates terminal visibility to one or more satellites; bottom curve is visibility to 2 or more satellites.

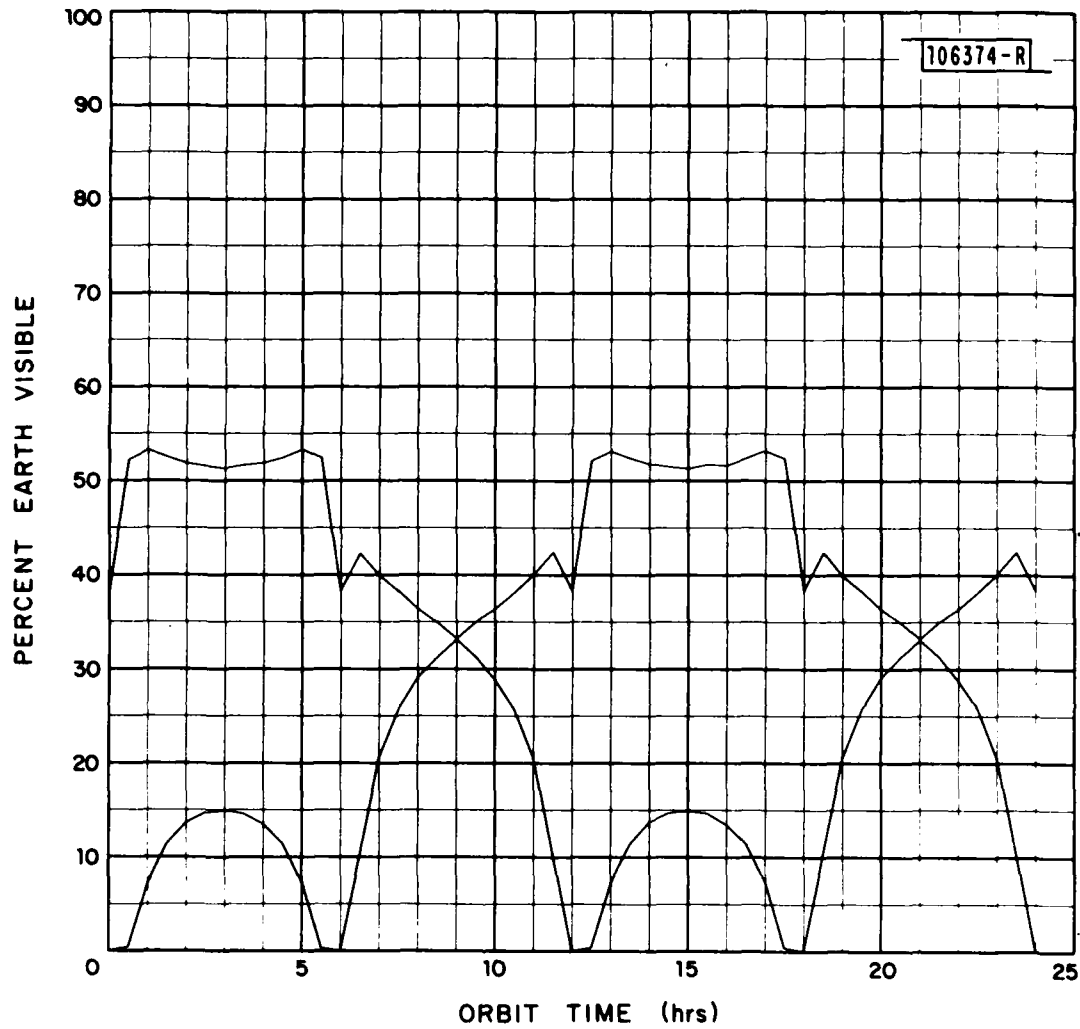


Fig. 6(b). Percent Earth coverage as a function of orbit time relative to perigee. Two satellites in critically inclined orbits; 12 hour periods; each satellite is phased by 6 hours with satellites in orthogonal orbital planes. Top curve illustrates terminal visibility to one or more satellites; bottom curve is visibility to 2 or more satellites. This case represents a configuration yielding identical ground tracks for the 2 satellites.

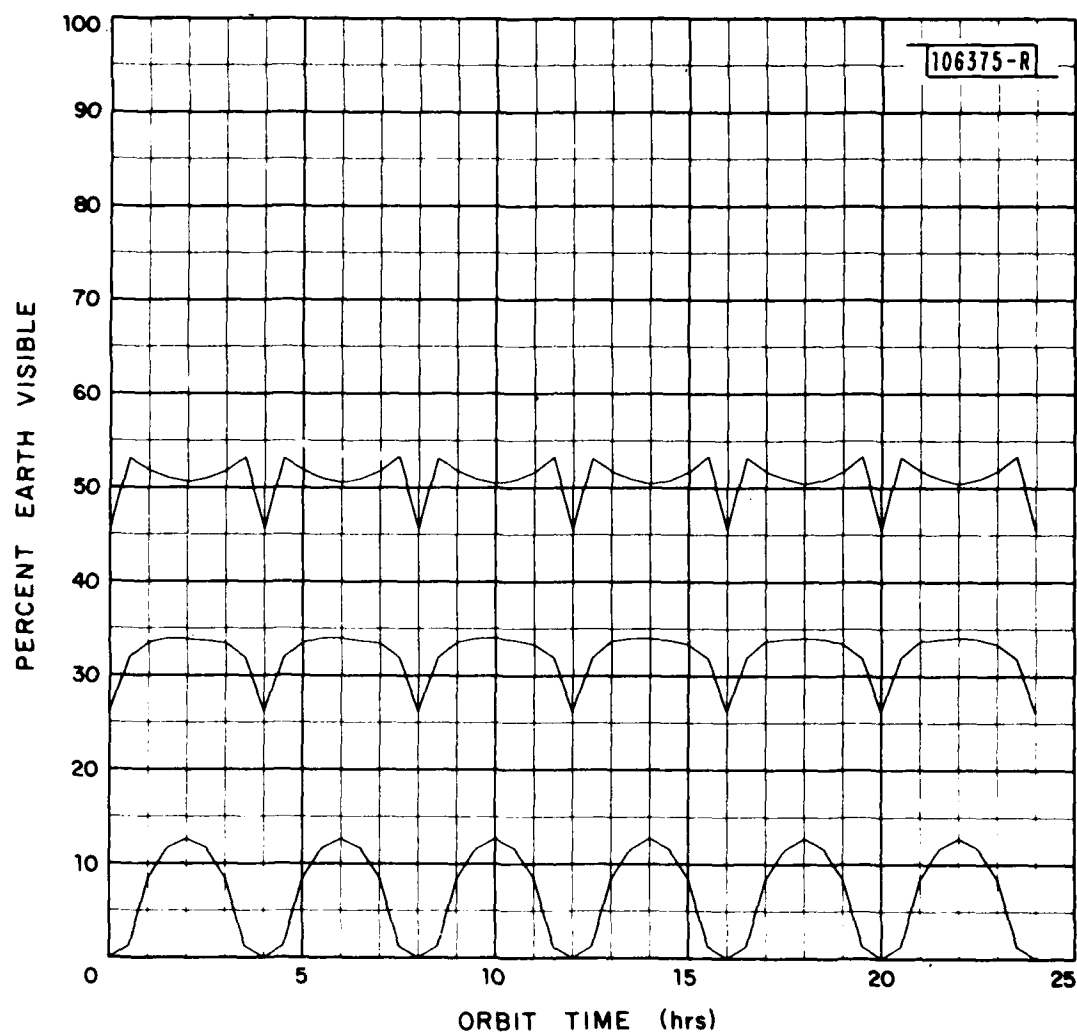


Fig. 6(c). Percent Earth coverage as a function of orbit time relative to perigee. Three satellites in critically inclined orbits; 12 hour periods; each satellite is phased by 4 hours with satellites in the same orbital plane. Top curve illustrates terminal visibility to one or more satellites; bottom curve is visibility to 3 or more satellites.

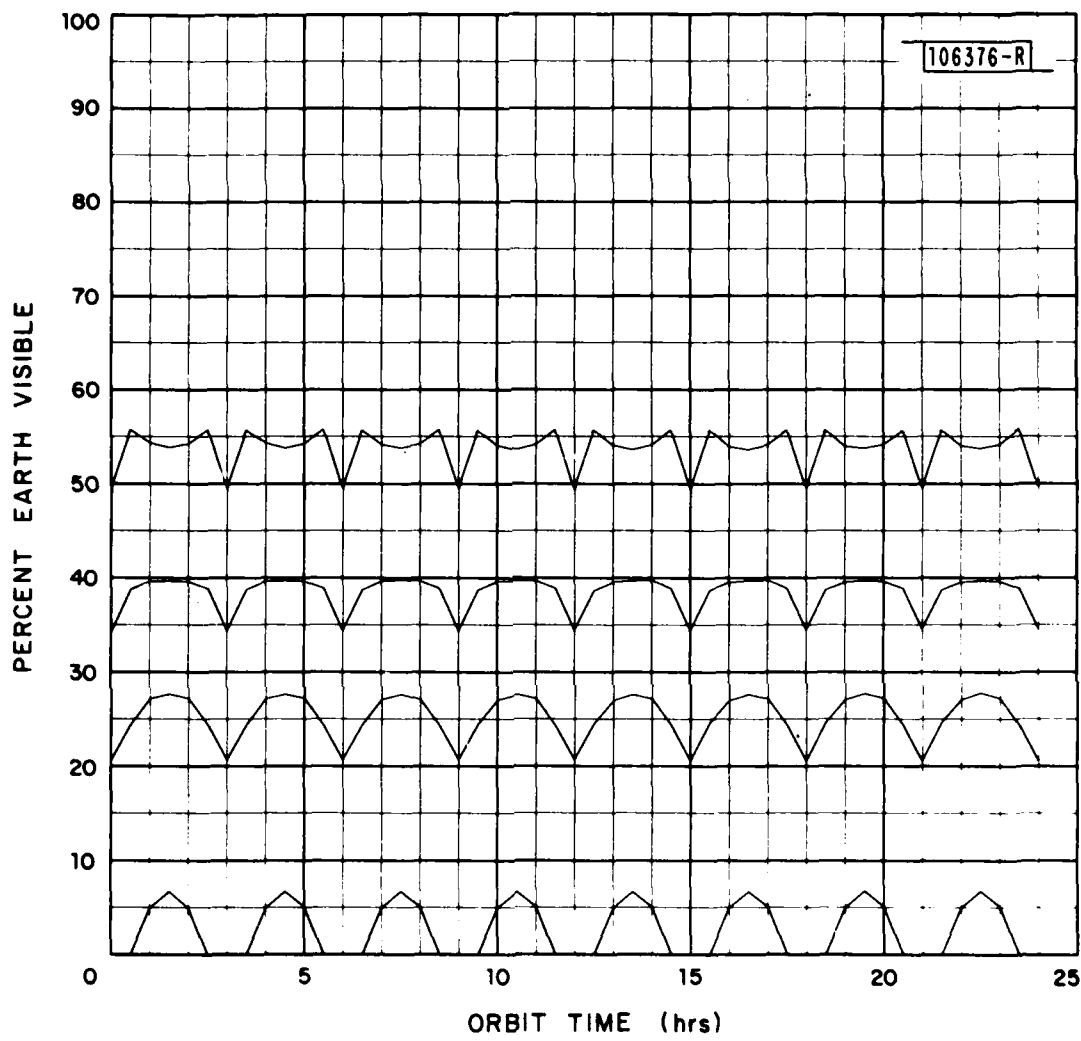


Fig. 6(d). Percent Earth coverage as a function of orbit time relative to perigee. Four satellites in critically inclined orbits; 12 hour periods; each satellite is phased by 3 hours with satellites in the same orbital plane. Top curve illustrates terminal visibility to one or more satellites; bottom curve is visibility to 4 or more satellites.

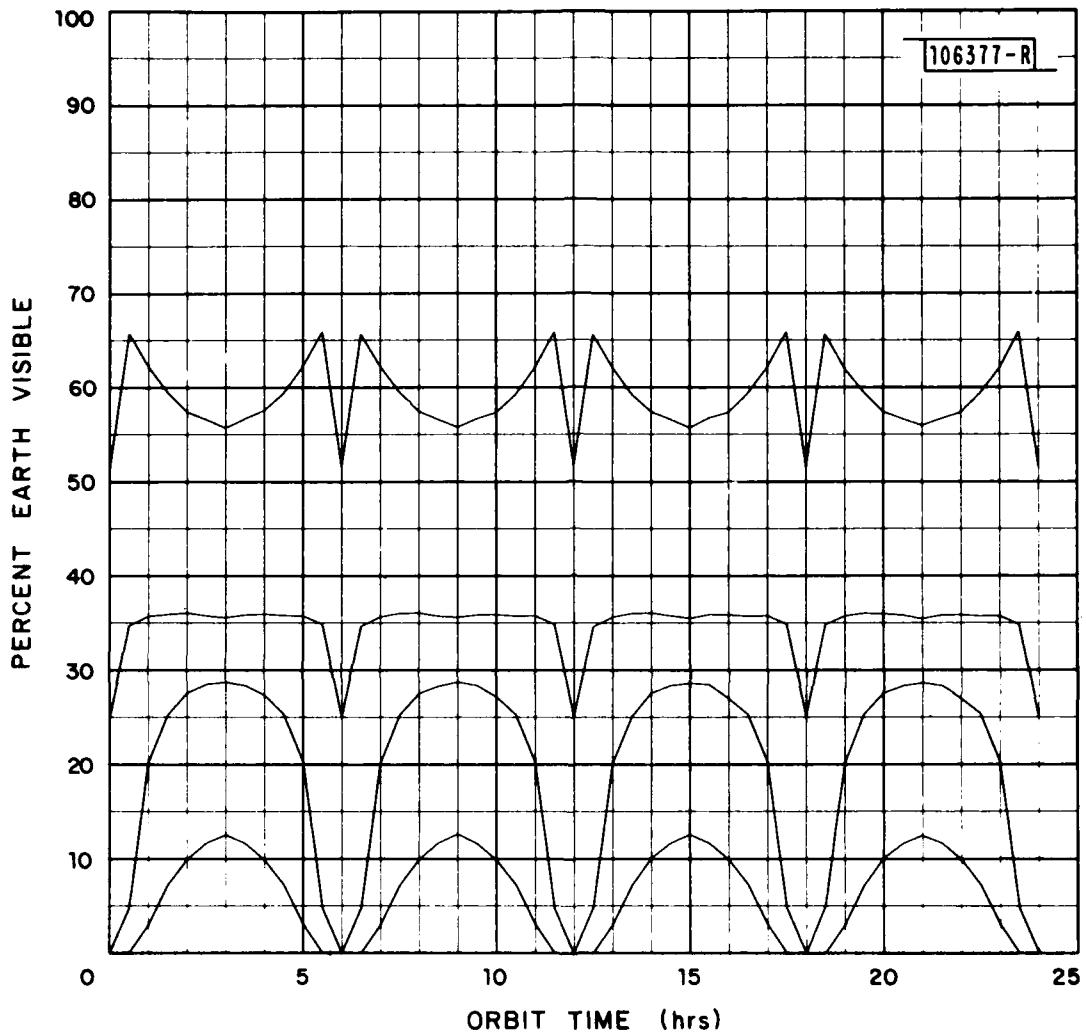


Fig. 6(e). Percent Earth coverage as a function of orbit time relative to perigee. Four satellites in critically inclined orbits; 12 hour periods; each satellite is phased by 6 hours with satellites in orthogonal orbital planes. This case represents a configuration of 2 identical ground tracks separated by 90° longitude. Top curve illustrates terminal visibility to one or more satellites; bottom curve is visibility to 4 or more satellites.

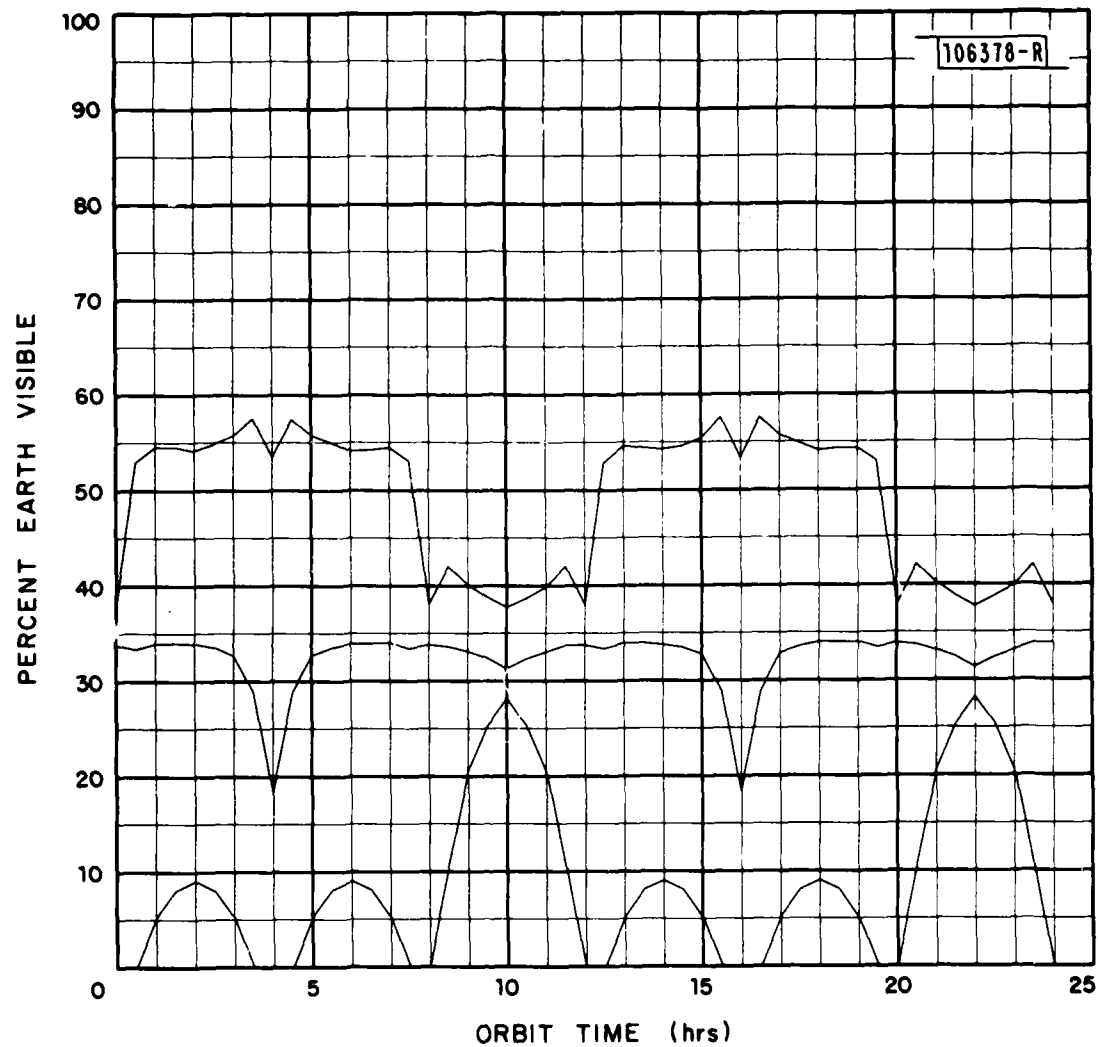


Fig. 6(f). Percent Earth coverage as a function of orbit time relative to perigee. Three satellites in critically inclined orbits; 12 hour periods; each satellite is phased by 4 hours with orbital planes separated by 60° . This case represents a configuration yielding identical ground tracks for the 3 satellites.

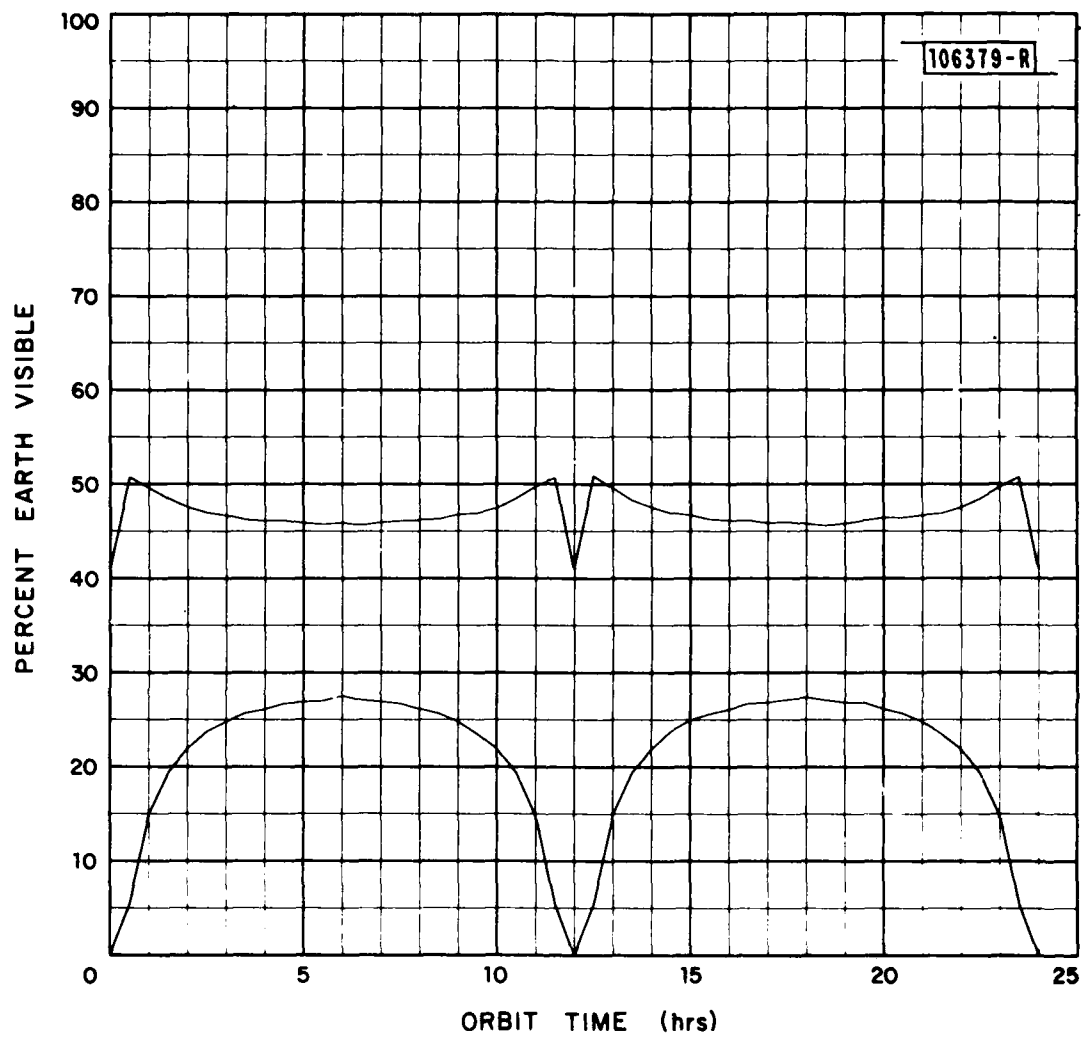


Fig. 7(a). Percent Earth coverage as a function of orbit time relative to perigee. Two satellites in critically inclined orbits; 24 hour periods; each satellite is phased by 12 hours with satellites in the same orbital plane. Top curve illustrates terminal visibility to one or more satellites; bottom curve is visibility to 2 or more satellites.

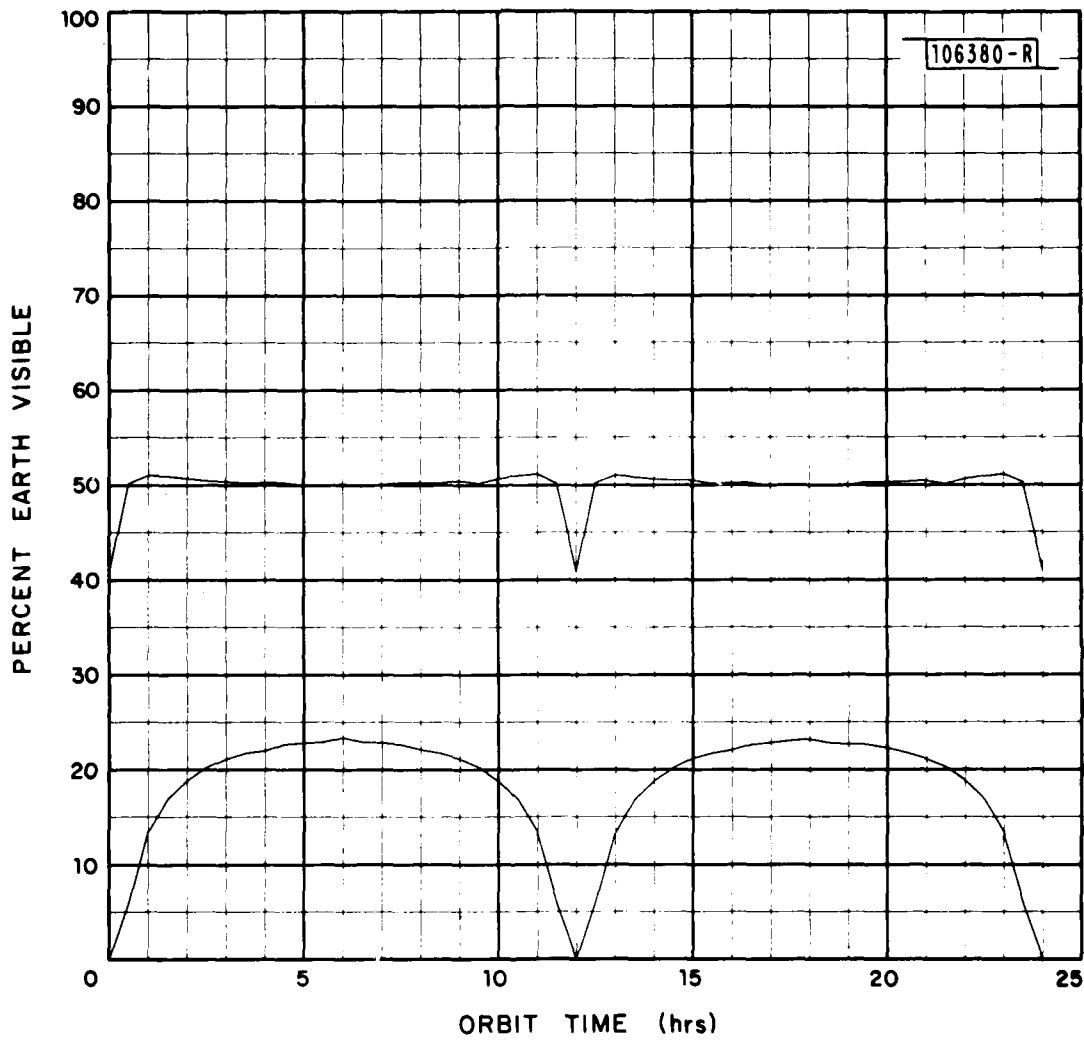


Fig. 7(b). Percent Earth coverage as a function of orbit time relative to perigee. Two satellites in critically inclined orbits; 24 hour periods; each satellite is phased by 12 hours with satellites in orbital planes 180° apart. This case represents a configuration yielding identical ground tracks for the satellites. Top curve illustrates terminal visibility to one or more satellites; bottom curve is visibility to 2 or more satellites.

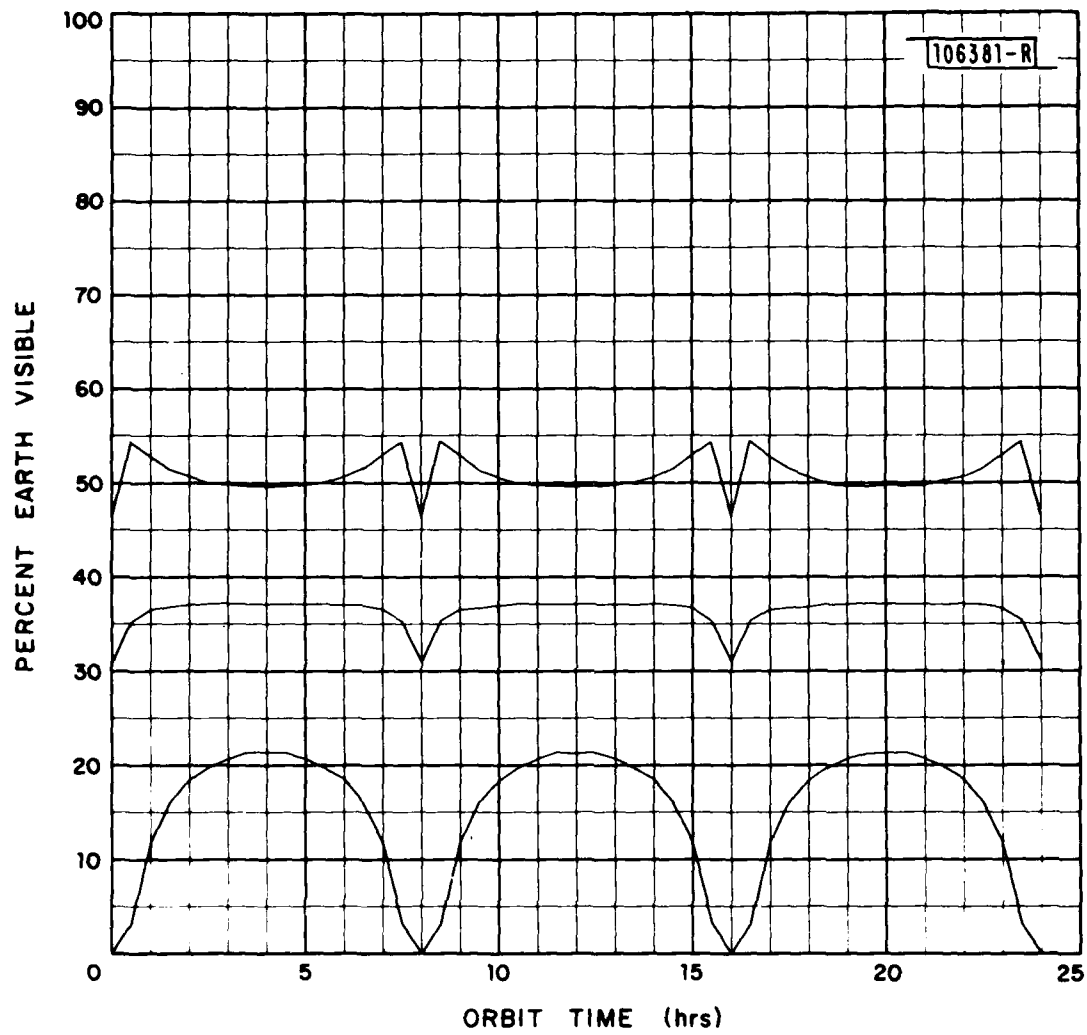


Fig. 7(c). Percent Earth coverage as a function of orbit time relative to perigee. Three satellites in critically inclined orbits; 24 hour periods; each satellite is phased by 8 hours with satellites in the same orbital plane. Top curve illustrates terminal visibility to one or more satellites; bottom curve is visibility to 3 or more satellites.

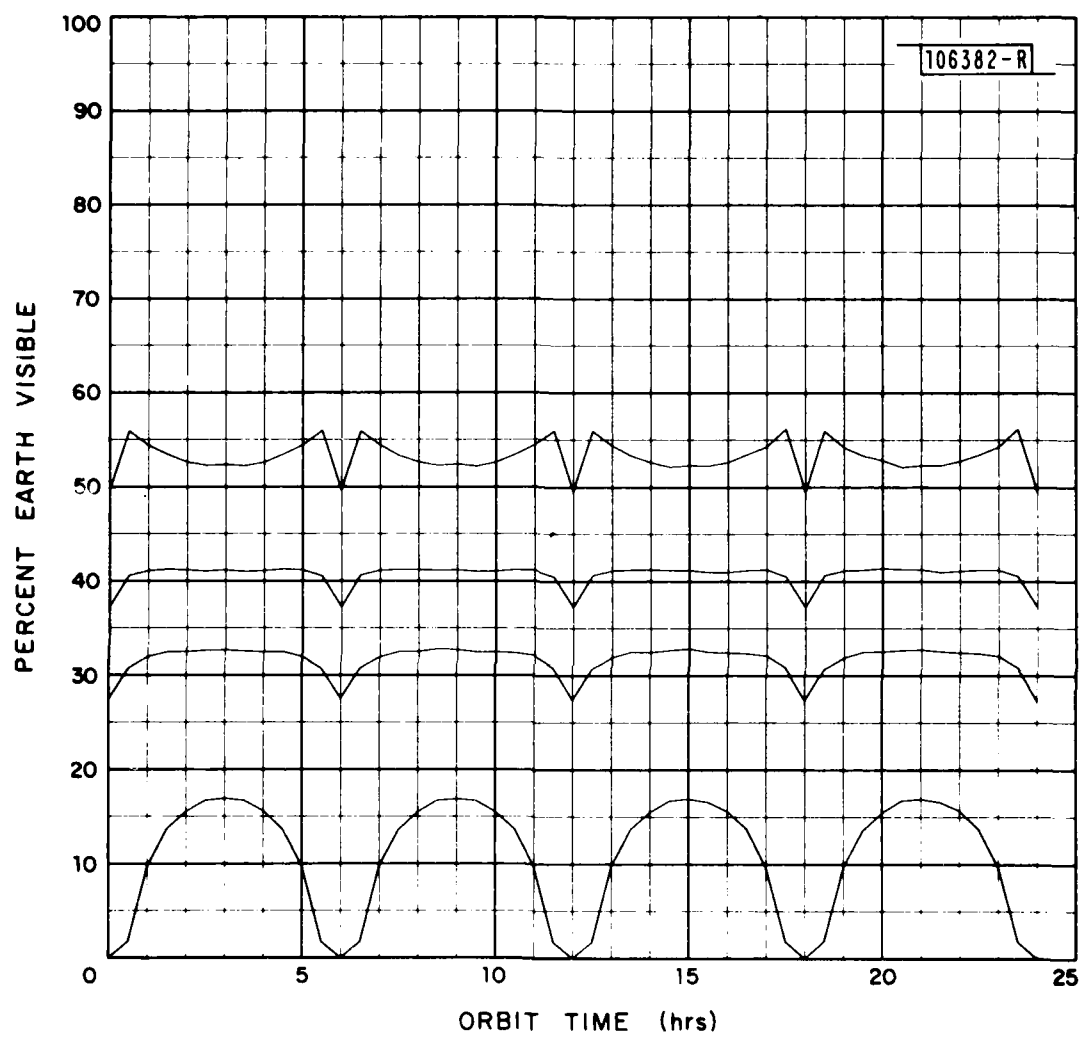


Fig. 7(d). Percent Earth coverage as a function of orbit time relative to perigee. Three satellites in critically inclined orbits; 24 hour periods; each satellite is phased by 6 hours with satellites in the same orbital plane. Top curve illustrates terminal visibility to one or more satellites; bottom curve is visibility to 4 or more satellites.

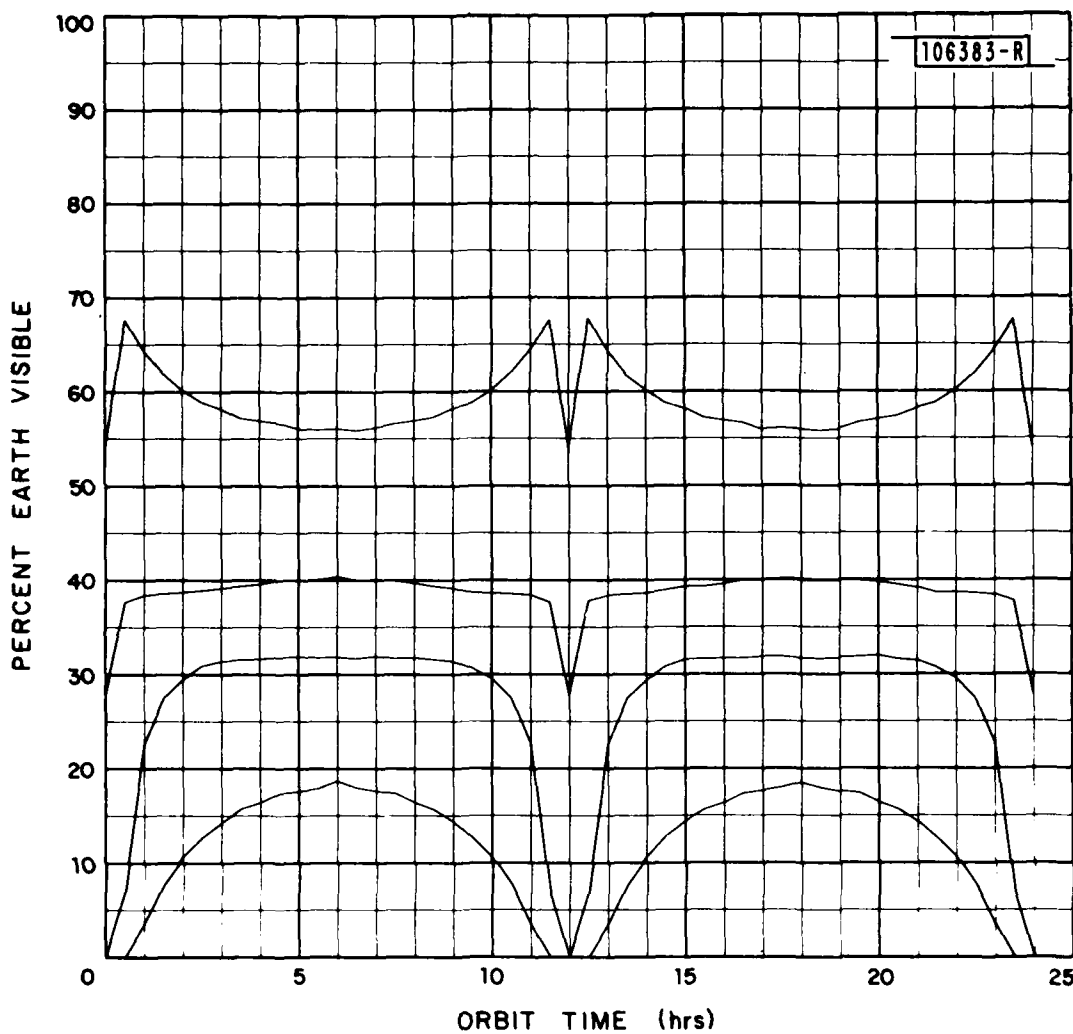


Fig. 7(e). Percent Earth coverage as a function of orbit time relative to perigee. Four satellites in critically inclined orbits; 24 hour periods; each satellite is phased by 12 hours with satellites in orthogonal orbital planes. Top curve illustrates terminal visibility to one or more satellites; bottom curve is visibility to 4 or more satellites.

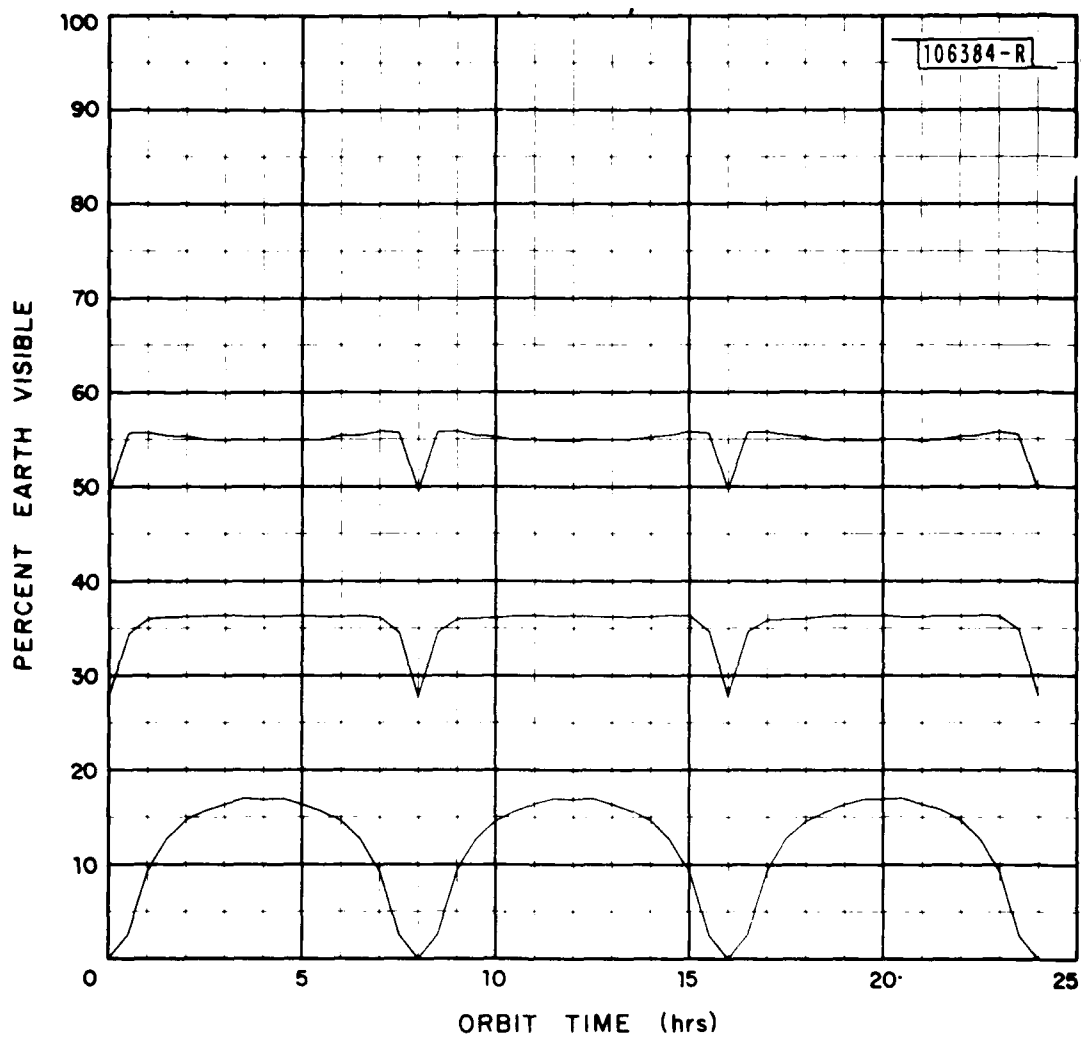


Fig. 7(f). Percent Earth coverage as a function of orbit time relative to perigee. Three satellites in critically inclined orbits; 24 hour periods; each satellite is phased by 8 hours with orbital planes separated by 120° . This case represents a configuration yielding identical ground tracks for the 3 satellites.

($M=1,2,\dots,N$) by taking the difference between the curve for M satellites and the curve for $(M-1)$ satellites. This procedure is analogous to the one described for Fig. 2 in part A of this section.

As alluded to earlier, there are several possible constellations of satellites in exclusively critically inclined orbits for which approximately full geometric Earth coverage (to the assumed 10° minimum terminal elevation angle) is available 24 hours per day. (Complete Earth coverage is achieved by doubling the constellations listed below to provide for second hemisphere coverage.) Those constellations are summarized as follows:

Fig. 6(d): 12 hour period; 4 satellites; identical orbital plane with perigees phased by 3 hours successively (i.e., 4 different ground tracks)

Fig. 6(e): 12 hour period; 4 satellites; 2 orthogonal orbital planes with perigees phased by 6 hours (i.e., 2 identical ground tracks separated by 90° longitude)

Fig. 7(d): 24 hour period; 4 satellites; identical orbital plane with perigees phased by 6 hours successively (i.e., 4 different ground tracks)

Fig. 7(e): 24 hour period; 4 satellites; 2 orthogonal orbital planes with perigees phased by 12 hours (i.e., 4 different ground tracks)

Fig. 7(f): 24 hour period; 3 satellites; 3 orbital planes separated by 120° longitude with perigees phased by 8 hours (i.e., a single identical ground track)

Examination of the computed ephemeris (which yields the ground track when projected on the Earth) for the 2 satellite identical ground track (Figs. 6(b) and 7(b)) cases shows that there is one point in the ephemeris pair where hand-off from a descending satellite to an ascending satellite is easily accomplished because both satellites are very close to one another. There is a small operational advantage (which occurs on every second handoff in the 2 satellite configuration), in terms of ground station antenna slewing requirements. However, since the operational advantage does not occur for all handoffs, it does not appear to be of significant value in considering system trade-offs.

It is recognized that other factors than those addressed in this section may also pose important considerations in the selection of a particular orbit configuration for a particular application. Examples of such added considerations include visibility to one or more specified ground stations, maximization of continuous (24 hr) coverage to some specified area of interest (e.g., the northern hemisphere), etc. The plots given in this section provide an added dimension by portraying the sensitivity or variation in visibility to multiple satellites. Specifically, the 4 satellite configurations considered in Figs. 6(d) and 7(d) show consistently high values of percent visibility to at least 2 satellites through an entire 24 hour cycle. The results provided in this section are intended for use in conjunction with other published orbital coverage data^{6,7} in selecting suitable orbital parameters for a specific application.

D. Critically Inclined Orbit: Weather Factor Included

The primary purpose in considering critically inclined orbits in the context of this report was to determine the possibility, from the geometric point of view, of accomplishing total Earth coverage using a constellation of satellites exclusively in critically inclined orbits. That question was affirmatively answered in the last section for five different constellations.

As an adjunct to the geostationary orbit coverage analysis including weather effects, a set of selected cases of satellite positions in 12 and 24 hour period critically inclined orbits was treated. The specific orbital/position data of the cases tested are given in Table II. The orbital times selected before and after apogee represent approximate limits to the usable portions of each orbit. The data is presented as conventional shaded contour plots for a 14 dB value of link margin and 0.99 availability on Mercator grid maps in Figs. 8 through 13. All plots are performed for apogees over the Northern Hemisphere. Based on an estimation of the Earth area below 0.99 availability on these maps, it is highly unlikely that constellations consisting exclusively of satellites in critically inclined orbits can achieve total Earth coverage at a 0.99 value of link availability.

TABLE II
CRITICALLY INCLINED ORBITS: PERIOD AND ORBITAL POSITION DATA*

<u>Figure No.</u>	<u>Period (hrs.)</u>	<u>Orbital Position (hrs. relative to apogee)</u>
8	12	T_A^{-4}
9	12	T_A
10	12	T_A^{+2}
11	24	T_A^{-4}
12	24	T_A
13	24	T_A^{+8}

*Margin = 14 dB and Availability = 0.99 for all cases

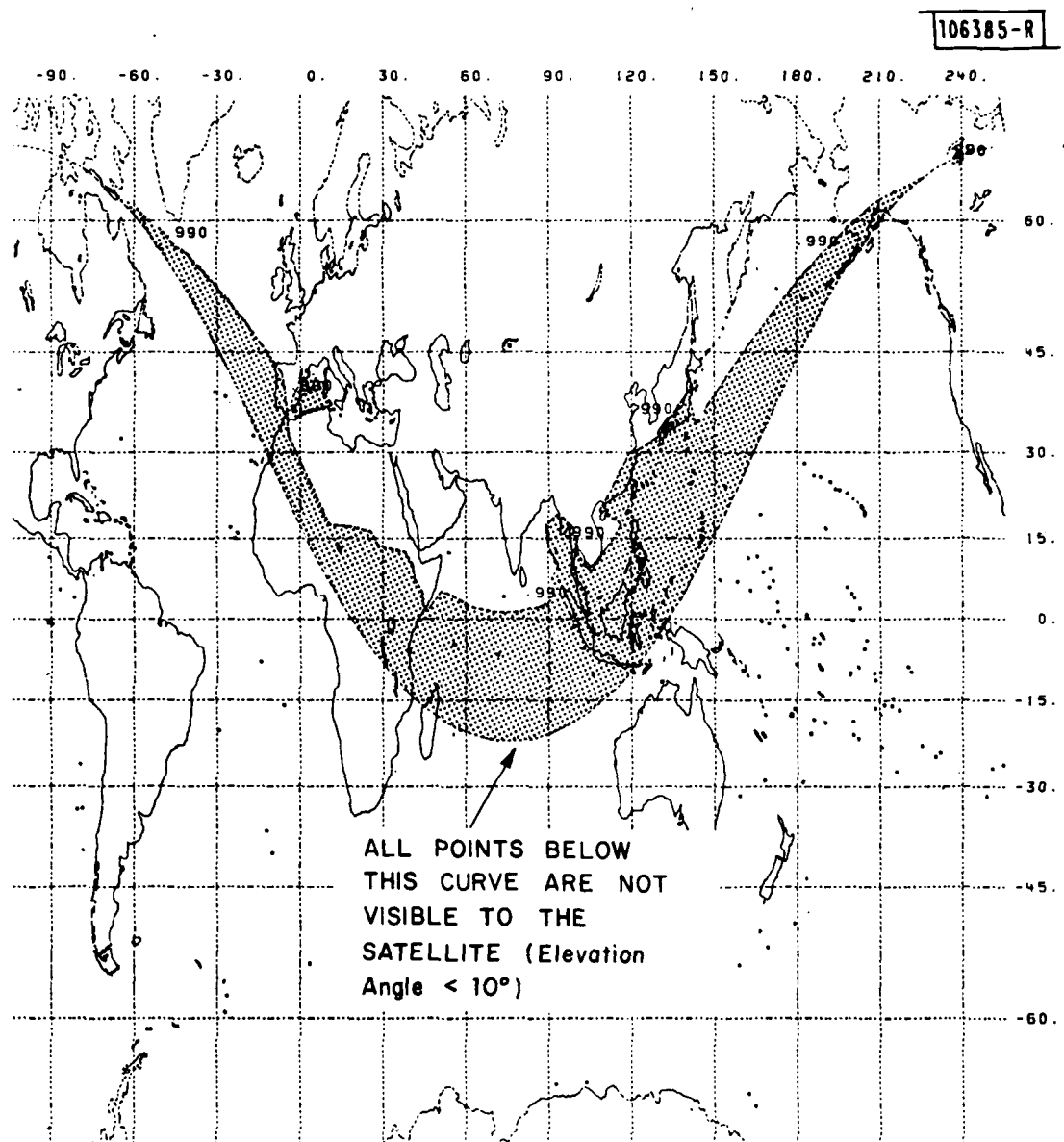


Fig. 8. Northern Hemisphere coverage for 0.99 link availability:
14 dB link margin at 44 GHz. Critically inclined orbit with 12 hour
period. 4 hours before apogee: 45.7N, 76.0E; $3.72 \times R_e$ altitude.

106386-R

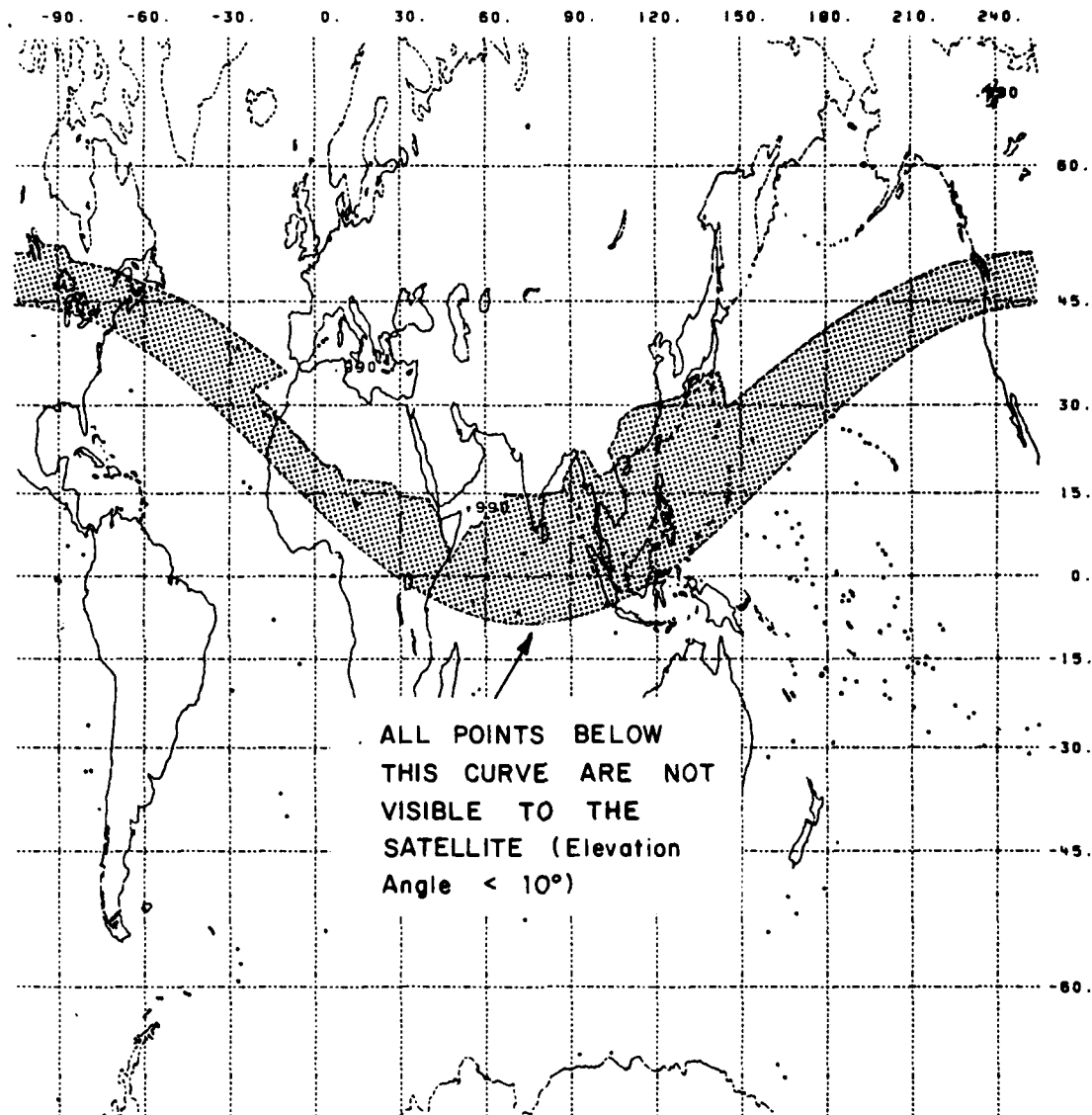


Fig. 9. Northern Hemisphere coverage for 0.99 link availability:
14 dB link margin at 44 GHz. Critically inclined orbit with 12 hour
period. Apogee: 63.4N, 75.0E; $6.16 \times R_E$ altitude.

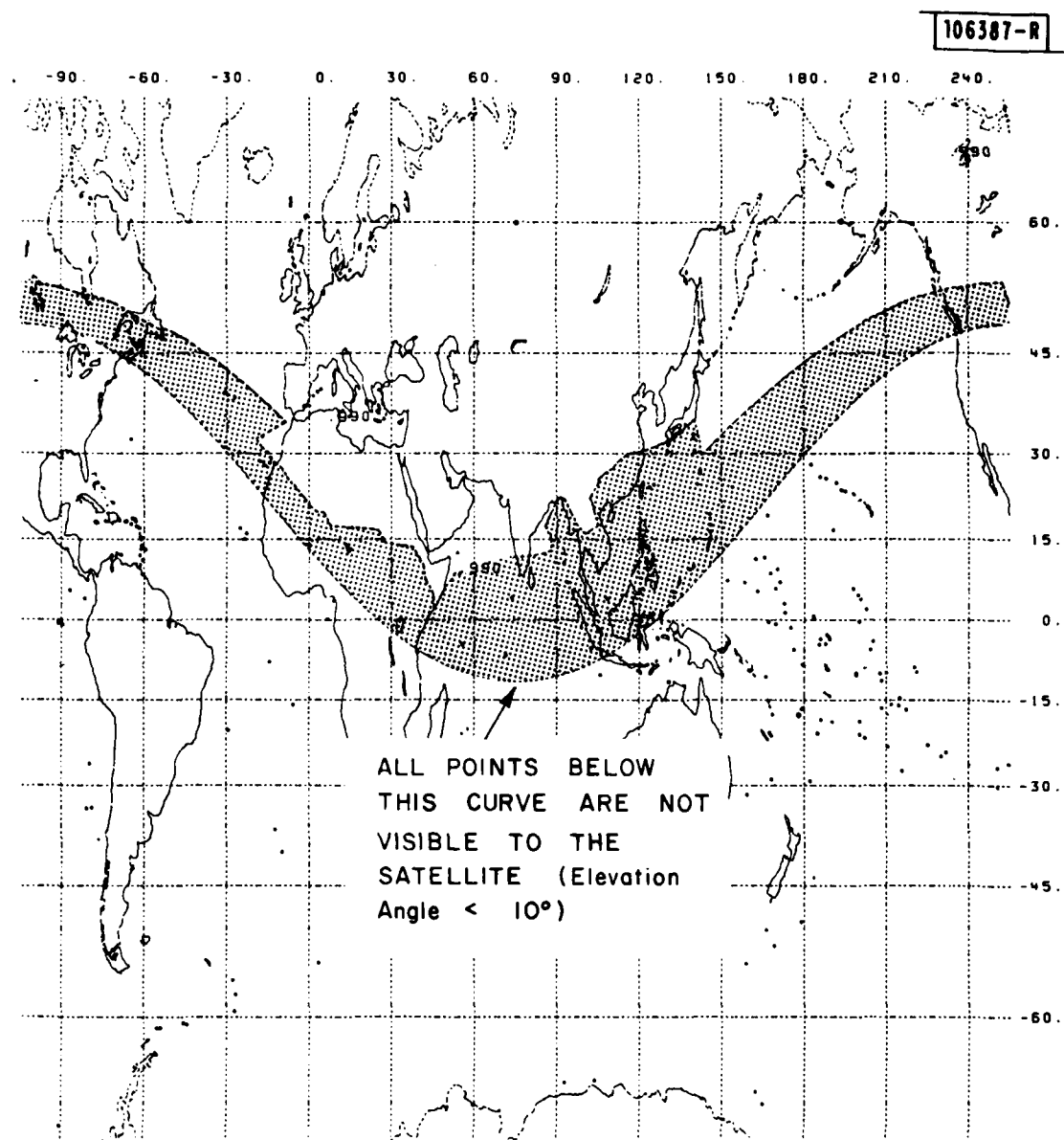


Fig. 10. Northern Hemisphere coverage for 0.99 link availability:
14 dB link margin at 44 GHz. Critically inclined orbit with 12 hour
period. 2 hours after apogee: 59.9N, 75.5E; $5.6 \times R_E$ altitude.

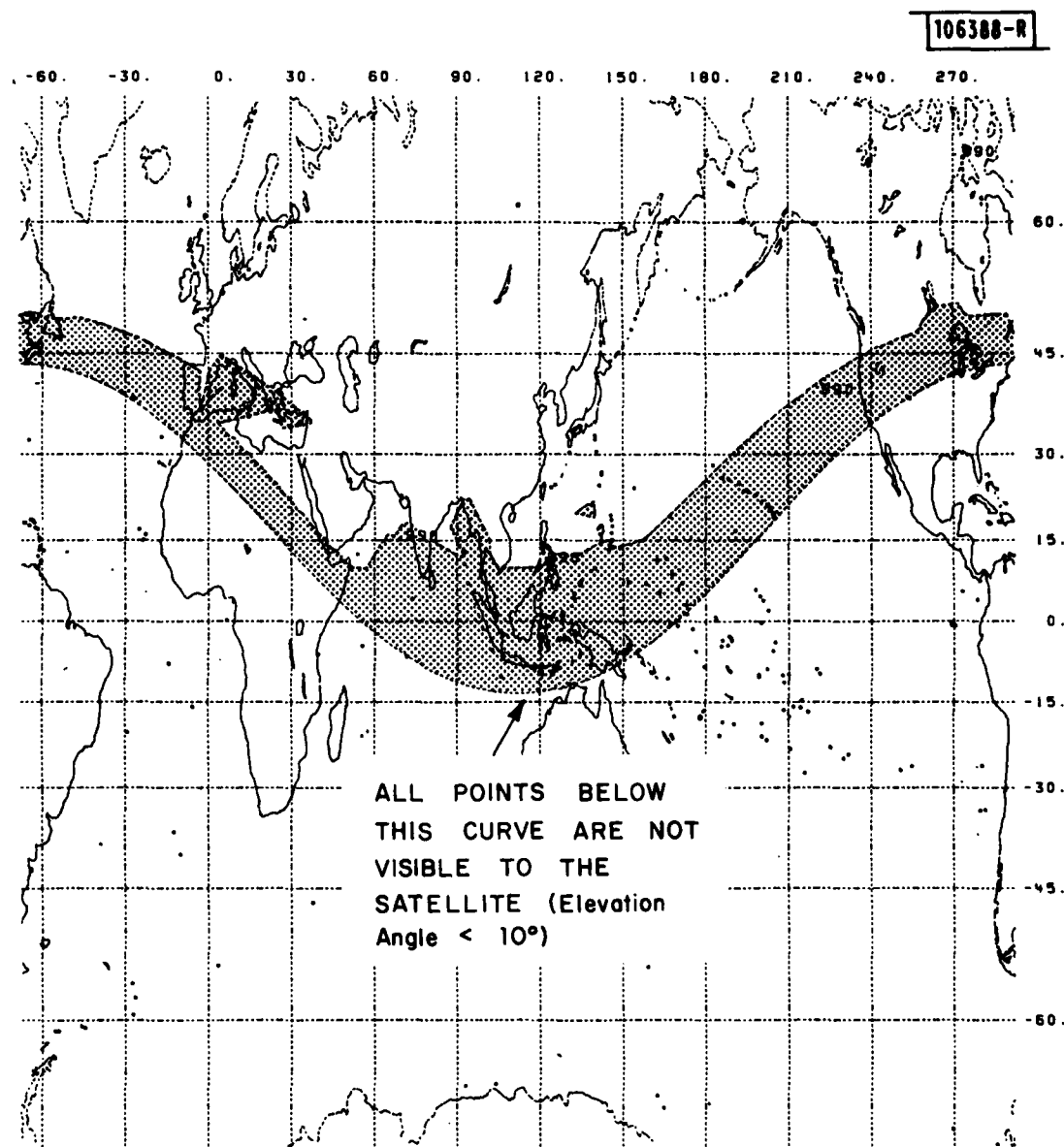


Fig. 11. Northern Hemisphere coverage for 0.99 link availability:
14 dB link margin at 44 GHz. Critically inclined orbit with 24 hour
period. 4 hours before apogee: 61.5N, 112.2E; 10.13°Re altitude.

106389-R

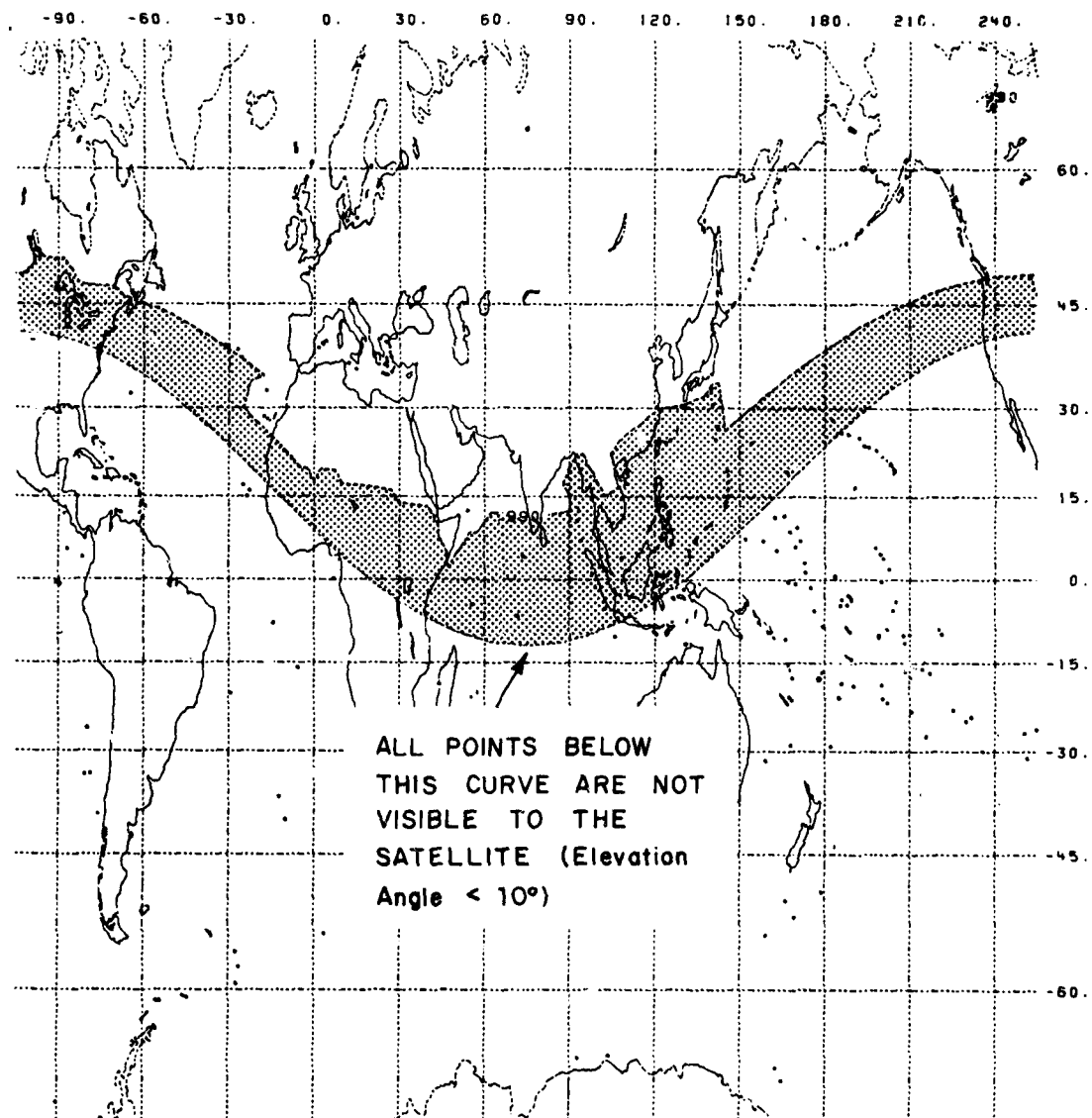


Fig. 12. Northern Hemisphere coverage for 0.99 link availability:
14 dB link margin at 44 GHz. Critically inclined orbit with 24 hour
period. Apogee: 63.4N, 75.0E; $11.05 \times R_E$ altitude.

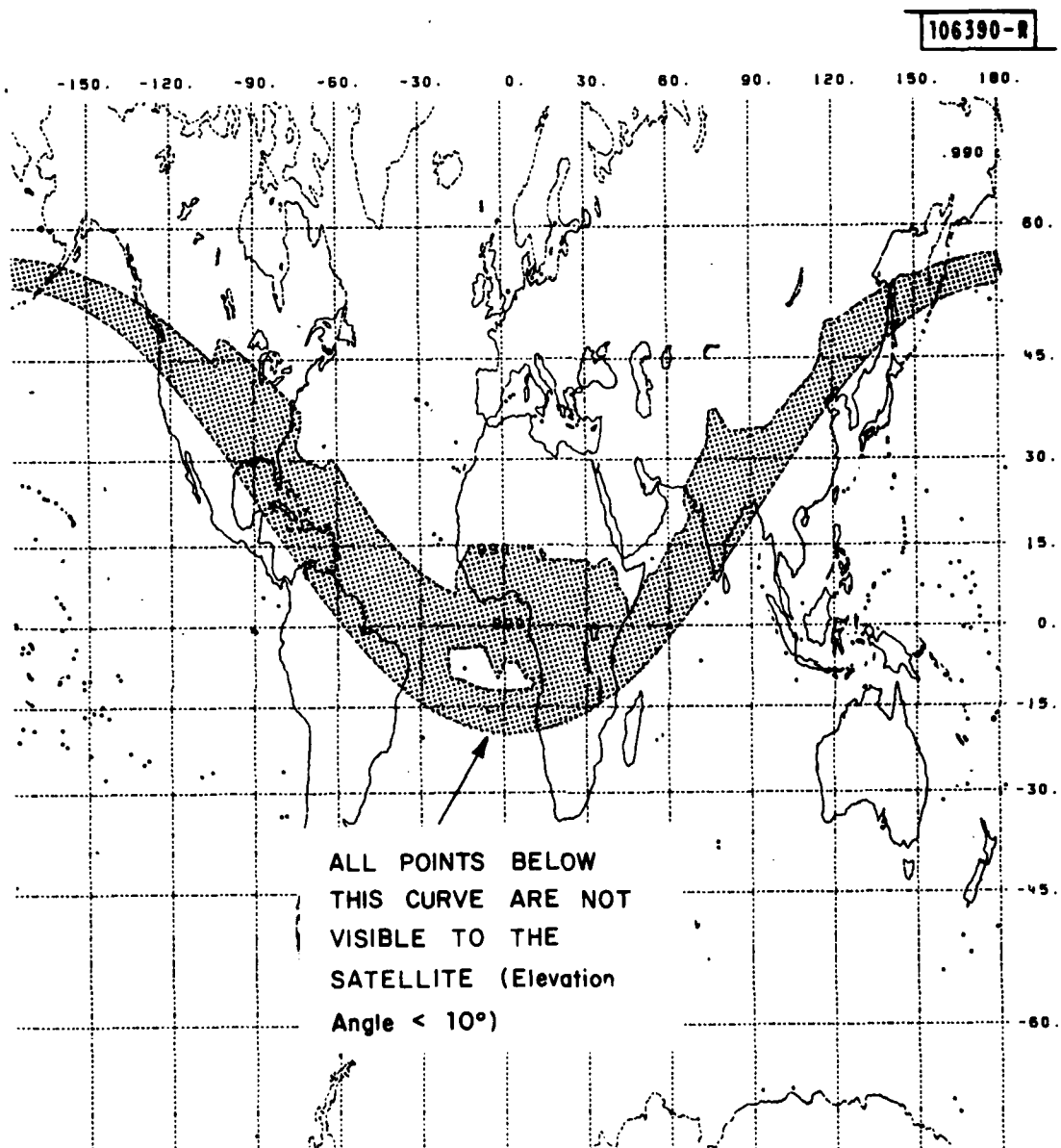


Fig. 13. Northern Hemisphere coverage for 0.99 link availability:
14 dB link margin at 44 GHz. Critically inclined orbit with 24 hour
period. 8 hours after apogee: 53.2N, 2.8E; $7.06 \times R_e$ altitude.

E. Relationship of Earth Coverage to Link Margin for Geostationary Orbit

The plots of Earth coverage vs link availability given in Figs. 3, 4, and 5 of Section II B are useful for examining the sensitivity of the Earth coverage - availability relationship, i.e., the partial derivative functions for fixed values of either Earth coverage or link availability as a function of the margin parameter. While they are helpful in that right, they do pose fundamental limitations of use to the MILSATCOM system designer in that the independent variable (availability) is usually interpreted and used as an "objective" or resultant parameter rather than a design parameter. The computed coverage data for the geostationary satellite constellations including the weather factor were replotted for a fixed number (3, 4, and 5) of equi-spaced geostationary satellites in a constellation and a fixed frequency (44 GHz) treating link margin as the independent variable and link availability as a parameter of the problem. Those plots, given in Figs. 14, 15 and 16 are more representative of the analytic sequence (i.e., accounting for the resources available, stating a level of efficiency desired, determining the resultant or output function) used by a systems designer. The range of values of link margin used (6 dB to 18 dB) and the range of the availability parameter are representative of values used in current MILSATCOM operational studies being performed at Lincoln Laboratory. These curves now provide the MILSATCOM system designer with a complete set of data to assess the classic trade-off problem of Earth coverage vs link margin vs availability vs number of satellites. The problem of applying linear programming techniques to this multivariable data to solve for an optimum operational configuration (i.e., in the sense of simultaneously achieving a relative maximum for Earth coverage, relative maximum for availability, relative minimum for margin and relative minimum for the number of satellites) will be addressed as a task subsequent to this report. It is recognized before such an analysis is even begun that the outcome may yield an optimum configuration which may violate physical operational requirements or limitations. The ability to impose initial constraints (e.g., a minimum acceptable Earth coverage factor, or a maximum achievable margin value) will be a requirement of such an analysis.

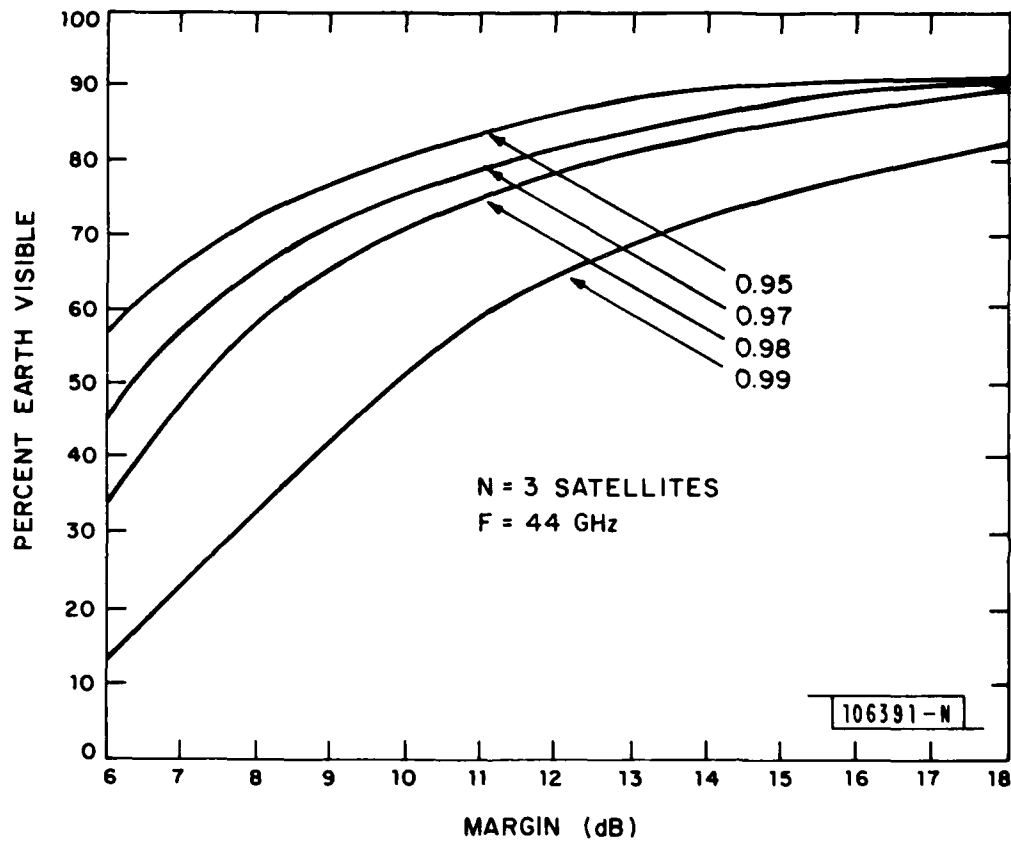


Fig. 14. Earth coverage as a function of link margin for parametric values of link availability. A constellation of 3 equi-spaced geostationary satellites and an operating frequency of 44 GHz are assumed.

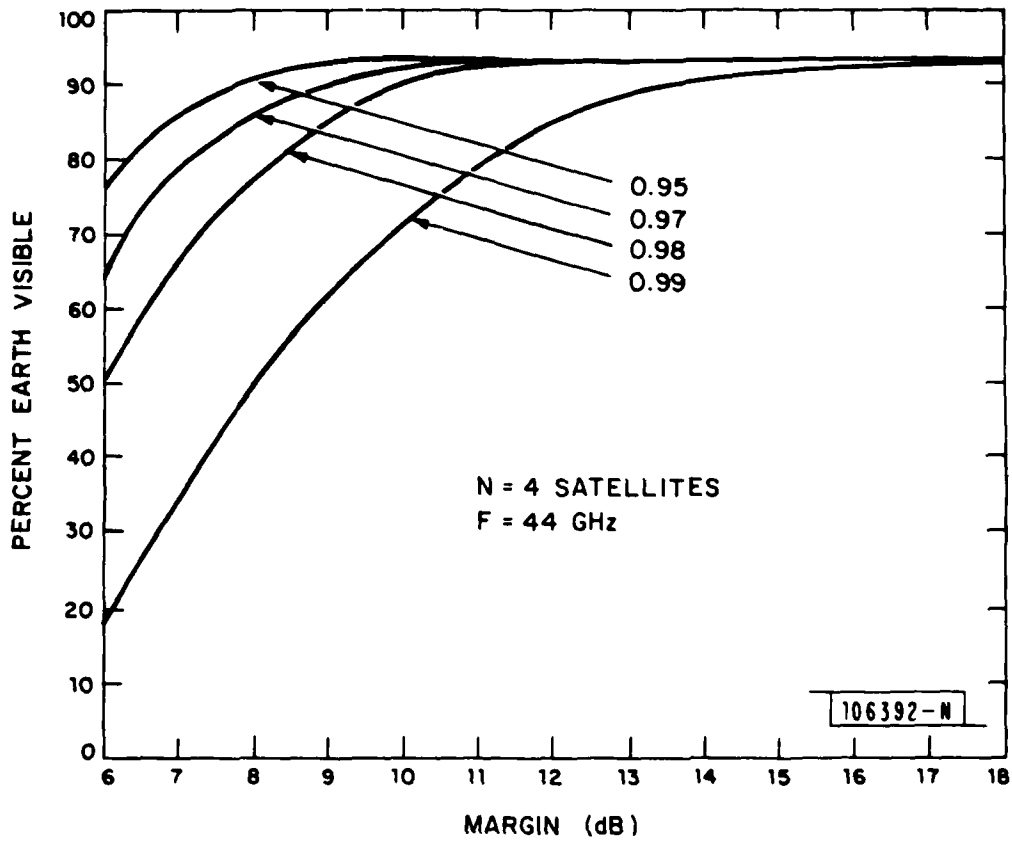


Fig. 15. Earth coverage as a function of link margin for parametric values of link availability. A constellation of 4 equi-spaced geostationary satellites and an operating frequency of 44 GHz are assumed.

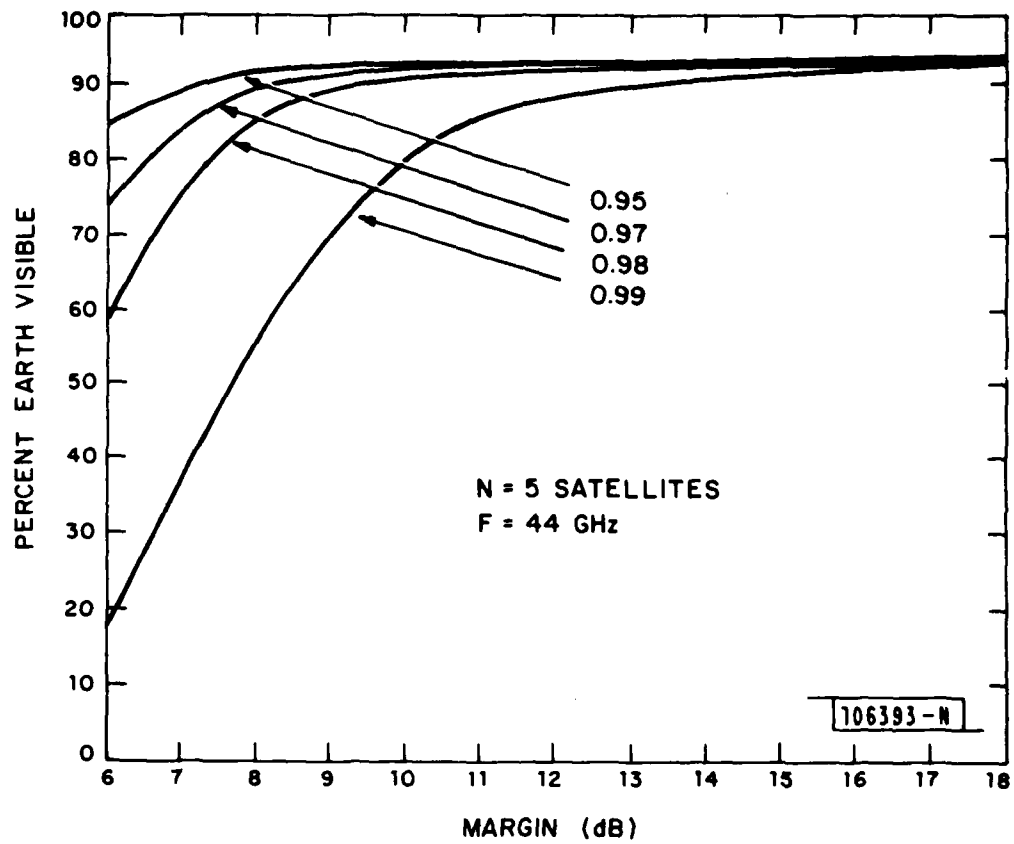


Fig. 16. Earth coverage as a function of link margin for parametric values of link availability. A constellation of 5 equi-spaced geostationary satellites at an operating frequency of 44 GHz are assumed.

III. LINK AVAILABILITY COVERAGE PROFILE MAPS

The percent Earth coverage plots given in Section II(B) provide numerically integrated values describing the relationship of coverage vs availability for a fixed margin or coverage vs margin for a fixed availability. However, those plots lend no insight to the MILSATCOM systems planner or designer in determining specific geographic areas which may have chronic weather-related system outage problems. For this important reason, the underlying software data used in the integration step was preserved and is provided here as coverage profiles of link availability plotted on Mercator maps.

The straight line boundaries of constant longitude between the equi-spaced satellites were determined from the relation of Eqn. (3)

$$\lambda_{\text{boundary}} = [\lambda_{\text{subpoint}} \pm \frac{360^\circ}{2 \cdot \text{No. of satellites}}] \quad (3)$$

This geometric relation has the effect of simply truncating the visible area of any given satellite at the average of the longitude values of adjacent satellite pairs. The technique could also be straightforwardly extended for unequally spaced subsatellite points yielding truncated visible areas of variable width. (The scope of this report does not include unequally spaced satellite constellations.)

With equally spaced satellites the geometric distance from adjacent satellites to the common visible area boundary is the same at any given value of latitude. Hence, it can be directly shown that, for equal (or isotropic) antenna patterns on both equi-spaced satellites, the contour plots of constant link availability must join at the boundary. Previous reports^{2,8} have presented multiple levels of availability contours for a single satellite operating at fixed frequency with a fixed link margin. For the sake of clarity, the multi-satellite coverage areas ("profiles") plotted in Figs. 17-34 are done for a single value of link availability each. The shaded areas shown in each figure represent Earth areas for which the link

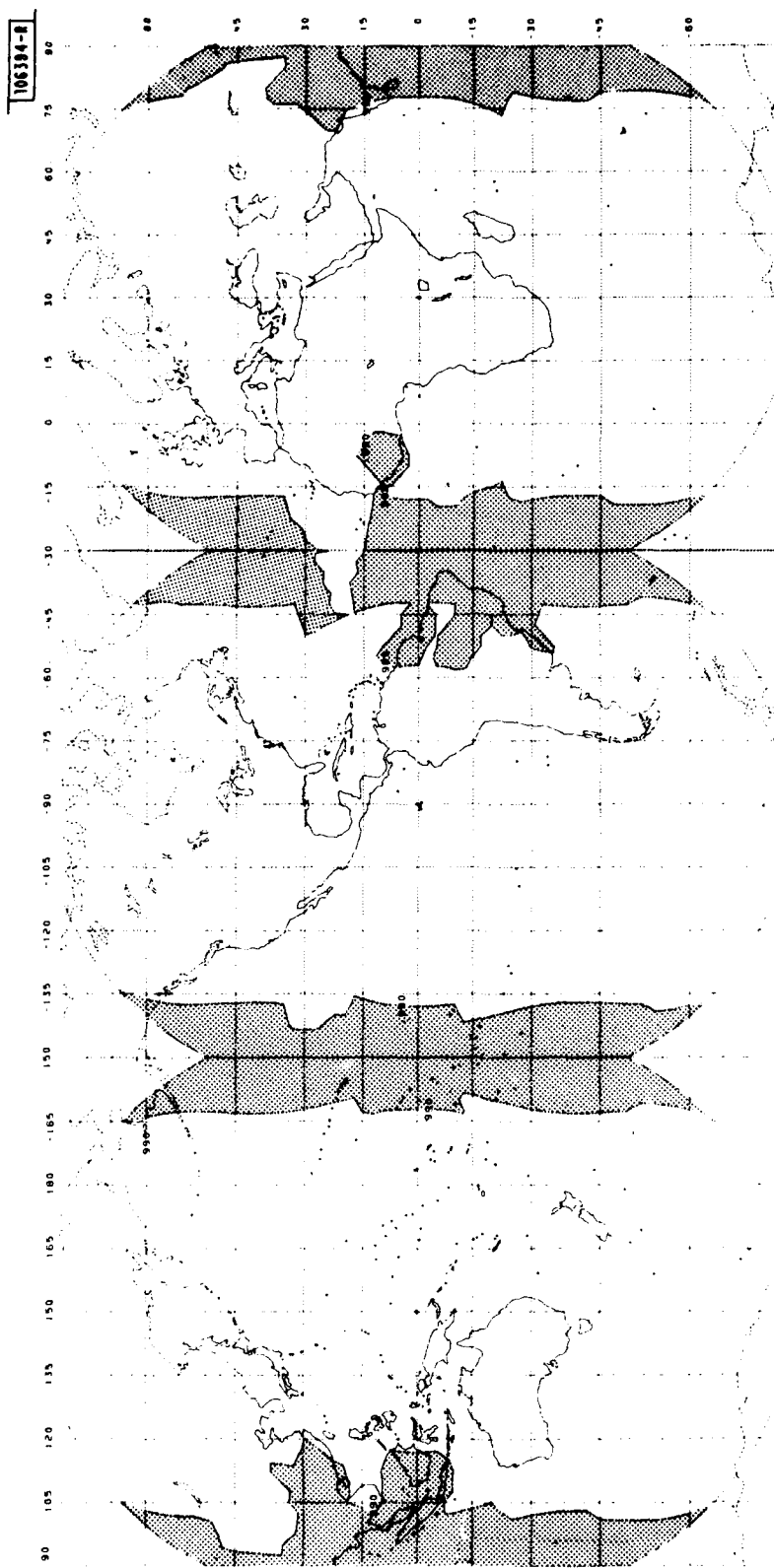


Fig. 17. Coverage area (unshaded) for 0.99 link availability for a constellation of 3 equispaced geostationary satellites. Operating frequency is 44 GHz and link margin equals 14 dB.

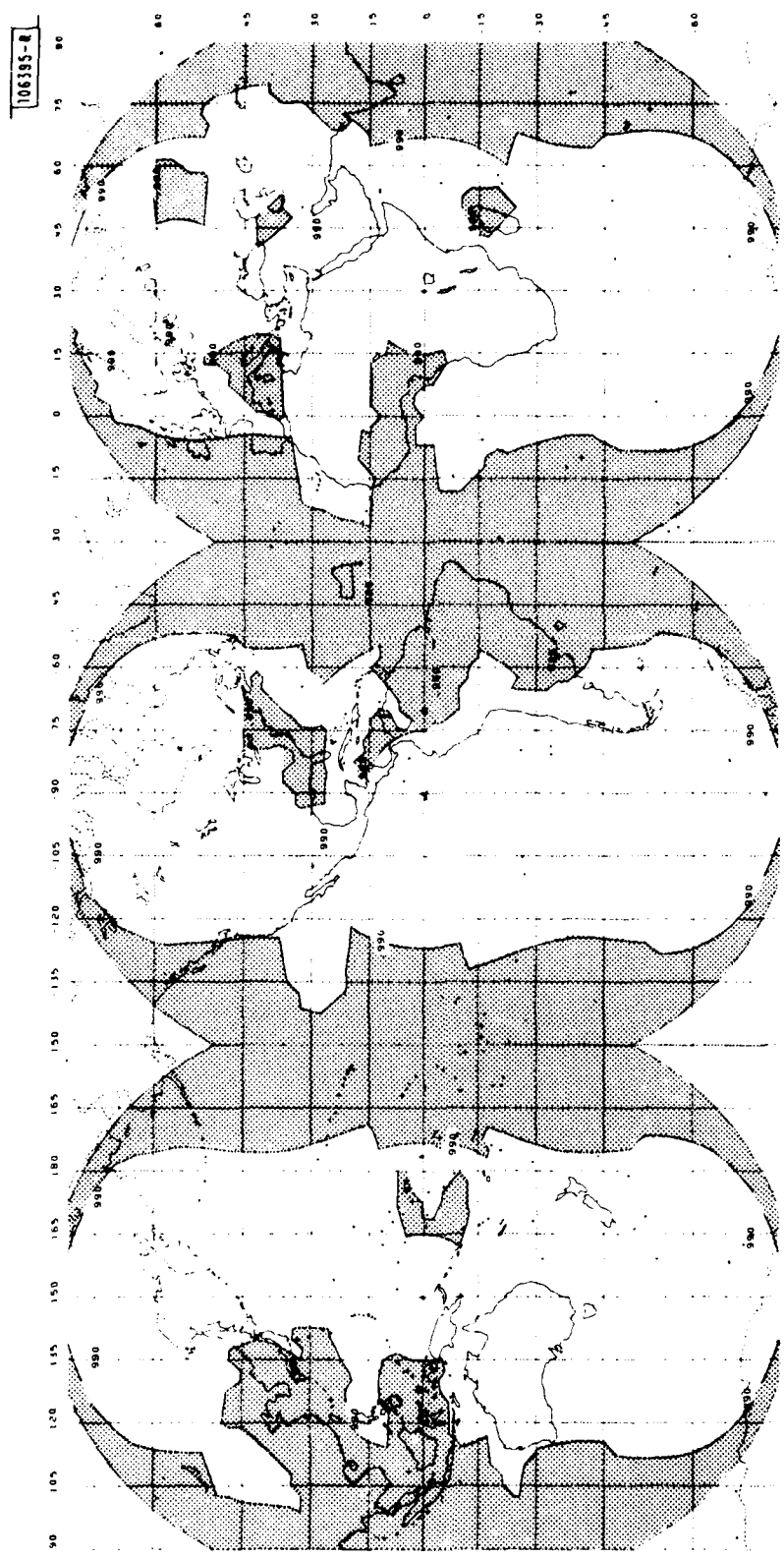


Fig. 18. Coverage area (unshaded) for 0.99 link availability for a constellation of 3 equi-spaced geostationary satellites. Operating frequency is 44 GHz and link margin equals 10 dB.

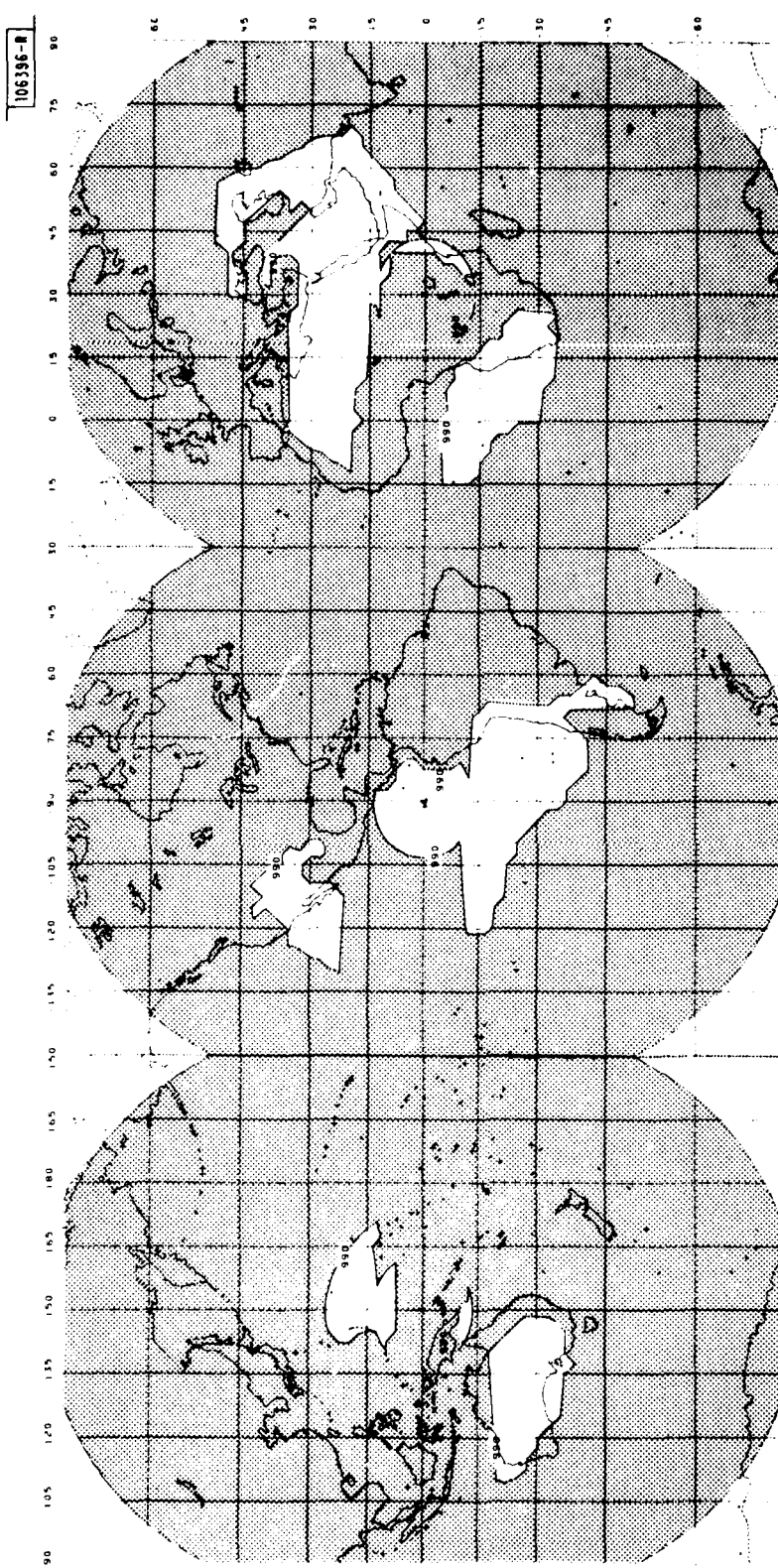


Fig. 19. Coverage area (unshaded) for 0.99 link availability for a constellation of 3 equispaced geostationary satellites. Operating frequency is 44 GHz and link margin equals 6 dB.

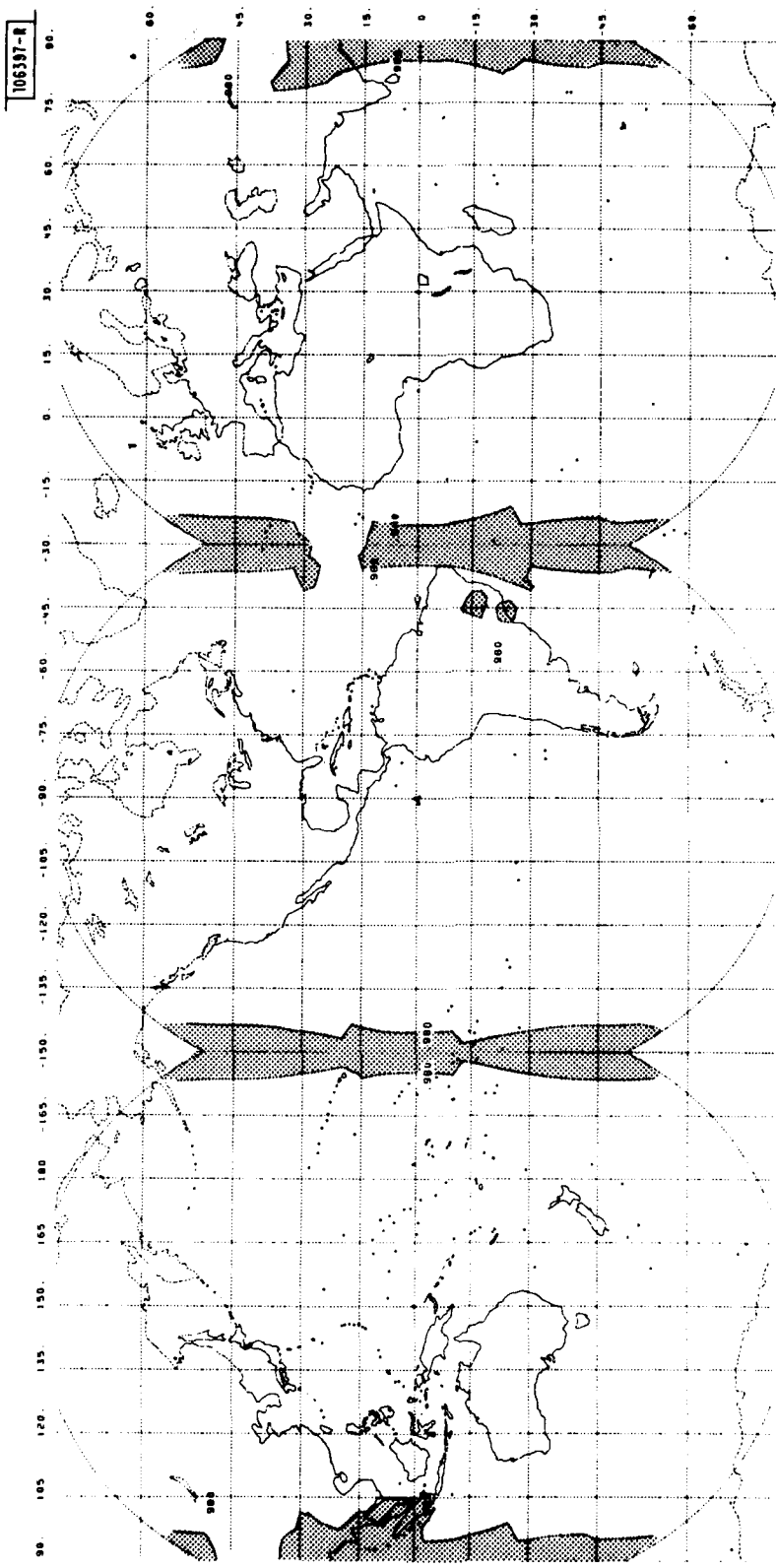


Fig. 20. Coverage area (unshaded) for 0.98 link availability for a constellation of 3 equi-spaced geostationary satellites. Operating frequency is 44 GHz and link margin equals 14 dB.

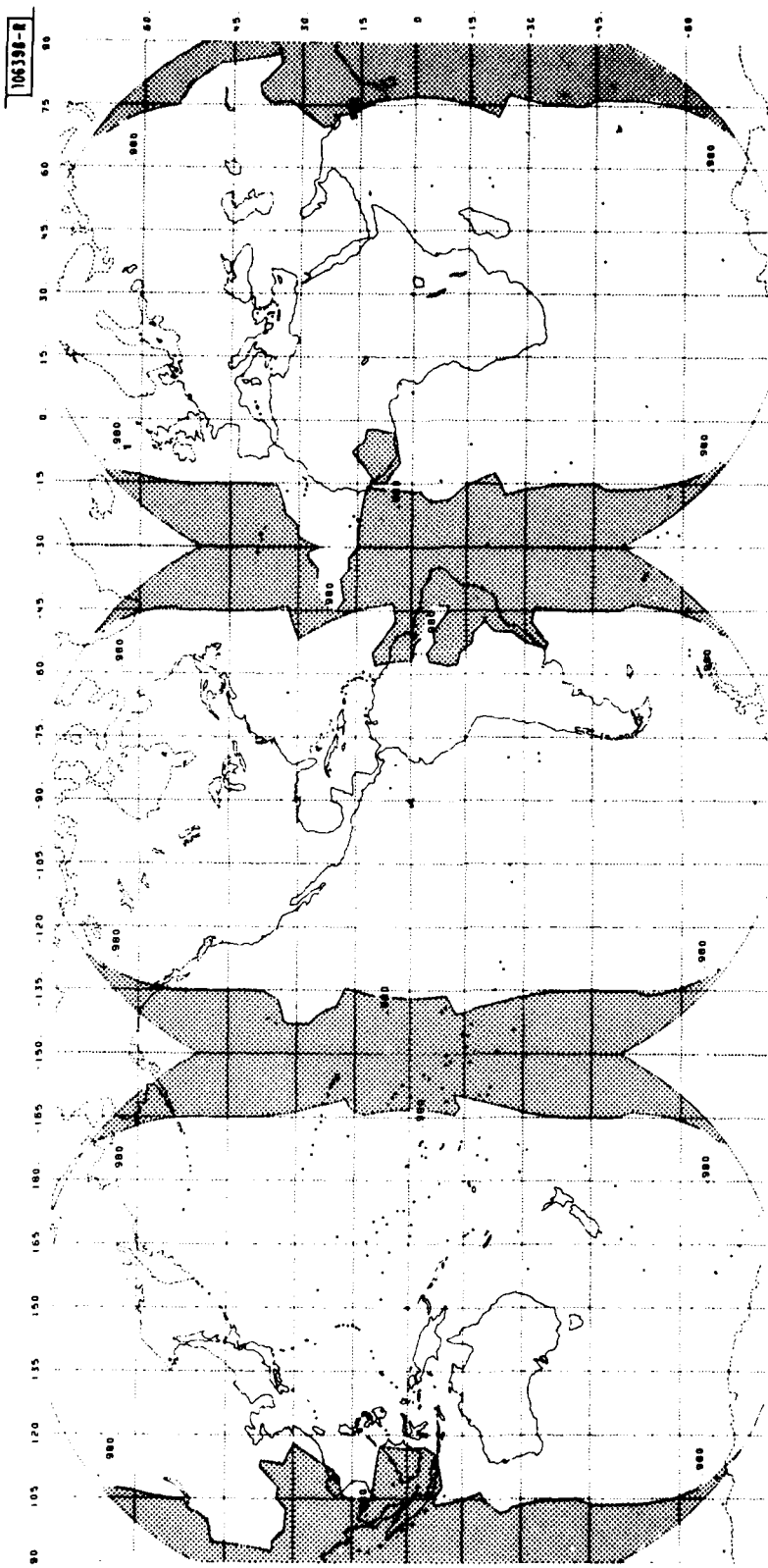


Fig. 21. Coverage area (unshaded) for 0.98 link availability for a constellation of 3 equispaced geostationary satellites. Operating frequency is 44 GHz and link margin equals 10 dB.

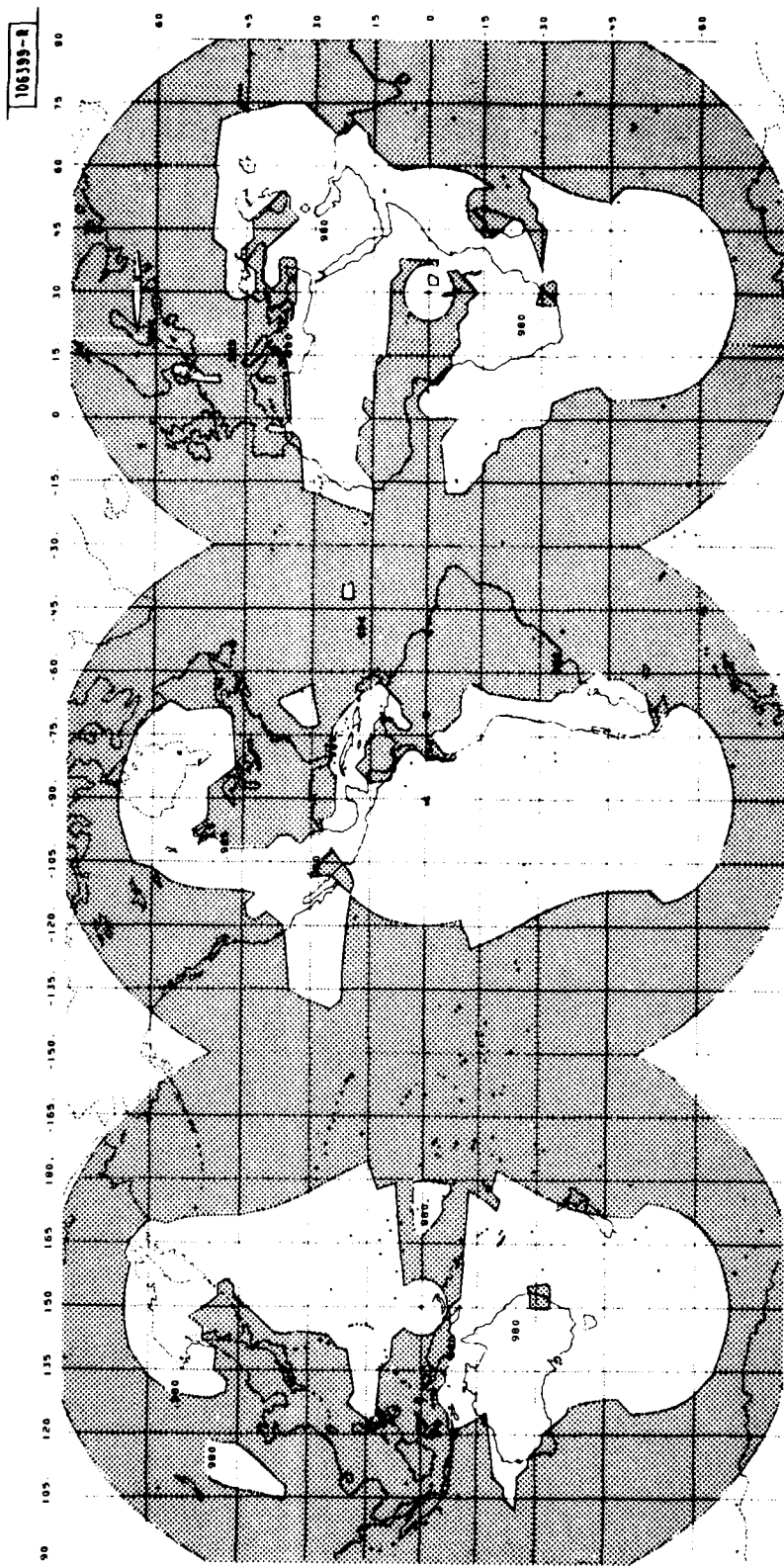


Fig. 22. Coverage area (unshaded) for 0.98 link availability for a constellation of 3 equispaced geostationary satellites. Operating frequency is 44 GHz and link margin equals 6 dB.

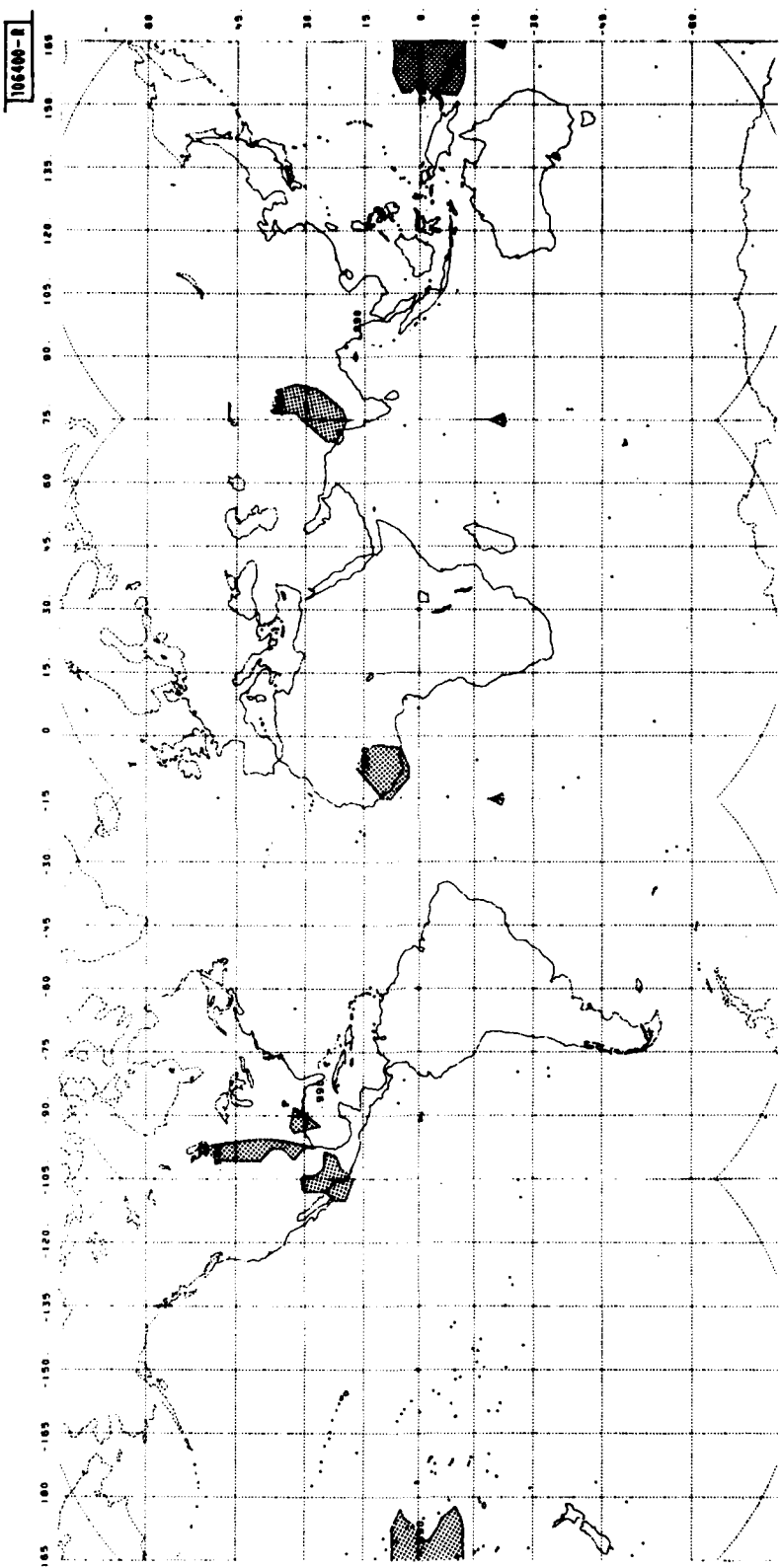


Fig. 23. Coverage area (unshaded) for 0.99 link availability for a constellation of 4 equispaced geostationary satellites. Operating frequency is 44 GHz and link margin equals 14 dB.

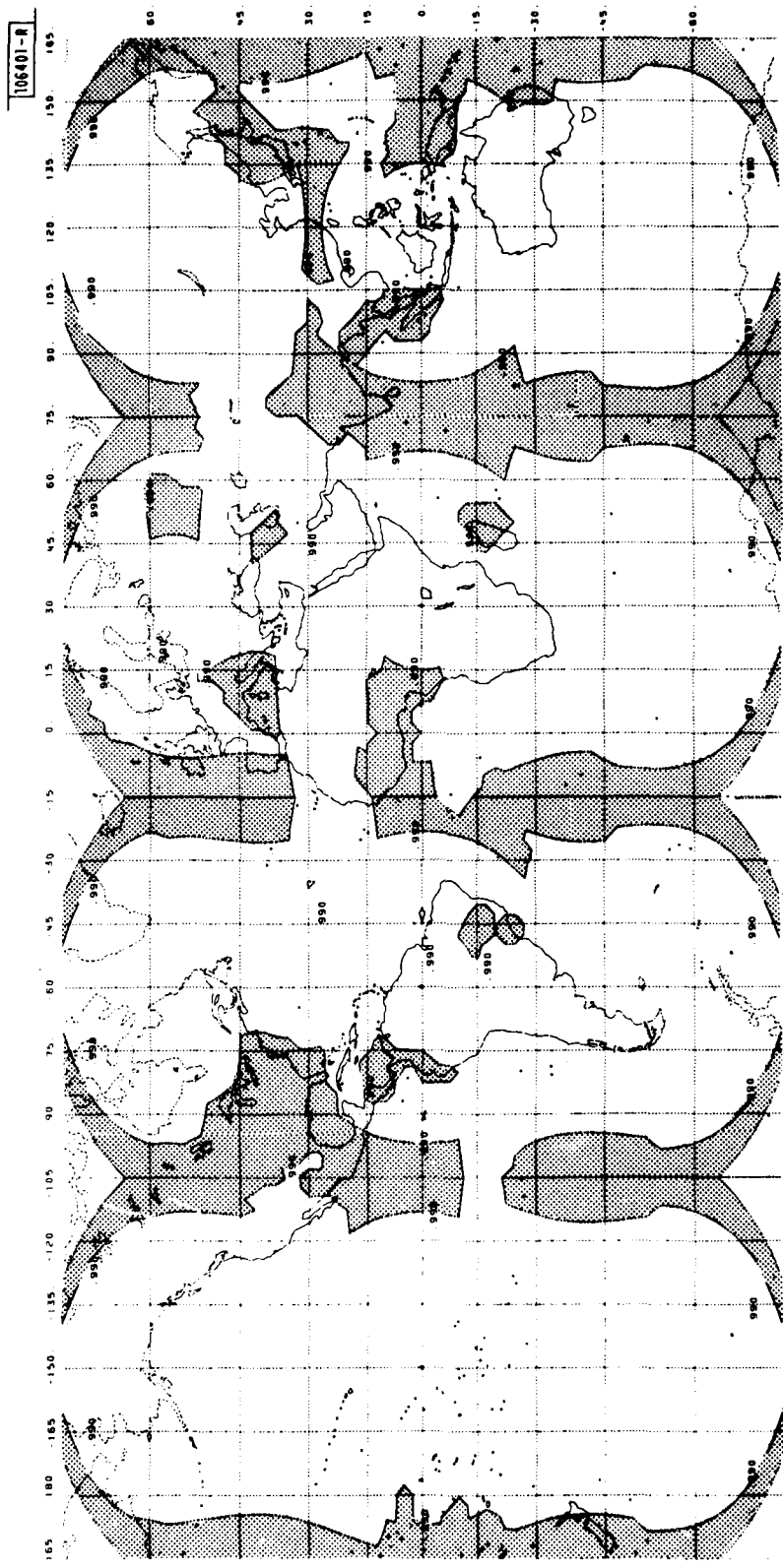


Fig. 24. Coverage area (unshaded) for 0.99 link availability for a constellation of 4 equi-spaced geostationary satellites. Operating frequency is 44 GHz and link margin equals 10 dB.

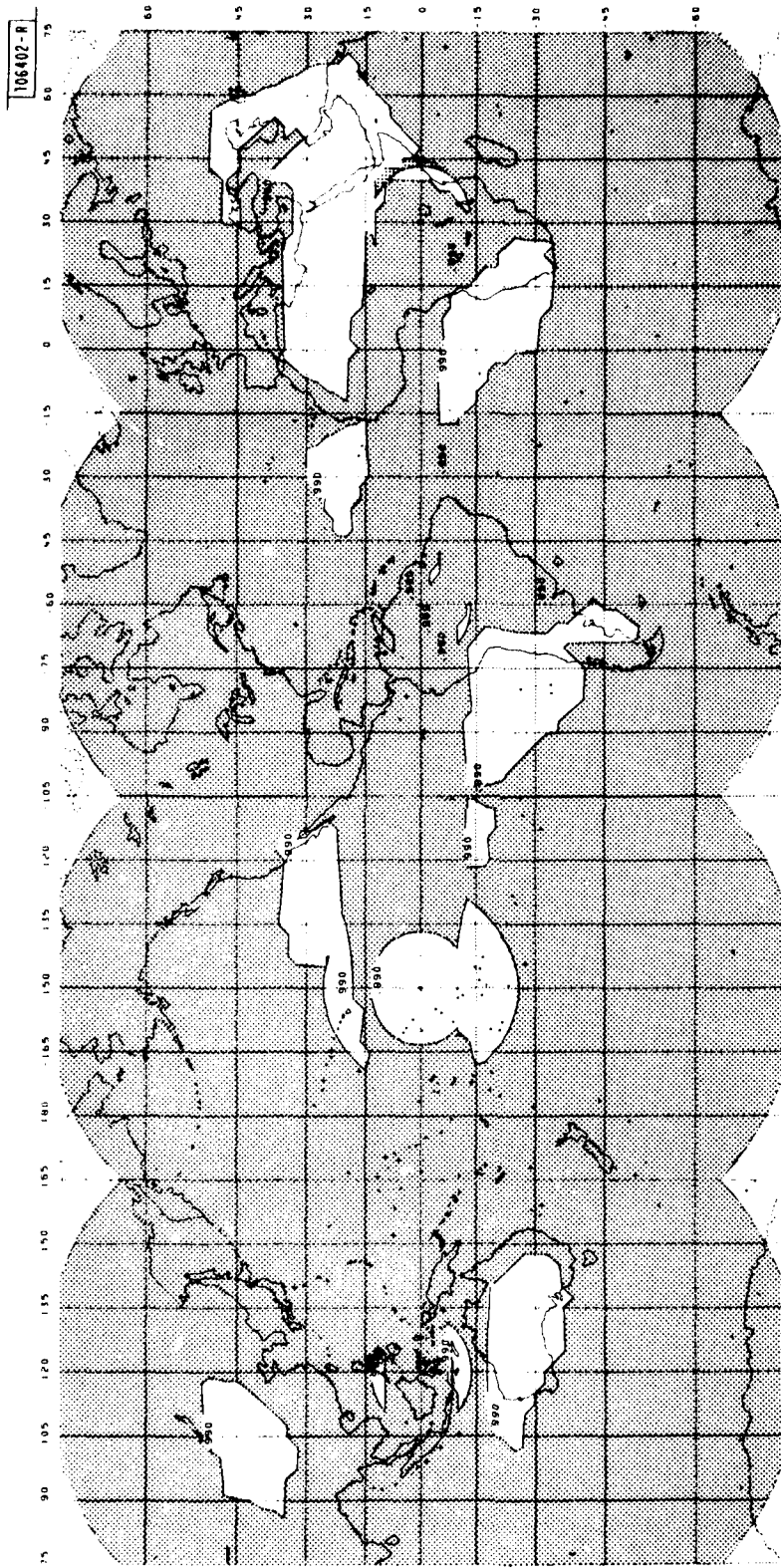


Fig. 25. Coverage area (unshaded) for 0.99 link availability for a constellation of 4 equi-spaced geostationary satellites. Operating frequency is 44 GHz and link margin equals 6 dB.

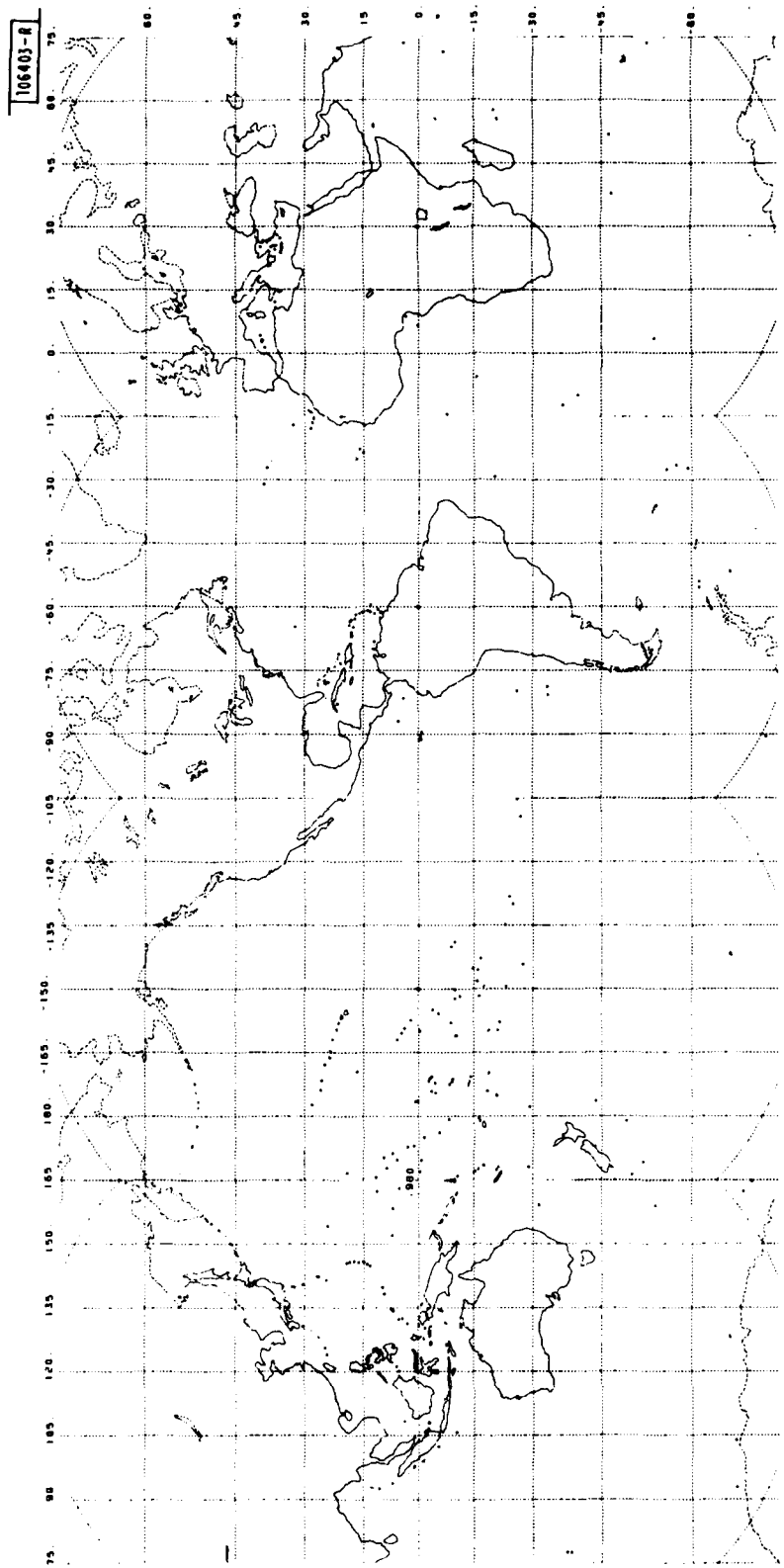


Fig. 26. Coverage area (unshaded) for 0.98 link availability for a constellation of 4 equi-spaced geostationary satellites. Operating frequency is 44 GHz and link margin equals 14 dB.

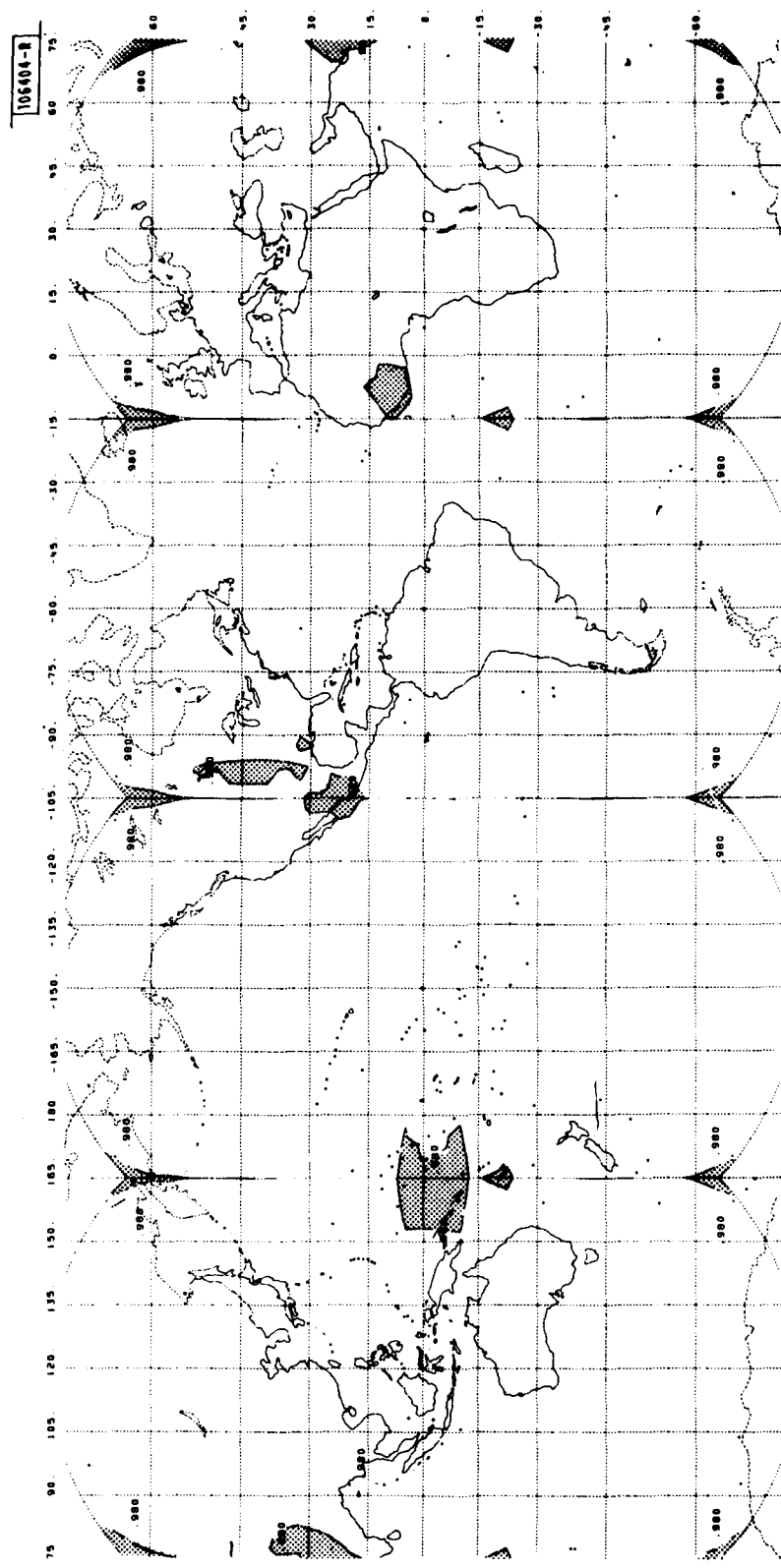


Fig. 27. Coverage area (unshaded) for 0.98 link availability for a constellation of 4 equispaced geostationary satellites. Operating frequency is 44 GHz and link margin equals 10 dB.

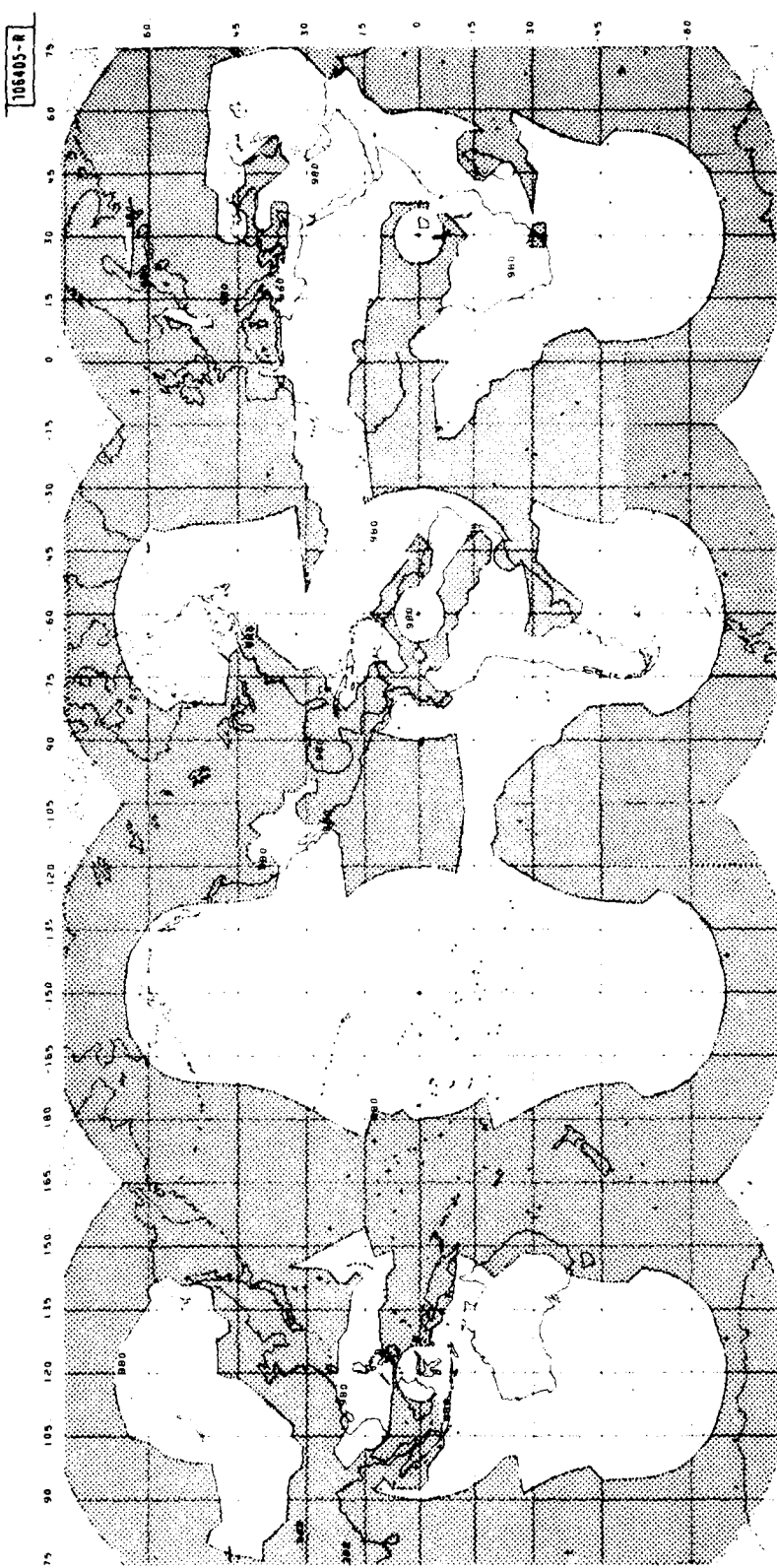


Fig. 28. Coverage area (unshaded) for 0.98 link availability for a constellation of 4 equi-spaced geostationary satellites. Operating frequency is 44 GHz and link margin equals 6 dB.

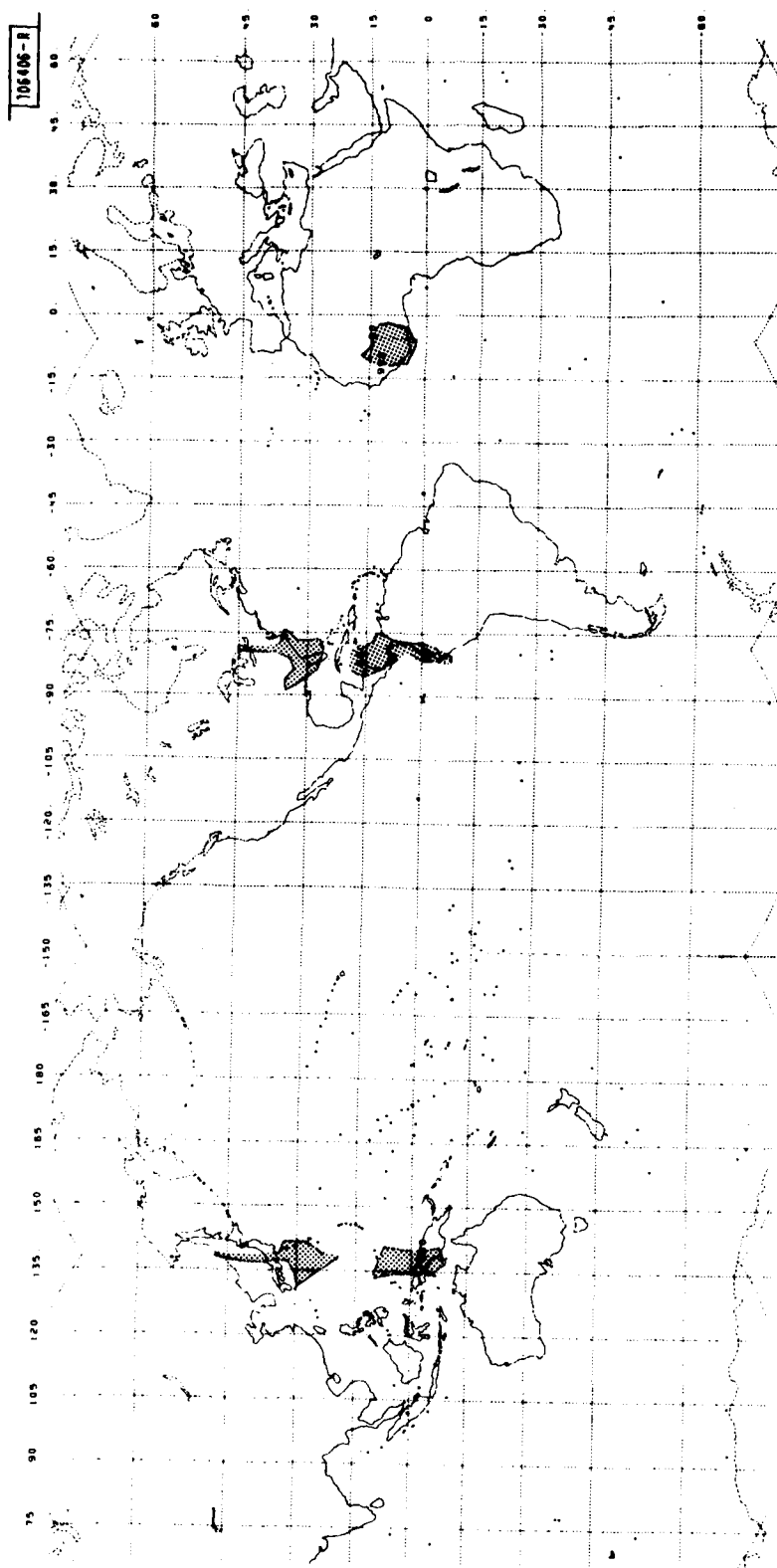


Fig. 29. Coverage area (unshaded) for 0.99 link availability for a constellation of 5 equispaced geostationary satellites. Operating frequency is 44 GHz and link margin equals 14 dB.

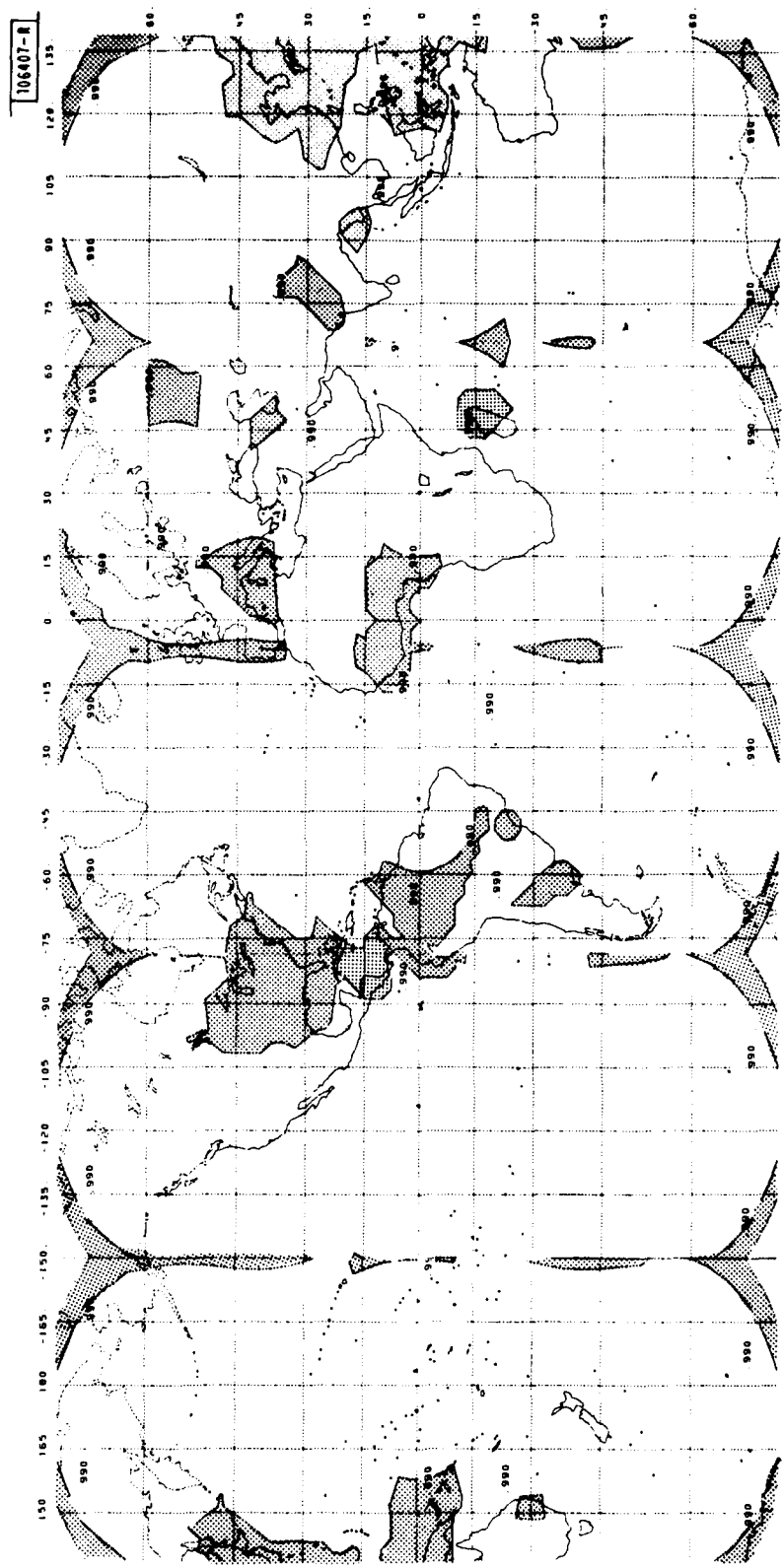


Fig. 30. Coverage area (unshaded) for 0.99 link availability for a constellation of 5 equi-spaced geostationary satellites. Operating frequency is 44 GHz and link margin equals 10 dB.

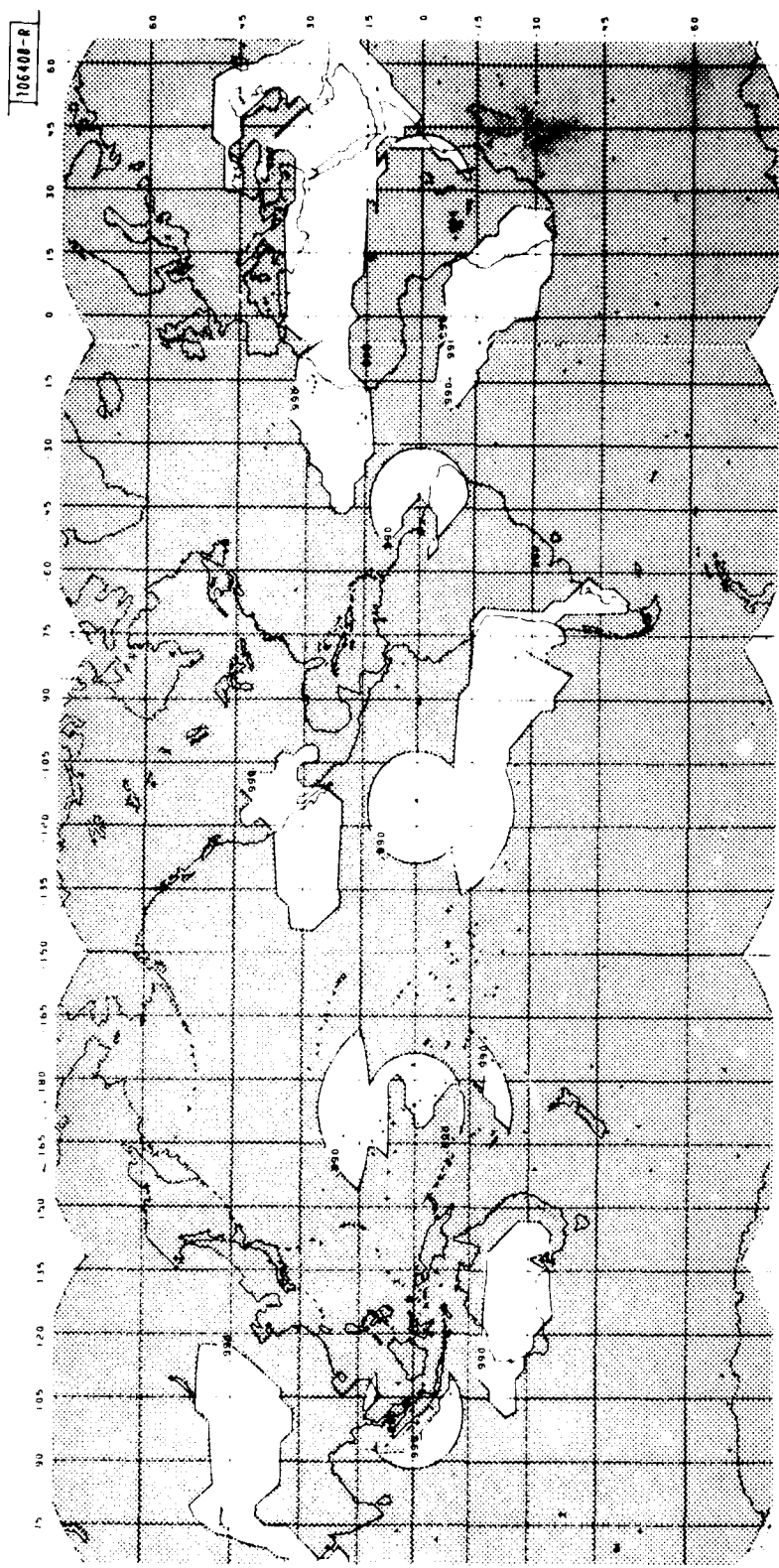


Fig. 31. Coverage area (unshaded) for 0.99 link availability for a constellation of 5 equispaced geostationary satellites. Operating frequency is 44 GHz and link margin equals 6 dB.

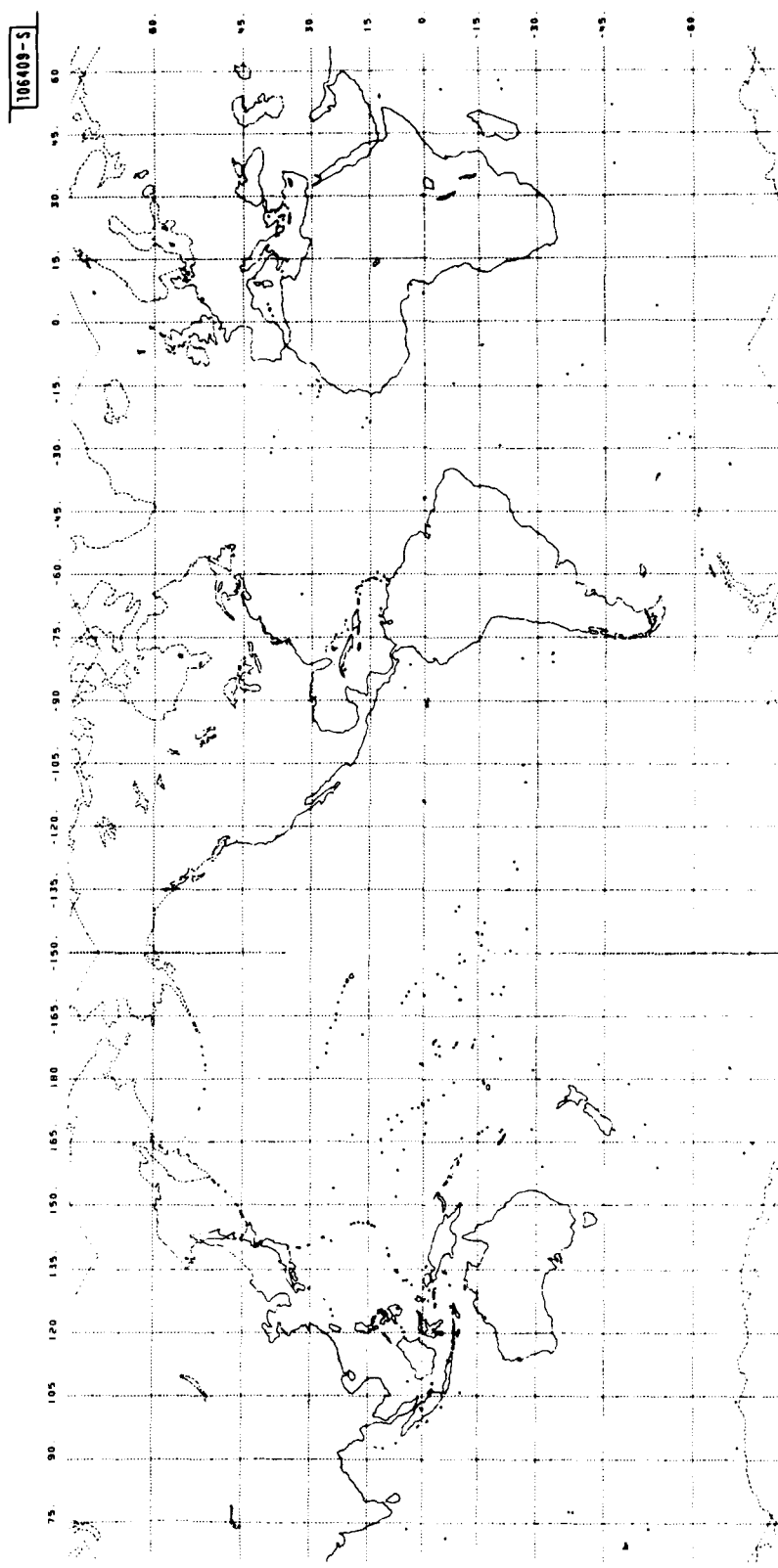


Fig. 32. Coverage area (unshaded) for 0.98 link availability for a constellation of 5 equi-spaced geostationary satellites. Operating frequency is 44 GHz and link margin equals 14 dB.

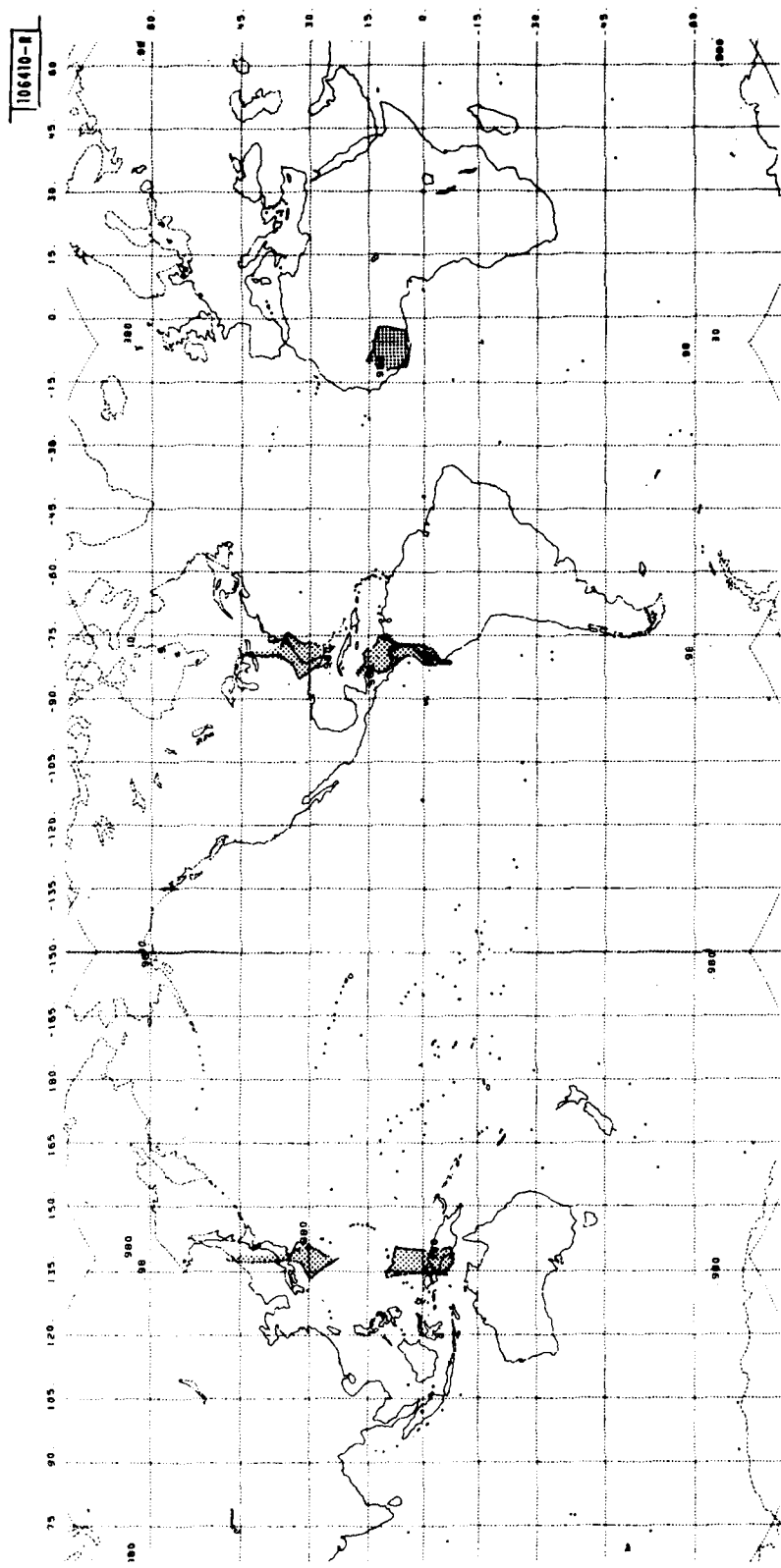


Fig. 33. Coverage area (unshaded) for 0.98 link availability for a constellation of 5 equispaced geostationary satellites. Operating frequency is 44 GHz and link margin equals 10 dB.

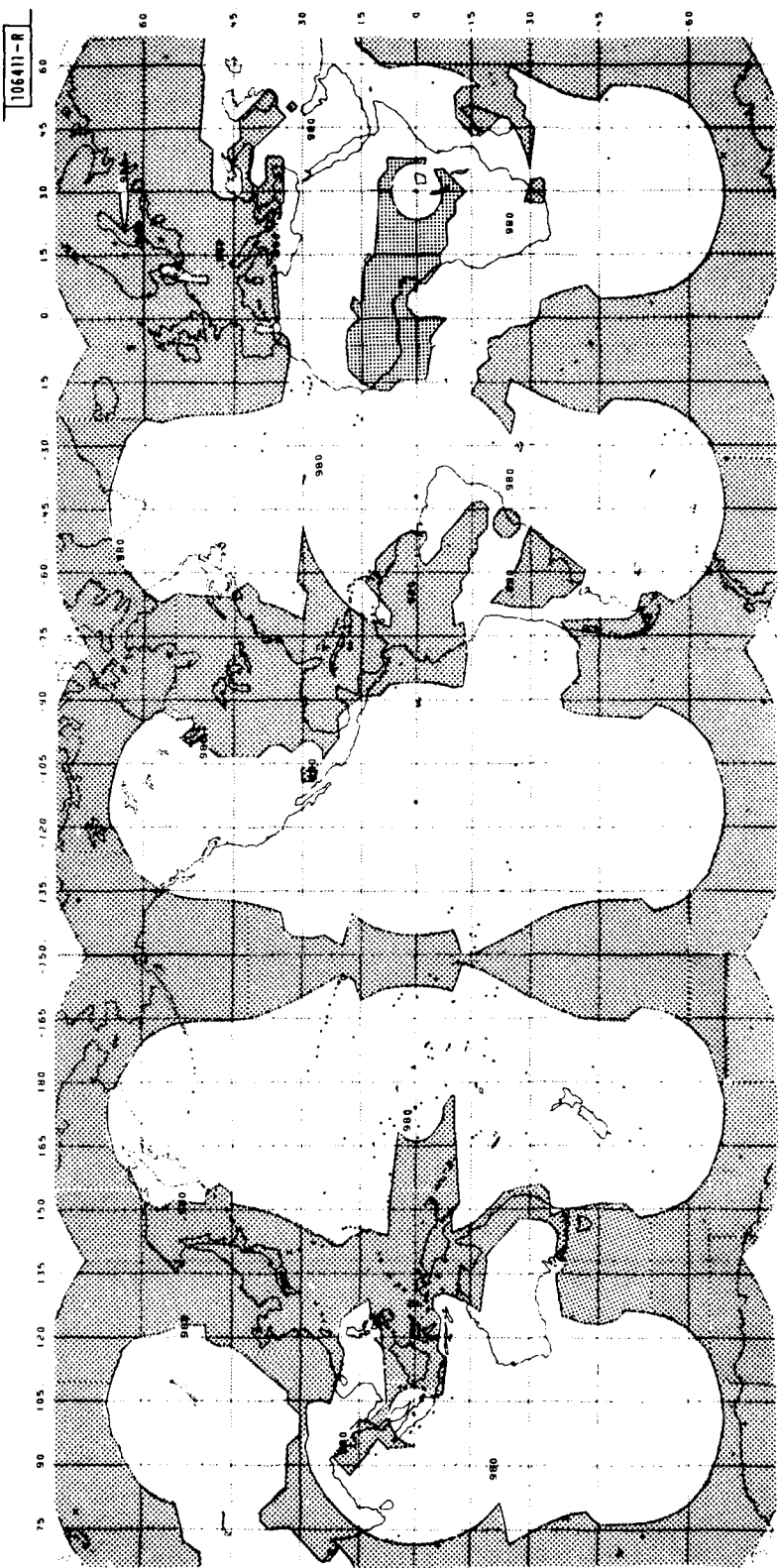


Fig. 34. Coverage area (unshaded) for 0.98 link availability for a constellation of 5 equispaced geostationary satellites. Operating frequency is 44 GHz and link margin equals 6 dB.

availability to the nearest satellite is below the indicated value. Figs. 17-22 present the coverage profiles for the 3 satellite constellation with link availabilities of 0.99 and 0.98, respectively, and link margins sequentially set to 14 dB, 10 dB and 6 dB. Figs. 23-28 present the coverage profiles for the 4 satellite constellation and Figs. 29-34 present the coverage profiles for the 5 satellite constellations. All plots are done for a frequency of 44 GHz.

IV. SATELLITE ANTENNA SUBSYSTEM DIRECTIVITY ALLOCATION CONSIDERATIONS

The coverage profile maps for fixed values of link availability given in the Section III for constellations of 3, 4, and 5 equi-spaced geostationary satellites clearly illustrate the fact that rain attenuation and slant range differential effects coupled together cause marked reductions in link availability near the constant longitude coverage boundaries of adjacent satellite pairs. This effect is especially noticeable at temperate-to-equatorial latitudes for the 3-satellite configuration. Allocation of satellite antenna directive gain to overcome attenuation due to rain will be modelled and parametrically investigated in this section. The 3-satellite configuration will be assumed; however, the technique is equally applicable to the less critical 4 and 5 satellite constellation cases. A 14 dB link margin will be assumed.

The use of a satellite antenna subsystem which provides for reconfigurable beams in near real time would allow MILSATCOM systems operators the option of increasing directivity only in those directions to the Earth's surface where localized storm cells are causing increased link bit error rates due to the rain attenuation. Even if the pattern cannot be reconfigured to match the instantaneous rain situation, improved availability can be obtained with a fixed (but non-uniform) pattern matched to long-term rain statistics. Reconfiguring a satellite antenna subsystem to provide enhanced directivity in some regions must, for a fixed aperture, result in reducing the directivity in other directions. The parametric solution given in this section defines the variables involved and provides a numerical example of the directive gain differential values to illustrate the desirability and limitations of using satellite receive antenna beam shaping for countering rain-induced link attenuation. Like the previous analyses contained in this report, "Earth coverage" antenna patterns are assumed for this parametric analysis. This assumption serves as a departure point for allocation of increased directive gain. The actual pattern shape can subsequently be prescribed as a goal to be achieved by an MBA (multi-beam antenna) or other variable coverage antenna.

For a spacecraft uplink receiving antenna with uniform Earth coverage, the nominal directive gain without (or prior to) gain reallocation can be approximated by the directivity integral in Eqn. (4)

$$D_o = \frac{4\pi}{\int \int_{\Omega_s} P_n(\theta, \phi) d\Omega} \quad (4)$$

where $P_n(\theta, \phi) = 1$ over the field of view

and $d\Omega = \sin\theta d\theta d\phi$

and the limits of integration are given by

$$[\phi_i; \phi_f] = [0^\circ; 360^\circ]$$

$$[\theta_i; \theta_f] = [0^\circ; 8.7^\circ]$$

The idealized pattern integration yields a value of 173.6 (=22.4 dB).

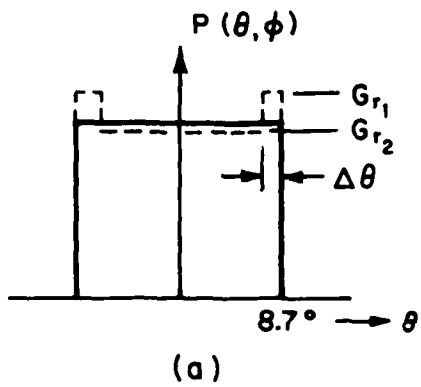
Recognizing that rain is a problem primarily at low elevation angles in the tropics, we are led to examine the idealized gain pattern function as shown by the dashed lines of Fig. 35(a). An isometric sketch of the three dimensional directive gain pattern is shown in Fig. 35(b), where directive gain is increased in the two 90° sectors along the fringes of the coverage area. The angular width of these sectors is $\Delta\theta$ degrees.

The new shaped pattern function is then applied to the standard directive gain expressions as follows.

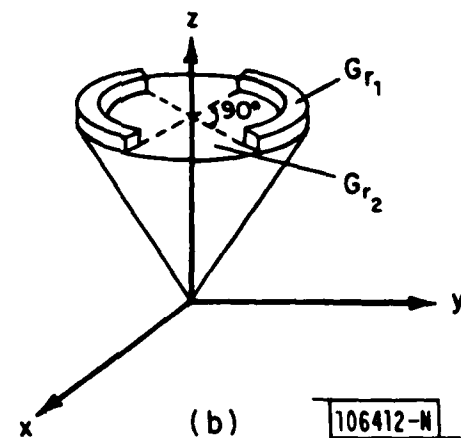
$$G_{r_1} = \frac{4\pi|E_{r_1}|^2}{P} ; G_{r_2} = \frac{4\pi|E_{r_2}|^2}{P}$$

where

$$P = [\int_0^{2\pi} \int_0^{(8.7^\circ - \Delta\theta)} |E_{r_2}|^2 d\Omega + \int_0^\pi \int_{(8.7^\circ - \Delta\theta)}^{8.7^\circ} |E_{r_2}|^2 d\Omega + \int_0^\pi \int_{(8.7^\circ - \Delta\theta)}^{8.7^\circ} |E_{r_1}|^2 d\Omega]$$



(a)



(b)

106412-N

Fig. 35(a). Idealized Earth coverage uplink receive pattern before reallocation (solid line) and after reallocation (dashed line); (b). Isometric sketch of reallocated gain pattern showing fringe area increase in relative directive gain.

Straightforward evaluation and substitution steps yield the following expression for the directive gain G_{r_1} as a function of the fringe area width $\Delta\theta$ (degrees) and the ratio (G_{r_1}/G_{r_2}) of the directive gains in the pattern fringes to the pattern central area.

$$G_{r_1} = \frac{G_{r_1}}{G_{r_2}} \cdot \frac{4}{(2-\cos(8.7^\circ-\Delta\theta)-\cos8.7)+(G_{r_1}/G_{r_2})(\cos(8.7^\circ-\Delta\theta)-\cos8.7)}$$

This expression was numerically evaluated and is plotted in Fig. 36 where all the gain values are expressed in dB. For a 1° fringe area width and gain difference value G_{r_1} (dB)- G_{r_2} (dB)=6 dB, one finds the enhanced fringe area directive gain is 27.2 dB (or 4.8 dB over the uniform Earth coverage value of 22.4 dB). The penalty paid in the remaining portion of the pattern is $(6-4.8)=1.2$ dB. Comparison of the coverage profile plot given in Fig. 20 for the case of 3 satellites, 14 dB margin and 0.98 availability with the plot of the 1° wide enhanced fringes projected onto the Earth as given in Fig. 37 shows that most of the areas with low availability are inside the enhanced fringe areas. A check of the percent Earth coverage vs link margin data given in Fig. 14 shows that, for the 3 satellite constellation case, an increase in gain to realize a $14+4.8=18.8$ dB margin increases coverage almost to the theoretically maximum value (approximate coverage increases from 82% at 14 dB margin to 90% at 18.8 dB margin).

In order to produce the assumed 1° width of the antenna pattern over which the directive gain is enhanced, an antenna aperture ~ 70 wavelengths (λ) is required. A 70λ aperture MBA can produce an Earth coverage gain of 19 dB minimum and 21 dB maximum (due to ripple in the pattern). Installation of the pattern, shaped to reallocate gain, as described here would reduce the Earth coverage directive gain to ≈ 18 dB and provide 23 dB directive gain in the direction of those terminals located in the sectoral-shaped fringes of the "coverage" area. The DSCS III uplink MBA would be capable of producing this shaped pattern with the enhanced sector width = $1 \frac{3}{4}^\circ$ resulting in a margin ≈ 18 dB. The margin in the "Earth coverage" area would be reduced to ≈ 12 dB.

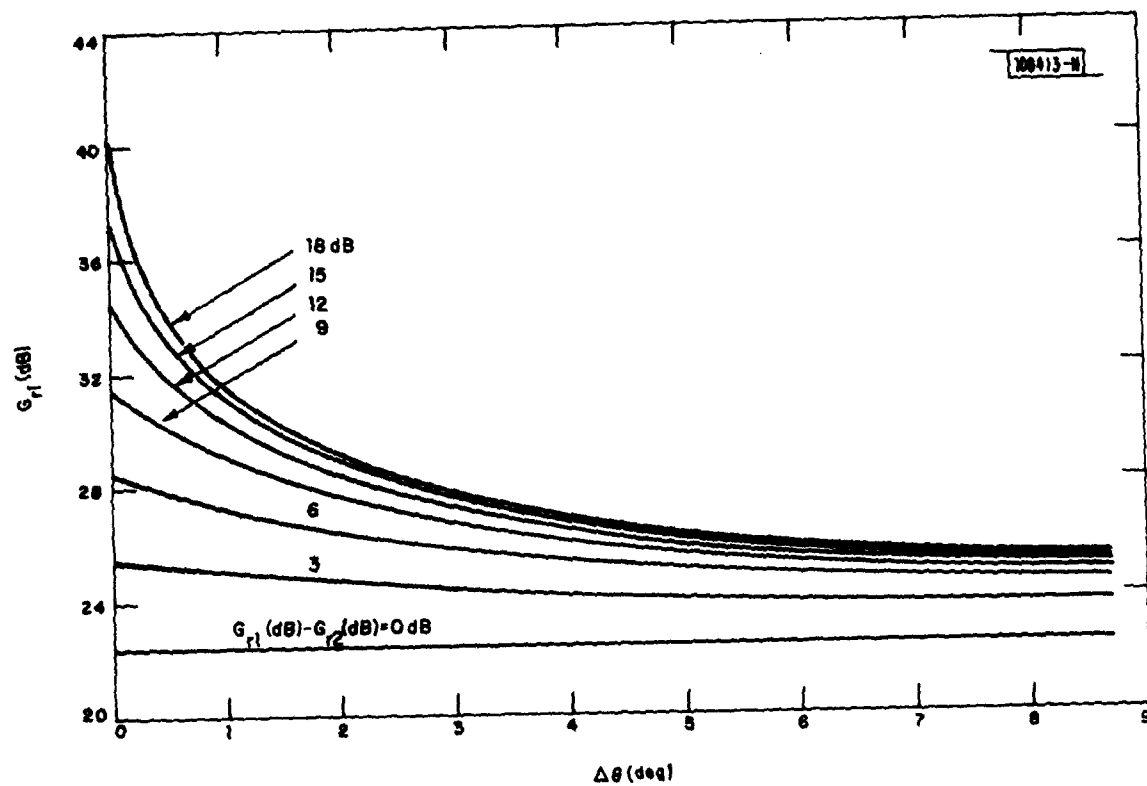


Fig. 36. Enhanced directive gain G_{r1} (dB) as a function of angular width ($\Delta\theta$) for two 90° sector pattern fringes and parametric values of difference in directive gains from 0 to 18 dB with increments of 3 dB.

106414-S

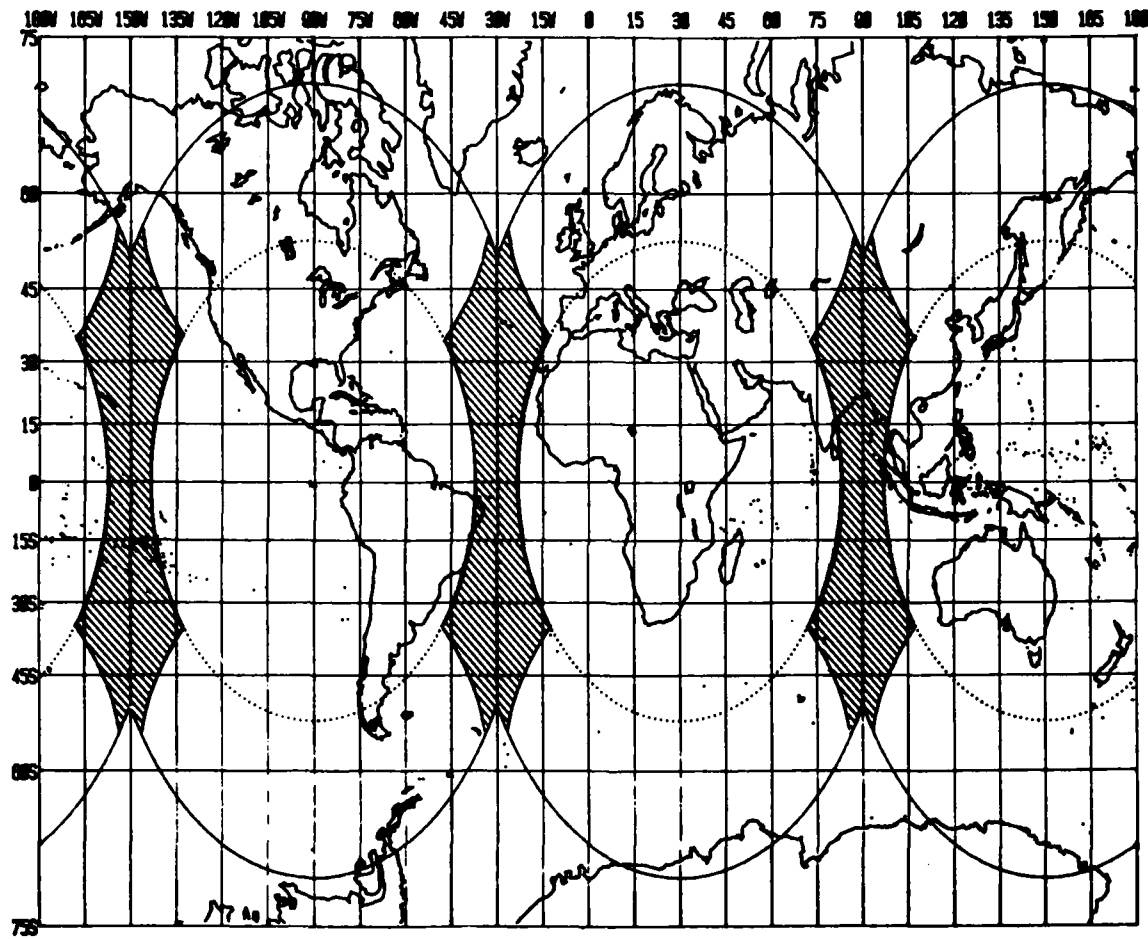


Fig. 37. Projection of an enhanced fringe area satellite antenna pattern on Earth's surface. Fringe sectors are 90° wide (azimuth sense) and 1° deep (polar sense) as measured from a line between the Earth center and the satellite (Mercator Projection).

Alternatively, one could derive and plot a contour of required margin to provide a fixed value of availability. Such a plot would depict the optimum differential antenna directive gain in a long term sense vis-a-vis the background rain statistics. This would be an appropriate and desirable adjunct to the design of a specific spacecraft array configuration.

The prospective usefulness of a directive gain reallocation capability for a satellite antenna subsystem is strongly related to matching the subsystem operating parameters to the rain characteristics which are the root of the problem. The rainfall characteristics described in this section were obtained from recent literature on the subject and will likely be superceded by more accurately measured data in the near future.

Both Crane⁹ and the ITU/CCIR¹⁰ agree that two types of storms are used to categorize rainfall: ITU designates them as stratiform and cumulus. Crane designates them as stratiform and convective. Both agree that stratiform type systems are usually horizontally homogeneous and display only a vertical variation in intensity (measured by radar reflectivity). On the point of horizontal distribution, Crane and the ITU use different terminology of definition but the measured data presented by both appear to agree to the first order. That data is in the form of storm cell size measured horizontally (in km).

Crane's (more recent) publication notes that, in practice, weather systems display both stratiform and convective elements in the same system. Crane asserts that "widespread rain generally has imbedded convective elements; convective showers are surrounded by relative uniform regions of lower reflectivity ...". Crane's definition of cell size is related to the -3 dB contour around the point of maximum radar reflectivity within a convective structure. His data was measured at the Millstone Hill Radar, Westford, MA, and appears to be representative of northeast US conditions. A contour plot in Crane's paper shows an event with multiple cells within one storm structure. The cell dimensions are not tabulated separately but use of the calibration scale provided shows that most of the cells have orthogonal cut dimensions of a few kilometers to at most (for one cell) about 8 km in one direction.

The ITU version is supplied in the form of a curve of average rain cell size (km) as a function of rain rate (mm/hr). That curve is reproduced in Fig. 38. Three sets of measured data points are superimposed on the curve. Two sets are indicated as having been derived from attenuation measurements in the 2 most rainy climate regions of the previously commonly used 5 region CCIR climate model. The other set of points were derived from radar measurements conducted in Switzerland (CCIR Region 3). For rain rates of 40 mm/hr or greater, the average rain cell size is 3 km or less. More important, the cell size diminishes with increasing rain rate. Recall that, for fixed values of link margin and frequency, the shaded areas below a given fixed value of link availability on the coverage profile maps (Figs. 17-34) represent terminal locations which will experience outages at high rain rates, i.e., rates high enough to negate the existing link margin.

The reallocation of gain on an almost real-time basis to overcome local rain cell attenuation poses additional array hardware implications in order to conclusively determine threshold fading due to rain. Such hardware implications are beyond the scope of this report.

The relatively small lateral dimensions of rain storm cells must be carefully qualified in attempting to scope likely areas of link outage. In particular, the vertical dimensions of the storm cells must be included in determining a "rain attenuation footprint" on the Earth surface due to low values of elevation angle encountered in the satellite overlap regions.

In summary, the entire spatial and temporal character of rain storm cell structure must be included in any effort to determine a statistically characterized outage profile which can be overcome on a highly localized basis by means of directive gain reallocation techniques. At present, a limited amount of such comprehensive cell structure data is available.

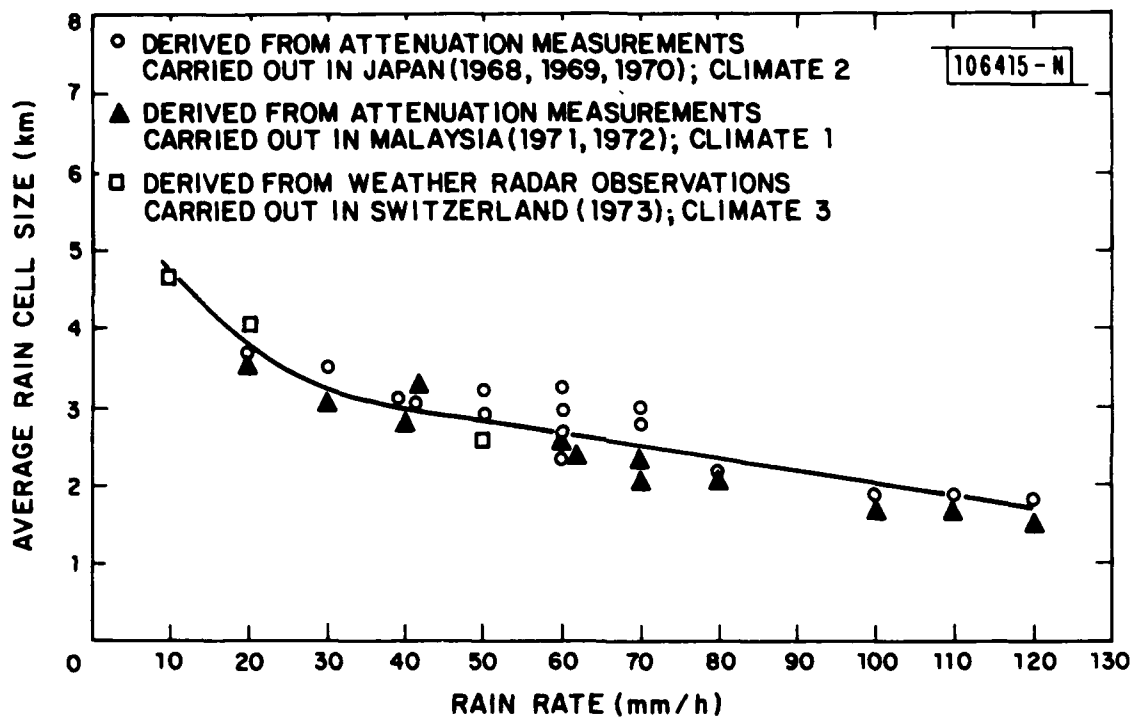


Fig. 38. Average rain cell size (km) as a function of rain rate. (From ITU/CCIR Rep. 563)

V. CONCLUSIONS

From the geometric coverage viewpoint only, it has been shown that the use of a constellation of 4 equi-spaced geostationary satellites provides substantial coverage (93%) of the Earth surface with visibility to 2 satellites available to almost one half of that amount (43% of the Earth's surface). Accomplishing a significant amount (i.e., > 90% coverage) of redundancy in terms of simultaneous satellite access requires at least 7 equi-spaced satellites. Several constellations of satellites in critically inclined orbits were found to provide full Earth coverage at all times in an unconditional sense, i.e., mutual visibility to a specific ground station is not required. Also, the constellation of 4 critically inclined satellites (4 per hemisphere apogee) in the same orbital plane (i.e., 4 separate ground tracks), provides higher levels of simultaneous coverage to 2 satellites than the other configurations considered. The constellations with 24 hour periods showed slightly better one and two satellite coverages in most cases when compared to analogous 12 hour period constellations.

The inclusion of the rain attenuation factor in computing percent Earth coverage for geostationary constellations as a function of margin or availability for fixed frequency has resulted in the following general conclusions:

The percent coverage vs availability curves possess part or all of an S-shape with the tails of the curves relatable to physical aspects of the problem.

Increasing the number of equi-spaced geostationary satellites in the constellation causes the knee of the visibility vs availability curve to become very pronounced; i.e., a threshold value of availability now becomes apparent above which Earth coverage area falls dramatically.

The slope of the percent coverage vs margin (for fixed number of satellites) curves monotonically decreases until the curves reach the geometric visibility asymptote for large margins. That asymptotic limit is reached more quickly for larger numbers of satellites in the constellation. Threshold values (or curve knees) are not obvious in the coverage vs margin plots. However, these latter plots provide the MILSATCOM system designer with new potent tools for assessing the classic trade-off of coverage vs margin vs availability vs number of satellites.

ACKNOWLEDGMENTS

The author wishes to acknowledge the efforts of Nancy Helfrich in modifying the system availability predictor model software and computing the results given in Sections II(B) and (C) and Section III. The geometric orbit coverage results for non-geostationary satellites were computed by the ORBCOV program based on constellation analysis software originated by Susan Schmidt and Gloria Lilias of Lincoln Laboratory Group 64. The author also wishes to thank Mr. William Cummings and Drs. Leon Ricardi and Alan Simmons of Lincoln Laboratory, Group 61, for many helpful technical discussions. Dr. Ronald Bauer of Lincoln Laboratory Group 64 provided the suggestion for use of the reversed log graphing of the coverage vs availability data of Figures 3 through 5. The patience of the typist, Maureen Bartlett, during the long evolution of this report is sincerely appreciated.

REFERENCES

1. W. C. Cummings, P. C. Jain, and L. J. Ricardi, "Fundamental Performance Characteristics That Influence EHF MILSATCOM Systems," *IEEE Trans. Commun.* COM-27, 1423 (1979).
2. L. M. Schwab, "A Predictor Model for SHF and EHF MILSATCOM System Availabilities in the Presence of Rain," Technical Note 1980-15, Lincoln Laboratory, M.I.T (21 February 1980), DTIC AD-A086714/3.
3. N. E. Feldman and L. G. Mundie, "The Feasibility of Employing Frequencies Between 20 and 300 GHz for Earth-Satellite Communications Links," Rand Corp. Project Report R-2275 DCA (May 1978) DDC AD-A056100.
4. R. K. Crane, "Prediction of Attenuation by Rain," *IEEE Trans. Commun.* COM-28 1717 (1980).
5. R. K. Crane, "A Global Model for Rain Attenuation Prediction," EASCON '78 Record, Washington, D.C., pp. 391-395 (September 1978), IEEE Publication No. 78CH 1354-4AES.
6. L. N. Rowell, "Satellite Constellations for Worldwide and Hemisphere Coverage," Rand Corp. Note N-1432-DCA (December 1979).
7. L. J. Ginsberg and R. D. Luders, "Earth Coverage Provided by Certain Systems of Q=2 Type Relay Satellites," Aerospace Corp., Report No. TOR-0075(5060-04)-2 (10 January 1975).
8. Y-L. C. Lo and L. M. Schwab, "Effect of Downlink Phased Array Patterns on System Availability Contour Predictions," Technical Note 1980-27, Lincoln Laboratory, M.I.T. (10 April 1980) DTIC AD-A088664.
9. R. K. Crane, "Automatic Cell Detection and Tracking," *IEEE Trans. Geosci. Electron.* GE-17, 250 (1979).
10. ITU/CCIR Rept. 563-1: Contained in Section 5C, "Effects of the Atmosphere," Vol. V - Propagation in Non-Ionized Media, Recommendations and Reports of the CCIR, 1978 (XIV Plenary Assembly; Kyoto, 1978).

UNCLASSIFIED

SECURITY CLASSIFICATION OF THIS PAGE (When Data Entered)

DD FORM 1473 EDITION OF 1 NOV 65 IS OBSOLETE
1 JAN 73

UNCLASSIFIED

SECURITY CLASSIFICATION OF THIS PAGE (When Data Entered)